Oxidative Medicine and Cellular Longevity

Crosstalk between Mechanical Forces, Cytoskeletal Dynamics and the Regulation of ROS and Autophagy in Health and Disease

Lead Guest Editor: Miguel Sánchez-Álvarez
Guest Editors: Marco Cordani, Raffaele Strippoli, Fidel Lolo, and Manuela Antonioli

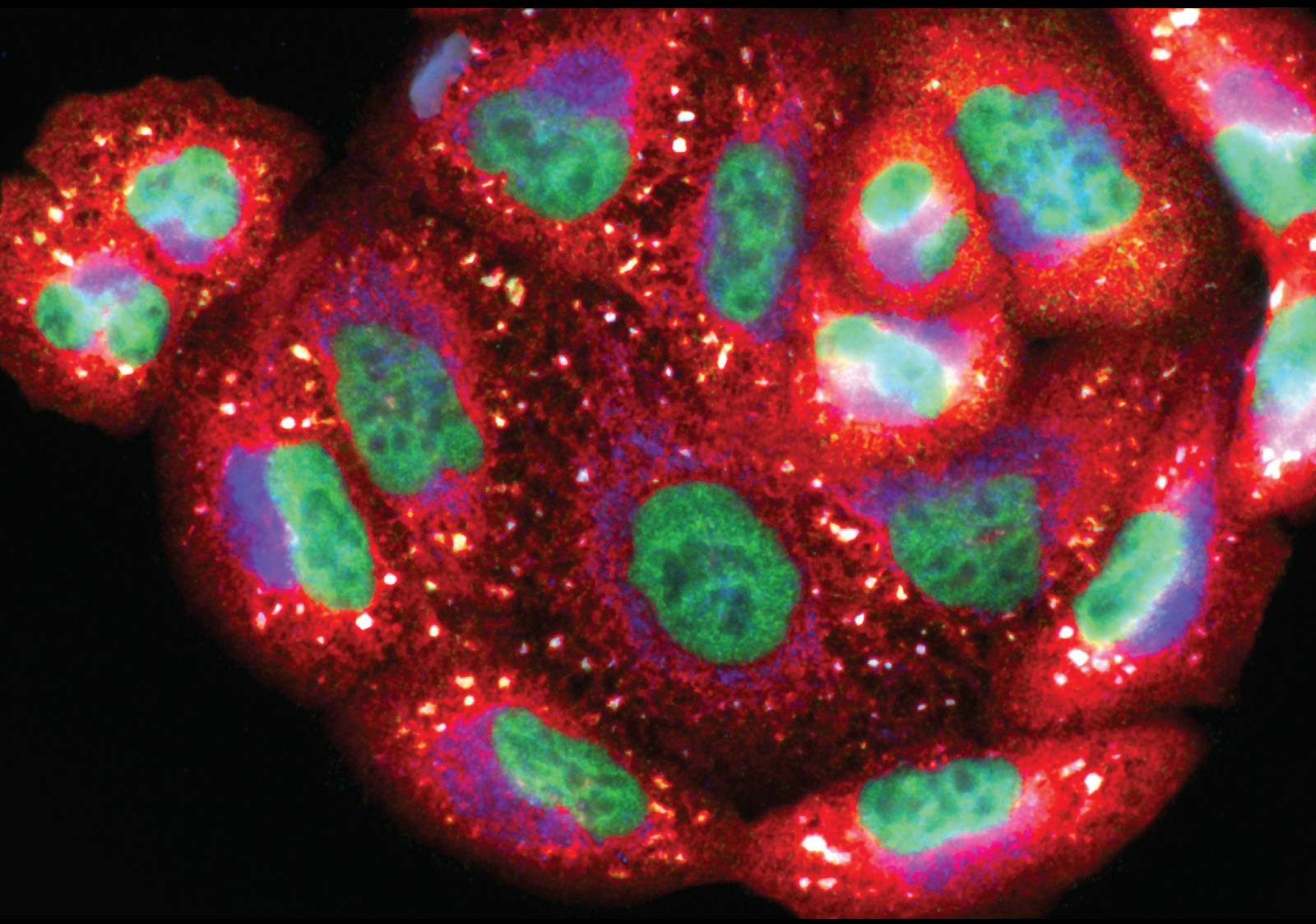

Crosstalk between Mechanical Forces, Cytoskeletal Dynamics and the Regulation of ROS and Autophagy in Health and Disease

Oxidative Medicine and Cellular Longevity

Crosstalk between Mechanical Forces, Cytoskeletal Dynamics and the Regulation of ROS and Autophagy in Health and Disease

Lead Guest Editor: Miguel Sánchez-Álvarez
Guest Editors: Marco Cordani, Raffaele Strippoli, Fidel Lolo, and Manuela Antonioli

Contents

Hindawi
Oxidative Medicine and Cellular Longevity
Volume 2020, Article ID 6425782, 15 pages
https://doi.org/10.1155/2020/6425782

Research Article

Molecular Mechanisms of Adiponectin-Induced Attenuation of Mechanical Stretch-Mediated Vascular Remodeling

Crystal M. Ghantous,[1,2] **Rima Farhat**,[1] **Laiche Djouhri**,[3] **Sarah Alashmar**,[3] **Gulsen Anlar**,[3] **Hesham M. Korashy**,[4] **Abdelali Agouni**,[4] **and Asad Zeidan**[3]

[1]*Department of Anatomy, Cell Biology and Physiology, Faculty of Medicine, American University of Beirut, Beirut, Lebanon*
[2]*Department of Nursing and Health Sciences, Faculty of Nursing and Health Sciences, Notre Dame University-Louaize, Beirut, Lebanon*
[3]*Department of Basic Sciences, College of Medicine QU Health, Qatar University, Doha, Qatar*
[4]*Department of Pharmaceutical Sciences, College of Pharmacy, QU Health, Qatar University, Doha, Qatar*

Correspondence should be addressed to Asad Zeidan; a.zeidan@qu.edu.qa

Received 6 December 2019; Revised 12 April 2020; Accepted 17 April 2020; Published 21 May 2020

Guest Editor: Fidel Lolo

Hypertension induces vascular hypertrophy, which changes blood vessels structurally and functionally, leading to reduced tissue perfusion and further hypertension. It is also associated with dysregulated levels of the circulating adipokines leptin and adiponectin (APN). Leptin is an obesity-associated hormone that promotes vascular smooth muscle cell (VSMC) hypertrophy. APN is a cardioprotective hormone that has been shown to attenuate hypertrophic cardiomyopathy. In this study, we investigated the molecular mechanisms of hypertension-induced VSMC remodeling and the involvement of leptin and APN in this process. To mimic hypertension, the rat portal vein (RPV) was mechanically stretched, and the protective effects of APN on mechanical stretch-induced vascular remodeling and the molecular mechanisms involved were examined by using 10 μg/ml APN. Mechanically stretching the RPV significantly decreased APN protein expression after 24 hours and APN mRNA expression in a time-dependent manner in VSMCs. The mRNA expression of the APN receptors AdipoR1, AdipoR2, and T-cadherin significantly increased after 15 hours of stretch. The ratio of APN/leptin expression in VSMCs significantly decreased after 24 hours of mechanical stretch. Stretching the RPV for 3 days increased the weight and [^{3}H]-leucine incorporation significantly, whereas APN significantly reduced hypertrophy in mechanically stretched vessels. Stretching the RPV for 10 minutes significantly decreased phosphorylation of LKB1, AMPK, and eNOS, while APN significantly increased p-LKB1, p-AMPK, and p-eNOS in stretched vessels. Mechanical stretch significantly increased p-ERK1/2 after 10 minutes, whereas APN significantly reduced stretch-induced ERK1/2 phosphorylation. Stretching the RPV also significantly increased ROS generation after 1 hour, whereas APN significantly decreased mechanical stretch-induced ROS production. Exogenous leptin (3.1 nM) markedly increased GATA-4 nuclear translocation in VSMCs, whereas APN significantly attenuated leptin-induced GATA-4 nuclear translocation. Our results decipher molecular mechanisms of APN-induced attenuation of mechanical stretch-mediated vascular hypertrophy, with the promising potential of ultimately translating this protective hormone into the clinic.

1. Introduction

Being a disease itself, hypertension is also a major risk factor for the development of other cardiovascular diseases, such as stroke, renal disease, and heart failure [1, 2]. In response to hypertension, small resistance vessels undergo vascular hypertrophy and remodeling [3]; their walls become thicker, stiffer, and less elastic, increasing the risk of vascular blockage and rupture, and potentially leading to organ damage and failure [4, 5]. Hypertension is not only associated with cardiovascular abnormalities in structure and function but also with dysregulated circulating levels of two important adipokines: leptin and adiponectin (APN). Plasma leptin levels are increased while APN levels are decreased in hypertensive

patients [6–8]. After their discovery and for a while, these adipokines were believed to be almost exclusively produced by adipocytes [9–15], but studies later showed that they are also produced by other kinds of cells, including cardiomyocytes [16–18]. However, little research has been done on whether leptin and APN are also produced by VSMCs and whether their expression is affected by hypertension.

Leptin is a hormone whose levels are directly associated with obesity [19], myocardial infarction [20], and hypertension [7, 21]. Studies have also shown a direct involvement of leptin in promoting hypertension-induced vascular hypertrophy [22, 23]. Leptin is synthesized by VSMCs in response to forces that mimic hypertension and, in turn, induces VSMC hypertrophy [22–24]. This hormone exerts a prohypertrophic effect on VSMCs by activating several signaling pathways and transducers, including the MAPK ERK1/2 [23], the RhoA/ROCK pathway [22, 25], and the prohypertrophic transcriptional factors serum response factor (SRF) and GATA-4 [22, 25, 26]. In addition, leptin-induced vascular remodeling has been associated with increased reactive oxygen species (ROS) production in the vascular wall [22]. Hypertension increases ROS production in VSMCs [27, 28], and this is partly mediated by leptin [22]. In turn, ROS induce hypertrophy of VSMCs [29, 30].

As opposed to leptin, APN levels are inversely associated with obesity [31–33], myocardial infarction [34, 35], and hypertension [8, 36]. Moreover, APN supplementation has been shown to be cardioprotective; for instance, APN administration protects against myocardial injury after ischemia-reperfusion and inhibits pressure overload-induced cardiac hypertrophy [37, 38]. To elicit its intracellular effects, APN can bind to three receptors: APN receptor 1 (AdipoR1), APN receptor 2 (AdipoR2), and T-cadherin [39–41]. Knockout mice lacking AdipoR1 and R2 have increased oxidative stress, inflammation, triglyceride content, glucose intolerance, and insulin resistance, indicating the predominant role of these receptors in mediating the metabolic effects of APN [42]. T-cadherin-null mice have exaggerated cardiac hypertrophy in response to pressure overload [43] and impaired revascularization in response to ischemia [44].

Binding of APN to its receptors activates 5′-AMP-activated protein kinase (AMPK) signaling, which plays a role in glucose utilization, insulin sensitivity, and fatty-acid oxidation [45]. AMPK is mainly activated by its upstream enzyme liver kinase B1 (LKB1), which is first activated by getting phosphorylated at its Ser428 residue [46, 47]. In turn, LKB1 activates AMPK by phosphorylating it at the Thr172 residue in the activation loop of the α subunit [46, 48, 49]. AMPK activation has been shown to exert protective actions, such as attenuating VSMC hypertrophy [50], improving endothelial function [51], and reducing agonist-induced blood pressure [52]. APN also stimulates the production of nitric oxide (NO) in endothelial cells by activating endothelial nitric oxide synthase (eNOS) [53, 54], a process that is mediated by AMPK activation [53]. As a result, more NO is produced to induce VSMC relaxation.

The goal of this research was to investigate the molecular mechanisms of hypertension-induced VSMC remodeling and the involvement of leptin and APN in this process. Moreover, APN's potential protective effect against hypertension-induced vascular remodeling and the mechanisms involved were examined. In order to achieve these aims, the rat portal vein (RPV) was mechanically stretched in a well-characterized organ culture model to mimic hypertension [23, 25, 55–57]. The RPV has distinct musculature; its tunica media is composed of an outer, thick layer of longitudinally oriented VSMCs, whereas its inner, thin layer has circularly oriented VSMCs [58, 59]. In order to mimic hypertension, the RPV was stretched with weights that lead to 10-15% stretch, which has been calculated using the force-length relationship [57, 58, 60]. Moreover, the RPV exhibits spontaneous myogenic tone and contractile activity [57, 58], and accordingly, this vessel has been used as an analogue for small precapillary resistance blood vessels [61]. Since physiological concentrations of APN range between 5 and 25 μg/ml [62], 10 μg/ml of exogenous APN was used to examine the potential protective effect of APN on mechanical stretch-induced VSMC hypertrophy and the molecular mechanisms involved, including LKB1-AMPK signaling, ERK1/2 activation, ROS production, and GATA-4 nuclear translocation.

2. Materials and Methods

2.1. Rat Portal Vein Organ Culture. Male Sprague-Dawley rats (200-250 gr) were euthanized using CO_2, as approved by The Animal Care Program and the Institutional Animal Care and Use Committee at the Faculty of Medicine, American University of Beirut. The RPV was dissected out in a sterile environment, placed in an ice-cold N-Hepes buffer solution (400 mM NaCl, 200 mM KCl, 100 mM $MgCl_2$, 100 mM Hepes, 11.5 mM Glucose, and 5% penicillin-streptomycin), stripped of its surrounding adipose and connective tissue, and denuded using forceps. It was then cut longitudinally into two halves. To mechanically stretch the RPV, silver weights of 0.6 grams (stretch the RPV slightly above optimal length) were tied to the end of one RPV strip, while the other was left unstretched and used as a negative control. The RPVs were then transferred to culture media of Dulbecco's Modified Eagle's Medium (DMEM)/F-12 HAM with 5% penicillin-streptomycin and incubated at 37°C, 5% CO_2 in air.

Since physiological concentrations of APN range between 5 and 25 μg/ml [62], 10 μg/ml of exogenous APN (Santa Cruz Biotechnology, California, USA) was used. APN was added to the culture media 1 hour before mechanical stretch was applied or agonists were added. Following incubation, the RPVs were taken out of the incubator and immediately either snap-frozen in liquid nitrogen for protein analysis, weighed, or embedded in frozen blocks and cut cross-sectionally for histological examination.

To measure changes in wet weight, RPVs were weighed before organ culture. They were then blotted gently using a filter paper and weighed after culture, as previously described [57]. To confirm that the changes in weight were due to actual hypertrophy and not just osmosis, dry weight/wet weight ratios were calculated. Dry weight was determined after placing the cultured RPVs at 100°C for 24 hours and

then weighing immediately. The dry weight/wet weight ratio was calculated by the ratio of the dry weight value to the wet weight after culture.

2.2. Immunoblotting. Protein extraction, sodium dodecyl sulfate polyacrylamide gel electrophoresis (SDS-PAGE), and Western blotting were done as previously described [22, 63]. Primary antibodies for APN (sc-26497), leptin (sc-842), p-LKB1 (cell-3482), p-AMPK (cell-2535), p-ERK1/2 (sc-81492), T-ERK1/2 (sc-292838), p-eNOS (sc-12972), actin (sc-1616), and GAPDH (sc-32233) were supplied by Santa Cruz Biotechnology (California, USA) or Cell Signaling Technology (Massachusetts, USA) and were added at 1 : 500 or 1 : 1000 ratio in 5% BSA for 1 hour.

2.3. Immunohistochemistry for APN Expression. To visualize the expression of APN, 5 μm thick cryosections were fixed using freshly prepared 4% paraformaldehyde for 15 minutes, rinsed twice with PBS, and permeabilized using 0.2% Triton X-100 in PBS for 20 minutes. The blocking solution (1% BSA, 0.1% Triton X-100 in PBS) was added for 1 hour to block nonspecific binding. Anti-APN (sc-26497, Santa Cruz Biotechnology, California, USA) primary antibody was then added at 1 : 100 ratio in 1% BSA, 0.05% Tween-20, in PBS and placed overnight at 4°C. The sections were then washed 5 times for 10 minutes each using 0.1% Tween-20 in PBS and then probed for 1 hour in the dark with donkey anti-goat secondary antibody conjugated to CruzFluor 594 (sc-362275, 1 : 250 ratio in 1% BSA, 0.05% Tween-20 in PBS, Santa Cruz Biotechnology, California, USA). Sections were then rinsed 5 times for 10 minutes each with 0.1% Tween-20 in PBS. The mounting media containing the nuclear counterstain 4′,6-diamidino-2-phenylindole (DAPI) (UltraCruz Hard-set Mounting Medium, sc-359850, Santa Cruz Biotechnology, Texas, USA) was then added for 20 minutes in the dark, and images were acquired with a laser scanning confocal microscope (LSM710, Carl Zeiss, Germany). APN positive intensity was quantified using ZEN software (Carl Zeiss, 2012).

2.4. RNA Extraction and Real-Time PCR. RNA extraction and real-time PCR analysis were performed as previously described [23]. The used primers were as follows: APN forward 5′-TCCCTCCACCCAAGGAAACT-3′ and APN reverse 5′-TTGCCAGTGCTGCCGTGATA-3′, AdipoR1 forward 5′-GCTGGCCTTTATGCTGCTCG-3′ and AdipoR1 reverse 5′-TCTAGGCCGTAACGGAATTC-3′, AdipoR2 forward 5′-CCACAACCTTGCTTCATCTA-3′ and AdipoR2 reverse 5′-GATACTGAGGGGTGGCAAAC-3′, T-cadherin forward 5′-TCGGGTCTGTCACTATCAAC-3′ and T-cadherin reverse 5′-TGAGGTCTCAAGCCCATA C-3′, and the housekeeping gene 18S rRNA forward 5′-GTAACCCGTTGAACCCCATT-3′ and 18S rRNA reverse 5′-CCATCCAATCGGTAGTAGCG-3′.

2.5. Protein Synthesis Measurement. Protein synthesis was measured by assessing [^{3}H]-leucine incorporation. RPVs were cultured for 2 days, followed by adding radioactively labelled [^{3}H]-leucine (Activity: 1 μCi/ml; Amersham, Illinois, USA) in the media for an additional day. [^{3}H]-leucine incorporation was measured by liquid scintillation counting, as described previously [57].

2.6. ROS Analysis. RPV sections (5 μm thickness) were stained with dihydroethidium (DHE) (Invitrogen, Oregon, USA) at a concentration of 10 μM in N-Hepes buffer and incubated at 37°C, 5% CO_2, for 30 minutes protected from light. The mounting media containing DAPI (UltraCruz Hard-set Mounting Medium, sc-359850, Santa Cruz Biotechnology, Texas, USA) was then added for 20 minutes in the dark. Images were acquired and DHE fluorescence intensity was quantified using a laser scanning confocal microscope (LSM710, Carl Zeiss, Germany) and ZEN software (Carl Zeiss, 2012).

2.7. Determination of GATA-4 Nuclear Translocation by Immunofluorescence. Rat aortic smooth muscle cells (RASMCs) were cultured ($50 \times 10^3 - 100 \times 10^3$ cells/ml) in complete media (DMEM (1 g/l glucose), 10% fetal bovine serum, 1% penicillin-streptomycin, 2 mM Glutamine, 20 mM Hepes) and incubated at 37°C, 5% CO_2, for 3 days, followed by serum-starvation. The next day, the RASMCs were treated with exogenous APN (10 μg/ml) and leptin (3.1 nM; equivalent to approximately 50 ng/ml). When the treatment was over, the media was aspirated and the cells were fixed with freshly prepared 4% paraformaldehyde for 15 minutes. Permeabilization was performed using 0.2% Triton X-100 for 30 minutes and blocking was done using 1% BSA, 0.1% Triton X-100, in PBS for 1 hour. The primary antibody for GATA-4 (sc-25310, Santa Cruz Biotechnology, California, USA) was added at 1 : 100 ratio in 1% BSA, 0.05% Tween-20, in PBS overnight at 4°C. Washing then followed, where 0.1% Tween-20 in PBS was added 5 times for 10 minutes each. The secondary antibody was CruzFluor 488-conjugated goat anti-mouse antibody (sc-362257, Santa Cruz Biotechnology, California, USA) used at 1 : 250 ratio in 1% BSA, 0.05% Tween-20, in PBS, which was added for 1 hour in the dark. The cells were rinsed again 5 times for 10 minutes each using 0.1% Tween-20 in PBS. To stain actin, phalloidin (100 nM; Acti-stain 555 phalloidin, Cytoskeleton, Colorado, USA) was added for 20 minutes followed by rinsing twice with 0.1% Tween-20 in PBS. Finally, the mounting media containing DAPI (UltraCruz Hard-set Mounting Medium, sc-359850, Santa Cruz Biotechnology, Texas, USA) was added for 20 minutes in the dark. Images were acquired using the Zeiss Axio Observer Z1 microscope (Carl Zeiss, Germany), and data were analyzed using ZEN software (Carl Zeiss, 2012). The purity of the cells as RASMCs was confirmed by immunostaining for alpha-smooth muscle actin (α-SMA).

2.8. Statistical Analysis. The results are presented as fold change with respect to the negative control, which was unstretched or untreated. The statistical analysis software SigmaStat (Systat Software, California, USA) was used to compute the mean and standard error of the mean (SEM) for each group. To compare 2 groups, *t*-test was used, while

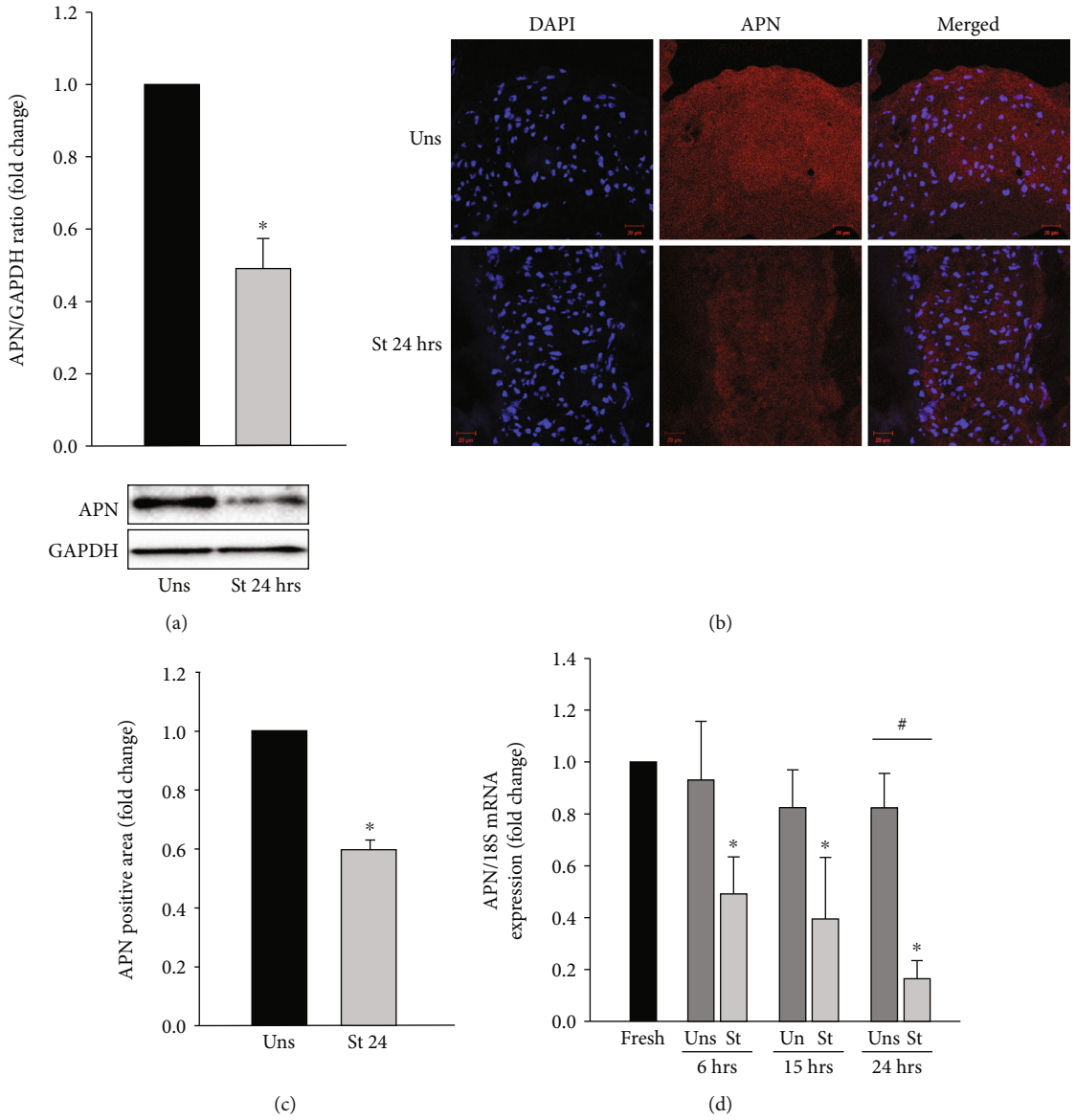

Figure 1: Mechanical stretch-induced downregulation of APN protein and mRNA expression in VSMCs. RPVs were stretched (St) for 24 hours or left unstretched (Uns). (a) APN protein expression was evaluated by Western blot and normalized to the unstretched RPVs. (b) Cryosections of the RPV wall were probed with primary anti-APN antibody and secondary antibody to mark APN (red). DAPI was used to stain the nuclei blue *(40x)*. (c) APN fluorescence intensity was measured using ZEN software and normalized to the unstretched RPVs. $^{*}p < 0.05$ versus unstretched. (d) Real-time PCR analysis was performed to examine APN mRNA expression in stretched RPVs for 6, 15, or 24 hours as well as unstretched and fresh RPVs. Data were normalized to the fresh RPVs. Results are represented as mean ± SEM. $n = 4 - 8$. $^{*}p < 0.05$ versus fresh. $^{\#}p < 0.05$ versus unstretched.

one-way analysis of variance (ANOVA) was used to compare 3 or more groups. The data are presented as mean ± SEM for each group in graphs using the graphing software SigmaPlot (Systat Software, California, USA). The difference between groups was considered to be statistically significant if p values were less than 0.05 (statistical significance: $p < 0.05$).

3. Results

3.1. Mechanical Stretch Reduces APN Expression in VSMCs. Hypertension is associated with reduced circulating levels of APN [8], which is mainly known to be produced by adipocytes [11, 15, 64]. To our knowledge, whether VSMCs produce APN and whether hypertension dysregulates its potential production in VSMCs have not been fully elucidated yet. To investigate this, RPVs were either mechanically stretched or left unstretched for 24 hours, followed by Western blot analysis. As shown in Figure 1(a), mechanically stretching the RPV for 24 hours significantly decreased APN expression compared to the control.

The ability of VSMCs to produce APN and the effect of mechanical stretch on APN expression in VSMCs were further examined by immunofluorescence. RPVs were stretched for 24 hours or left unstretched, cut into 5 μm thick

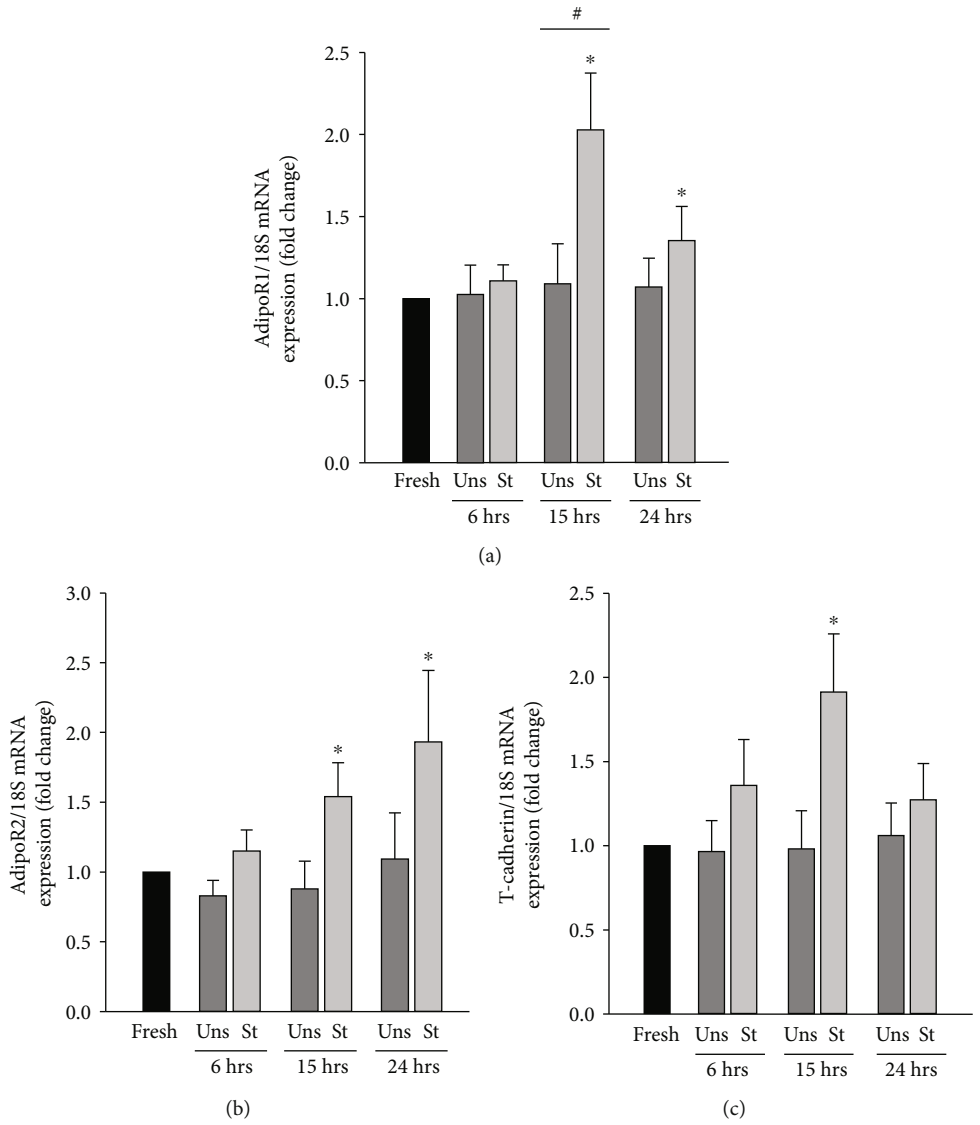

Figure 2: Mechanical stretch-induced increase in the mRNA expression of the APN receptors in VSMCs. RPVs were mechanically stretched (St) for 6, 15, or 24 hours or left unstretched (Uns), followed by real-time PCR analysis to examine AdipoR1 (a), AdipoR2 (b), and T-cadherin (c) mRNA expression. Results are represented as mean ± SEM and normalized to fresh RPVs. $n = 5 - 9$. $^{*}p < 0.05$ versus fresh. $^{\#}p < 0.05$ versus unstretched.

cryosections, and probed with anti-APN antibody to mark APN. DAPI was used to stain the nuclei. APN positive intensity was measured using ZEN software (Carl Zeiss, 2012). In agreement with the Western blot findings, APN expression in the mechanically stretched RPVs was significantly reduced compared to the unstretched RPVs (Figures 1(b) and 1(c)).

To examine whether the decrease in intracellular APN levels in response to mechanical stretch occurred at the transcriptional level, real-time PCR analysis was done to examine the effect of stretch on APN mRNA expression in VSMCs. RPVs were mechanically stretched for 6, 15, or 24 hours, and their APN mRNA expression levels were compared to those of unstretched RPVs for 6, 15, or 24 hours and fresh RPVs. As shown in Figure 1(d), mechanical stretch for 6 hours caused a significant decrease in APN mRNA expression compared to fresh RPVs. Stretch for 15 hours caused a more pronounced and significant decrease in APN mRNA expression, while mechanically stretching the RPV for 24 hours led to an even more pronounced reduction in APN mRNA expression compared to fresh and unstretched RPVs for 24 hours (Figure 1(d)).

3.2. Mechanical Stretch Increases the APN Receptors' mRNA Expression in VSMCs. Mechanical stretch downregulates the expression of APN in VSMCs (Figure 1), but whether it affects the expression of its receptors remains unclear. To elicit its intracellular effects, APN binds to its receptors AdipoR1, AdipoR2, and T-cadherin [39–41]. To investigate whether mechanical stretch affects the expression of these receptors, real-time PCR analysis was performed to study their mRNA expression levels in RPVs stretched for 6, 15, or 24 hours. As shown in Figure 2(a), AdipoR1 mRNA

expression was not affected by mechanical stretch for 6 hours. Stretching the RPV for 15 hours, however, induced a significant increase in AdipoR1 mRNA expression as compared to fresh RPVs and unstretched RPVs for 15 hours (Figure 2(a)). Stretching the vessels for 24 hours also induced a significant upregulation in AdipoR1 mRNA expression compared to fresh RPVs (Figure 2(a)). These data indicate that mechanical stretch upregulates AdipoR1 gene transcription with a peak at 15 hours of stretch.

Stretching the RPVs for either 15 hours or 24 hours significantly upregulated AdipoR2 mRNA expression compared to fresh RPVs (Figure 2(b)), indicating that mechanical stretch also promotes an increase in AdipoR2 gene transcription. Figure 2(c) shows that mechanically stretching the RPV for 6 hours slightly increased T-cadherin mRNA expression as compared to fresh and unstretched RPVs for 6 hours. In response to 15 hours of stretch, T-cadherin mRNA expression level increased significantly compared to fresh RPVs, while mechanical stretch for 24 hours did not significantly affect T-cadherin mRNA expression (Figure 2(c)). Thus, mechanical stretch upregulates T-cadherin gene expression after 15 hours in VSMCs. Collectively, these data indicate that mechanical stretch, which downregulates the expression of APN, induces an upregulation in the expression of the APN receptors, perhaps in an attempt to compensate for the reduced APN levels.

3.3. Mechanical Stretch Reduces the APN/Leptin Ratio in VSMCs. The plasma leptin/APN ratio is emerging as a marker for metabolic syndrome and insulin resistance [65, 66]. To study the effect of mechanical stretch on the ratio of APN/-leptin expression in VSMCs, RPVs were stretched for 24 hours followed by Western blot analysis to detect and measure endogenous APN and leptin levels. Figure 3 reveals that the ratio of APN/leptin was significantly decreased by mechanical stretch for 24 hours, indicating that the hypertensive state is characterized by a low APN/leptin ratio not only in the plasma but also within VSMCs.

3.4. APN Attenuates Mechanical Stretch-Induced VSMC Hypertrophy. We have previously shown that both mechanical stretch and leptin increase VSMC hypertrophy [22, 23, 57]. On the other hand, APN has been reported as a cardioprotective protein that attenuates pressure overload-induced cardiac hypertrophy and protects against myocardial injury after ischemia-reperfusion [37, 38]. However, it is unclear whether APN exerts a vascular protective effect against hypertension-induced vascular hypertrophy. In order to examine this, RPVs were cultured mechanically stretched for 3 days or left unstretched with or without APN (10 μg/ml), and changes in wet weight and protein synthesis (using [^{3}H]-leucine incorporation) were measured [57]. 10 μg/ml of APN was used because this concentration belongs to the physiological range of APN, which is 5 to 25 μg/ml [62].

As shown in Figures 4(a) and 4(b), mechanically stretching RPVs for 3 days significantly increased their wet weight and protein synthesis compared to unstretched RPVs. Treating unstretched RPVs with exogenous APN (10 μg/ml) had no effect on wet weight change (Figure 4(a)) or protein synthesis (Figure 4(b)), whereas treating mechanically stretched RPVs with APN significantly attenuated the stretch-induced increase in wet weight (Figure 4(a)) and protein synthesis (Figure 4(b)). These results indicate that APN exerts a protective effect on the vasculature under mechanical stretch by inducing an antihypertrophic effect on VSMCs. The ratio of dry weight to wet weight was also assessed in order to examine the possibility of water retention or osmosis as a reason for hypertrophy. The different groups did not have significant changes in dry weight/wet weight ratios, indicating that hypertrophy is not due to osmosis, but rather to protein synthesis.

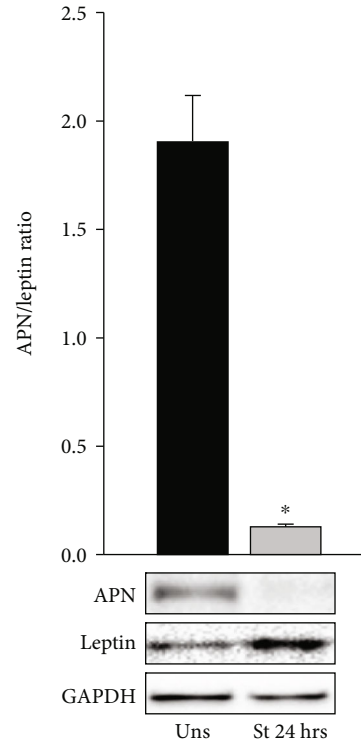

Figure 3: Mechanical stretch-induced reduction in the APN/leptin ratio in VSMCs. RPVs were mechanically stretched (St) for 24 hours or left unstretched (Uns), followed by Western blot analysis to study endogenous protein expression of APN and leptin in VSMCs. Results are represented as mean ± SEM. $n = 4$. $^*p < 0.05$ versus unstretched.

3.5. APN Increases LKB1 and AMPK Phosphorylation in Mechanically Stretched RPVs. AMPK and its upstream kinase LKB1 exert protective cellular effects in diabetes and are activated by diabetic treatments like metformin [47, 51]. Moreover, AMPK activation has been shown to attenuate VSMC contractility, reduce blood pressure, and decrease VSMC hypertrophy [50, 52]. To study the effect of mechanical stretch on AMPK and LKB1 activation in VSMCs, RPVs were stretched for 10 minutes followed by Western blot analysis. As shown in Figures 5(a) and 5(b), mechanical stretch significantly reduced both LKB1 and AMPK phosphorylation after 10 minutes, indicating that the detrimental effects of stretch on the vasculature are likely to be mediated by

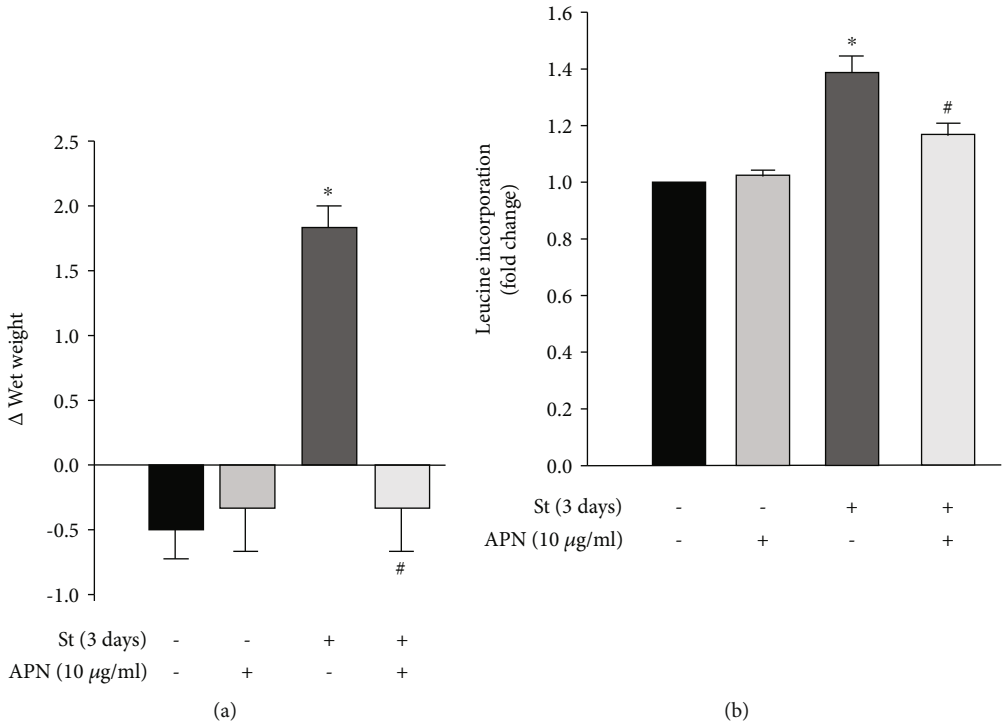

Figure 4: Exogenous APN-induced attenuation of mechanical stretch-mediated VSMC hypertrophy. RPVs were mechanically stretched (St) for 3 days or left unstretched with or without APN (10 μg/ml). Changes in wet weight (a) and [^{3}H]-leucine incorporation (b) were measured as indicators for hypertrophy. Results are represented as mean ± SEM. $n = 6$. $^*p < 0.05$ versus unstretched. $^\#p < 0.05$ versus stretched.

reduced activation of LKB1 and AMPK and thus an attenuation of their protective effects.

To examine whether APN's observed antihypertrophic effect on VSMCs in response to mechanical stretch is mediated by LKB1-AMPK signaling, RPVs were treated with APN (10 μg/ml) and stretched for 10 minutes. Western blot analysis was then performed to assess LKB1 and AMPK phosphorylation. Exogenous APN significantly increased LKB1 and AMPK phosphorylation in mechanically stretched RPVs compared to the untreated, stretched RPVs (Figures 5(a) and 5(b)). Thus, APN exerts a protective effect on VSMCs by activating LKB1-AMPK signaling under mechanical stretch. It is important to note that AMPK phosphorylation, although significantly increased by APN in stretched RPVs, remained significantly lower than unstretched RPVs, indicating that perhaps other signaling pathways activated by mechanical stretch are causing AMPK dephosphorylation.

3.6. APN Increases eNOS Activation in Mechanically Stretched RPVs. When activated by phosphorylation at the Ser1177 residue, eNOS exerts a protective role on the vasculature by producing NO, which promotes vasorelaxation and exerts antihypertrophic effects on VSMCs [67, 68]. However, hypertension is associated with both hypertrophy and an impaired vasorelaxation response [23, 69, 70]. To examine the effect of mechanical stretch on eNOS phosphorylation at Ser1177 (which marks its activation), RPVs were stretched for 10 minutes followed by Western blot using a specific antibody that recognizes the phosphate group at Ser1177. Mechanically stretching the RPVs for 10 minutes significantly decreased eNOS phosphorylation compared to unstretched RPVs (Figure 6(a)), suggesting that the harmful effects of stretch are mediated by reduced eNOS activation.

To examine whether eNOS is involved in APN's observed antihypertrophic effect on mechanical stretch-induced VSMC hypertrophy, RPVs were treated with exogenous APN (10 μg/ml) and either stretched for 10 minutes or left unstretched. As shown in Figure 6(a), APN increased eNOS activation in mechanically stretched vessels compared to untreated stretched RPVs. APN treatment on unstretched RPVs also significantly increased eNOS phosphorylation compared to stretched RPVs. These findings suggest that APN's protective effect against stretch-induced VSMC remodeling is mediated by activating eNOS.

3.7. APN Inhibits Mechanical Stretch-Induced ERK1/2 Phosphorylation in VSMCs. One of the mechanisms by which mechanical stretch leads to VSMC hypertrophy is by inducing ERK1/2 phosphorylation and subsequent activation [23, 56, 57, 60]. To investigate whether APN induces its antihypertrophic effect on mechanically stretched RPVs by affecting ERK1/2 signaling, RPVs were treated with exogenous APN (10 μg/ml) and stretched for 10 minutes, followed by Western blot analysis to examine ERK1/2 phosphorylation. Mechanically stretching the RPVs for 10 minutes significantly increased ERK1/2 phosphorylation compared to unstretched RPVs (Figure 6(b)). Treating unstretched RPVs with exogenous APN (10 μg/ml) had no effect on ERK1/2 activation (Figure 6(b)). Treating stretched RPVs with 10 μg/ml of APN significantly reduced mechanical stretch-induced ERK1/2 phosphorylation (Figure 6(b)). Therefore, one of the mechanisms by which APN exerts its

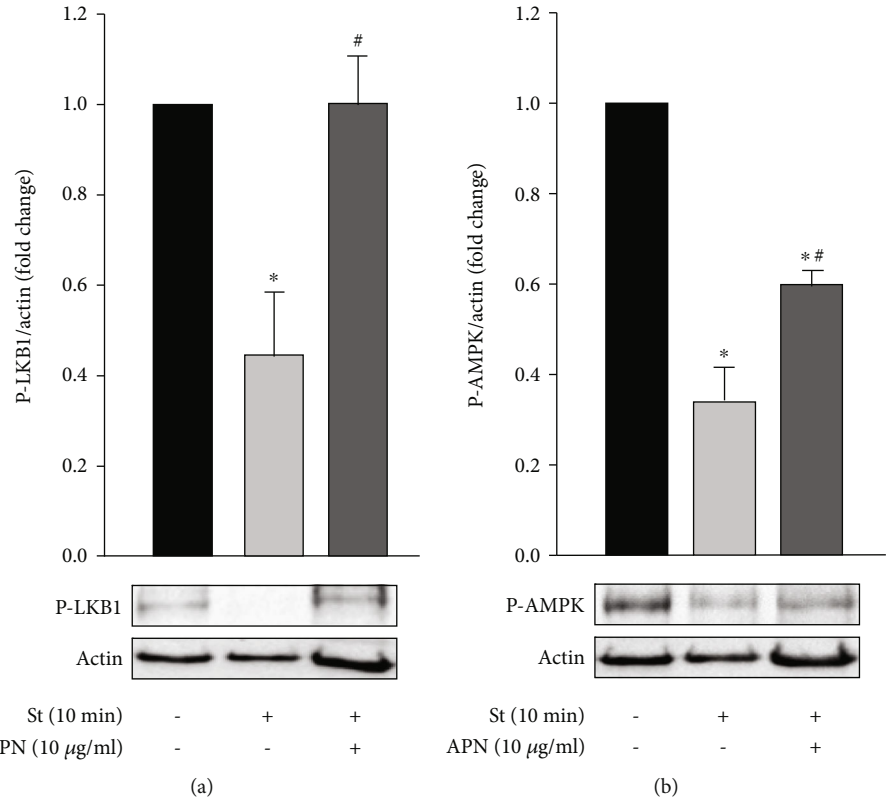

Figure 5: Exogenous APN-mediated increase in mechanical stretch-induced LKB1 and AMPK phosphorylation in VSMCs. RPVs were stretched for 10 minutes (St) and treated with APN (10 μg/ml), followed by Western blot analysis to study LKB1 (a) and AMPK (b) phosphorylation. Data are represented as mean ± SEM and normalized to the unstretched RPVs. $n = 4 - 7$. $^{*}p < 0.05$ versus unstretched. $^{\#}p < 0.05$ versus stretched.

antihypertrophic effect on mechanical stretch-induced VSMC hypertrophy is by inhibiting ERK1/2.

3.8. APN Attenuates Mechanical Stretch-Induced ROS Formation in VSMCs. We have previously studied the effect of mechanical stretch, mimicking hypertension, on ROS production in VSMCs [22]. Mechanical stretch increases ROS, which in turn promote vascular remodeling and induce hypertrophy [29, 30]. To investigate the effect of APN on stretch-induced ROS production in VSMCs, RPVs were stretched for 1 hour and treated with APN (10 μg/ml), and DHE was used to detect ROS. As shown in Figure 7, unstretched RPVs that were treated with APN (10 μg/ml) did not exhibit any marked changes in ROS production. Mechanical stretch significantly increased ROS production after 1 hour, while treating stretched RPVs with 10 μg/ml of APN significantly decreased ROS generation (Figures 7(a) and 7(b)), indicating that APN's antihypertrophic effect on VSMCs during mechanical stretch is likely mediated by a reduction in ROS production.

3.9. APN Attenuates Leptin-Induced GATA-4 Nuclear Translocation in VSMCs. Exogenous leptin activates translocation of the prohypertrophic transcription factor GATA-4 from the cytoplasm to the nucleus in RASMCs [22], indicating that leptin-induced GATA-4 nuclear translocation is likely a prominent mechanism by which leptin induces VSMC hypertrophy. To study whether GATA-4 is involved in the pathway of APN-induced attenuation of VSMC hypertrophy, RASMCs were pretreated with APN (10 μg/ml), followed by leptin (3.1 nM) addition for 1 hour. Immunofluorescence was then performed to detect GATA-4 by using anti-GATA-4 antibody and secondary antibody conjugated to CruzFluor 488. As shown in Figure 8, exogenous leptin for 1 hour markedly increased GATA-4 nuclear translocation, whereas APN significantly attenuated leptin-induced GATA-4 nuclear translocation. These findings indicate that APN most likely inhibits VSMC hypertrophy by attenuating GATA-4 activation.

4. Discussion

The major findings in this study are as follows: (1) VSMCs synthesize APN and express its receptors. (2) Mechanical stretch, which mimics hypertension, decreases APN expression and increases leptin synthesis in VSMCs, thereby decreasing the APN/leptin ratio in VSMCs. (3) APN exerts an antihypertrophic effect on mechanical stretch-induced VSMC hypertrophy. (4) APN attenuates mechanical stretch-induced vascular remodeling by inhibiting ERK1/2 phosphorylation and ROS production and by increasing LKB1, AMPK, and eNOS phosphorylation. (5) APN attenuates leptin-induced GATA-4 nuclear translocation in VSMCs.

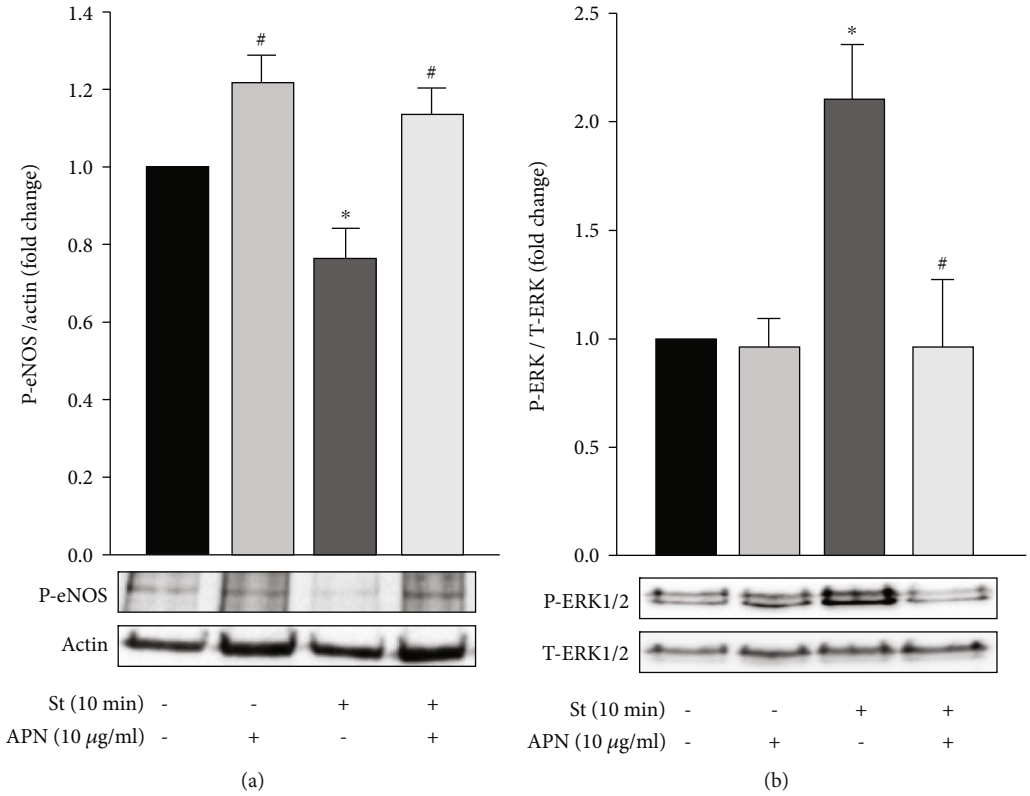

Figure 6: APN-mediated changes in mechanical stretch-induced eNOS and ERK1/2 phosphorylation in VSMCs. RPVs were stretched for 10 minutes (St) or left unstretched and treated with exogenous APN (10 μg/ml), followed by Western blot analysis to detect eNOS phosphorylation (a) and ERK1/2 phosphorylation (b). Results are represented as mean ± SEM and normalized to the unstretched RPVs. $n = 4 - 12$. $^{*}p < 0.05$ versus unstretched. $^{\#}p < 0.05$ versus stretched.

The force exerted by blood pressure on the vascular wall continuously exposes it to mechanical stretch. The higher the blood pressure, the higher the force of stretch, leading to vascular remodeling and hypertrophy [23, 70, 71]. Although it is a compensatory mechanism to hypertension, vascular hypertrophy is detrimental because it structurally and functionally changes the blood vessels, leading to reduced tissue perfusion and further inducing hypertension [72]. In order to study mechanical stretch-induced vascular hypertrophy, RPV organ culture was used as a well-established model to mimic hypertension [23, 25, 56, 57]. Being the bulk of the RPV wall, the pronounced longitudinal muscular coat makes it an ideal vessel to stretch by weight loading at a force that leads to 10-15% stretch, which has been calculated using the force-length relationship [57, 58, 60]. Mechanical stretch preserves the differentiated, contractile phenotype of the VSMCs in this *ex vivo* model of organ culture, as evidenced by the increased force of contraction and preservation of SM22 expression, a differentiation marker of VSMCs [56, 57, 73]. Moreover, this pre- and postcapillary blood vessel has spontaneous myogenic activity and has been used as an analogue for small precapillary resistance blood vessels [57, 58, 61].

Upon their discovery and for some time, leptin and APN were believed to be almost exclusively produced by adipocytes [9–15, 74]. We have shown that VSMCs produce the leptin protein and that its production is significantly upregulated by mimicking hypertension [22]. However, little is known about whether VSMCs synthesize APN and whether hypertension affects its production at the site of VSMCs. We began our research by investigating these two questions and found that APN is indeed produced by VSMCs and that the VSMC synthesis of APN is decreased by mimicking hypertension (Figure 1). When RPVs were stretched for 24 hours, APN expression in the VSMCs was significantly downregulated (Figure 1). Real-time PCR analysis was also performed to examine the effect of 6, 15, and 24 hours of mechanical stretch on APN mRNA expression and showed that mechanical stretch decreased APN mRNA expression in a time-dependent manner (Figure 1(d)). Thus, APN is indeed expressed in VSMCs, not only in adipocytes, and mechanical stretch downregulates its expression at both the gene and protein expression levels. Using real-time PCR analysis, we also examined the mRNA expression of the APN receptors AdipoR1, AdipoR2, and T-cadherin and found that they are all expressed in VSMCs. Mechanical stretch increased the mRNA expression of these receptors, perhaps as a feedback mechanism to compensate for the reduced levels of APN in the VSMCs as well as in the circulation during hypertension (Figure 2).

Although our findings are consistent with the prior knowledge that circulating plasma APN levels are decreased [6, 8] and leptin levels are increased [7] in hypertensive patients, their dysregulated synthesis and expression by VSMCs in hypertension proposes a new mechanism and

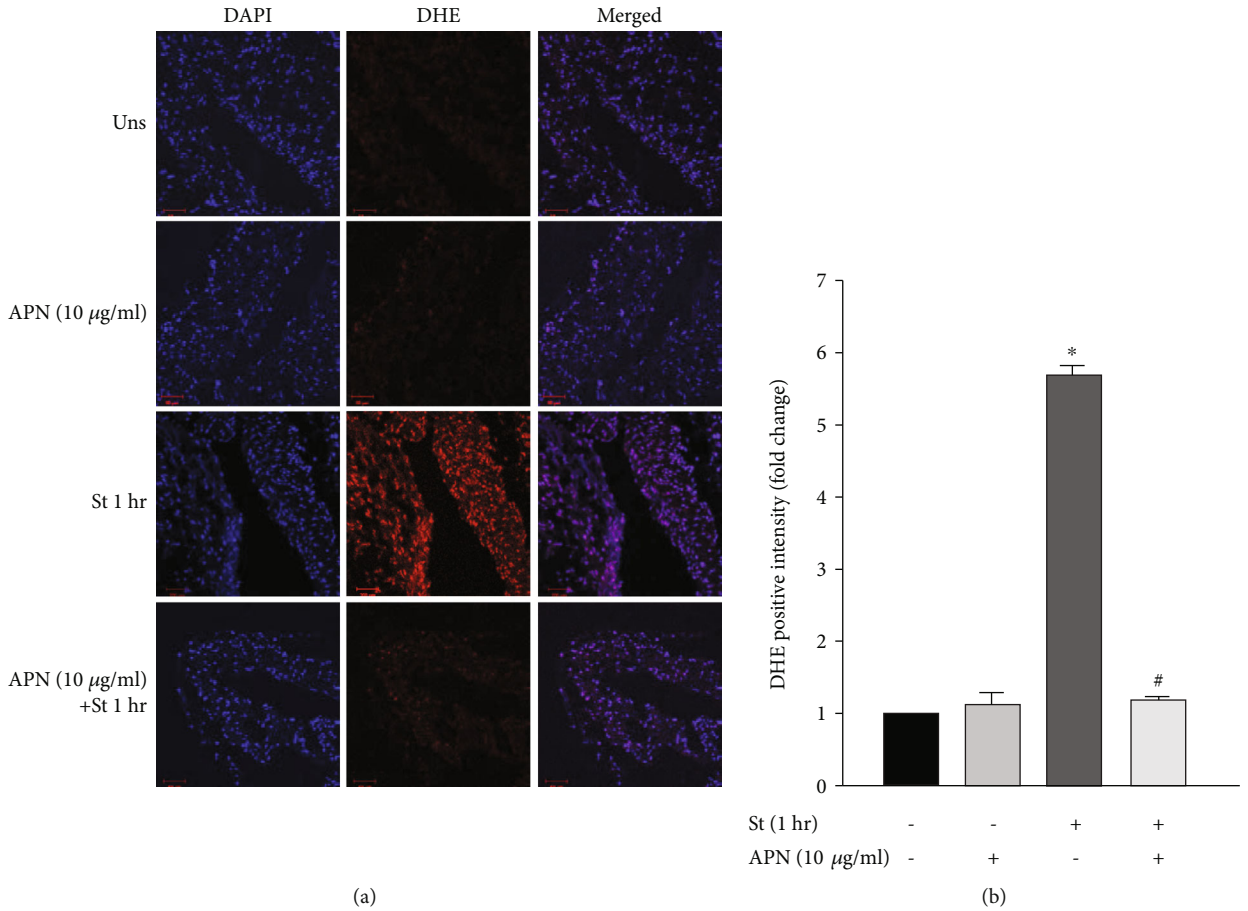

Figure 7: Exogenous APN-induced reduction in mechanical stretch-mediated ROS production in VSMCs. RPVs were unstretched (Uns) or stretched (St) for 1 hour and treated with 10 μg/ml of APN. (a) Cryosections of the RPV wall were stained with DHE to detect ROS (red), and DAPI was used to detect the nuclei (blue) *(40x)*. (b) DHE fluorescence intensity was measured using ZEN software. Data are represented as mean ± SEM and normalized to the unstretched RPVs. $n = 4$. $^{*}p < 0.05$ versus unstretched. $^{\#}p < 0.05$ versus stretched.

possible explanation for this process, as opposed to just their production by adipocytes. The APN/leptin ratio in VSMCs was drastically reduced by mechanical stretch compared to unstretched vessels (Figure 3). The ratio of circulating APN/-leptin is emerging as a marker for metabolic syndrome [65, 66], which includes hypertension, and our results indicate that VSMCs can now be viewed as contributors to this change in ratio.

Adiponectin supplementation has been shown to inhibit pressure overload-induced cardiac hypertrophy and protect against myocardial injury after ischemia-reperfusion [37, 38]. Zeidan et al. have previously shown that mechanical stretch and leptin, individually and together, significantly induce VSMC hypertrophy [23]. However, whether APN exerts a vascular protective or harmful effect on hypertension-induced VSMC hypertrophy has not been fully elucidated yet. In order to examine this, we treated RPVs with 10 μg/ml of APN, which belongs to its normal physiological range [62].

The adiponectin used in our experiments is the purified recombinant murine globular domain of adiponectin. Being the larger portion of full-length adiponectin, this globular domain has been shown to exhibit greater potency than full-length adiponectin [75–79], which is why we decided to conduct our study using this form. However, the next step of our experimental investigation will focus on using the metabolically active high molecular weight oligomer and compare its effect with the low molecular weight trimer and the medium molecular weight hexamer in order to decipher which form of adiponectin is most potent in attenuating hypertension-induced vascular remodeling.

Hypertrophy was evaluated by the hypertrophic markers wet weight change and [^{3}H]-leucine incorporation. APN significantly attenuated mechanical stretch-induced RPV hypertrophy by decreasing both weight change and protein synthesis in stretched vessels (Figure 4). Thus, APN exerts a protective, antihypertrophic effect against mechanical stretch-induced VSMC hypertrophy.

APN activates AMPK in several cell types, including ECs, VSMCs, and skeletal muscle cells [80, 81]. AMPK has been shown to exert several protective effects, such as attenuating VSMC hypertrophy [50], reducing blood pressure [52], and improving endothelial function [51]. We were interested in studying whether AMPK and its upstream kinase LKB1 were involved in the mechanotransduction of mechanical stretch-induced vascular remodeling. RPVs were stretched for 10 minutes, which corresponds to a time-point of significant

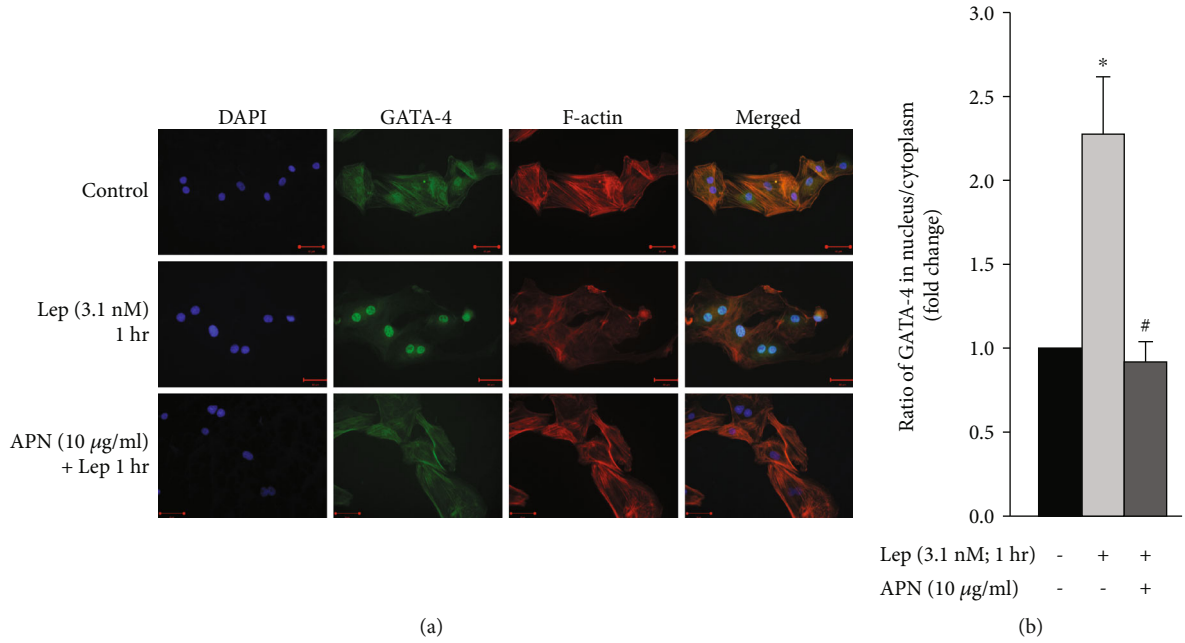

Figure 8: APN-mediated attenuation of leptin-induced GATA-4 nuclear translocation. RASMCs were treated with leptin (Lep; 3.1 nM) for 1 hour with or without APN (10 μg/ml). (a) GATA-4 was visualized using anti-GATA-4 primary antibody and secondary antibody conjugated to CruzFluor 488 (green; second panel). DAPI was used to stain the nuclei blue (first panel), while Acti-stain 555 phalloidin stained F-actin (red; third panel). The overlay of DAPI, GATA-4, and F-actin is shown in the right panel (merged) *(40x)*. (b) GATA-4 fluorescence intensity was measured using ZEN software, and the ratio of GATA-4 in the nucleus/cytoplasm was assessed. Results are represented as mean ± SEM. $n = 4$. $^{*}p < 0.05$ versus untreated. $^{\#}p < 0.05$ versus leptin treatment.

LKB1 and AMPK phosphorylation in VSMCs [50]. To detect activation of LKB1 and AMPK, specific antibodies were used that mark their activating phosphorylation sites at Ser428 and Thr172, respectively. Mechanically stretching the RPV significantly reduced LKB1 and AMPK phosphorylation (Figure 5), adding LKB1-AMPK signaling to the pathways involved in stretch-induced VSMC remodeling.

When RPVs were treated with APN (10 μg/ml) and mechanically stretched, LKB1 and AMPK phosphorylation was rescued (Figure 5), pointing towards a potential mechanism by which this protective hormone attenuates mechanical stretch-induced VSMC hypertrophy. In the APN-treated stretched vessels, LKB1 phosphorylation increased back to control (untreated and unstretched) levels, but AMPK phosphorylation, although significantly higher than that in untreated stretched RPVs, remained significantly lower than control levels (Figure 5). This may be due to other signaling pathways that are activated by mechanical stretch that APN does not attenuate. Future studies will investigate this notion. Moreover, it is particularly interesting to see that APN increased LKB1 activation in VSMCs, because, to our knowledge, the effect of APN on LKB1 activation has not been studied in VSMCs.

Downstream to AMPK activation is the phosphorylation and subsequent activation of the enzyme eNOS in ECs and cardiomyocytes [82–84]. When eNOS is activated by phosphorylation at its Ser1177 residue [85, 86], it produces NO which exerts protective actions on the vasculature that include antihypertrophic effects in VSMCs [63, 67, 68]. Moreover, APN has been shown to attenuate angiotensin II-induced contractility in a NO-dependent manner [63]. Although it was thought that VSMCs lack eNOS, studies have shown that eNOS is also expressed in VSMCs [87, 88], and our data has shown that mechanical stretch reduces eNOS phosphorylation at Ser1177 (Figure 6(a)). This is consistent with the knowledge that hypertension is associated with an impaired vasorelaxation response [69]. Moreover, when RPVs were treated with APN (10 μg/ml), eNOS phosphorylation increased in both unstretched and stretched RPVs (Figure 6(a)), indicating that APN's protective antihypertrophic effect most likely occurs via the LKB1-AMPK-eNOS signaling axis in VSMCs.

NO has been shown to exert protective effects against vascular hypertrophy by inhibiting ERK1/2 activation in VSMCs [68], and research has shown that activated ERK1/2 itself mediates mechanical stretch-induced VSMC hypertrophy [23, 56, 57, 60]. In our study, mechanical stretch for 10 minutes (a time point of significant ERK1/2 phosphorylation [23, 29]) significantly increased ERK1/2 phosphorylation (Figure 6(b)), indicating a mechanism by which mechanical stretch induces VSMC hypertrophy. When stretched RPVs were treated with 5 μg/ml of APN, ERK1/2 phosphorylation decreased, but this was not statistically significant (data not shown). When the concentration of APN was increased to 10 μg/ml, which still belongs to the lower range of normal physiological APN concentration, ERK1/2 phosphorylation was significantly reduced in mechanically stretched RPVs compared to untreated stretched RPVs (Figure 6(b)). Thus, APN exerts its antihypertrophic effects on VSMCs by reducing ERK1/2 activation.

Mechanical stretch-induced vascular remodeling has been associated with increased ROS production in the vascular wall [22]. Vessels exposed to hypertension produce excessive levels of ROS [28], which in turn promote vascular hypertrophy [29, 30]. To investigate whether ROS production belongs to the mechanism of APN-induced attenuation of VSMC remodeling, RPVs were treated with APN and mechanically stretched for 1 hour, a time-point of significant ROS production in response to stretch [22]. Treatment with 5 μg/ml of APN significantly reduced mechanical stretch-induced ROS formation (data not shown), while 10 μg/ml of APN even further reduced ROS generation (Figure 7). Thus, APN exerts a protective effect on VSMC remodeling via reduction of mechanical stretch-induced ROS production, indicating the potential for APN as an anti-oxidant in the vasculature during hypertension. Interestingly, mechanical stretch increases the expression of leptin protein, which has a pro-oxidative effect [22] but decreases that of APN, which has an anti-oxidative effect. Whether the observed increase in ROS production in the RPV was directly induced by the upregulation of leptin and downregulation of APN has not been elucidated yet. Future studies will aim at examining this.

GATA-4 is a transcription factor that promotes cardiac hypertrophy by translocating to the nucleus and activating hypertrophic gene expression [26, 89, 90]. Research by Zeidan et al. has shown that exogenous leptin (3.1 nM) activates GATA-4 in cardiomyocytes [91], a mechanism by which leptin induces cardiomyocyte hypertrophy. In VSMCs, exogenous leptin (3.1 nM), which also induces VSMC hypertrophy [22, 23], activates GATA-4 nuclear translocation in a time-dependent manner and markedly after 1 hour [22]. In this study, we investigated whether GATA-4 is involved in the molecular mechanisms of APN-induced attenuation of VSMC hypertrophy and found that exogenous APN (10 μg/ml) significantly reduced leptin-induced GATA-4 nuclear translocation in RASMCs (Figure 8). Thus, the mechanism of leptin-induced vascular hypertrophy via GATA-4 nuclear translocation is inhibited by APN in VSMCs.

5. Conclusion

Our study identifies molecular mechanisms involved in mechanical stretch-induced vascular remodeling and the role of APN and leptin in this process. It also provides evidence of APN's important protective effect against VSMC remodeling during hypertension. APN attenuates hypertrophy, ERK1/2 phosphorylation, ROS production, and GATA-4 nuclear translocation in VSMCs. It also increases the activation of the protective enzymes LKB1, AMPK, and eNOS in mechanically stretched RPVs. Hence, APN supplementation, upregulating its endogenous production, or using an agonist that mimics its effects provide a promising potential therapeutic strategy in attenuating the detrimental vascular effects of hypertension.

Data Availability

The data used to support the findings of this study are available from the corresponding author upon request.

Conflicts of Interest

The authors declare that the research was conducted in the absence of any commercial or financial relationships that could be construed as a potential conflict of interest.

Acknowledgments

This work was supported by the Medical Practice Plan (MPP), Faculty of Medicine at AUB to AZ, the National Council for Scientific Research of Lebanon (CNRS-L) to CMG, and the graduate teaching/research assistantship support from Qatar University to SA. The publication of this article was funded by the Qatar National Library.

References

[1] O. A. Carretero and S. Oparil, "Essential hypertension. Part I: definition and etiology," *Circulation*, vol. 101, no. 3, pp. 329–335, 2000.

[2] J. W. Levenson, P. J. Skerrett, and J. M. Gaziano, "Reducing the global burden of cardiovascular disease: the role of risk factors," *Preventive Cardiology*, vol. 5, no. 4, pp. 188–199, 2002.

[3] C. Rosendorff, "Vascular hypertrophy in hypertension: role of the renin-angiotensin system," *Mount Sinai Journal of Medicine*, vol. 65, no. 2, pp. 108–117, 1998.

[4] R. P. Lifton, A. G. Gharavi, and D. S. Geller, "Molecular mechanisms of human hypertension," *Cell*, vol. 104, no. 4, pp. 545–556, 2001.

[5] K. G. Shyu, "Cellular and molecular effects of mechanical stretch on vascular cells and cardiac myocytes," *Clinical Science*, vol. 116, no. 5, pp. 377–389, 2009.

[6] M. Adamczak, A. Wiecek, T. Funahashi, J. Chudek, F. Kokot, and Y. Matsuzawa, "Decreased plasma adiponectin concentration in patients with essential hypertension," *American Journal of Hypertension*, vol. 16, no. 1, pp. 72–75, 2003.

[7] C. de Haro Moraes, V. N. Figueiredo, A. P. de Faria et al., "High-circulating leptin levels are associated with increased blood pressure in uncontrolled resistant hypertension," *Journal of Human Hypertension*, vol. 27, no. 4, pp. 225–230, 2013.

[8] D. H. Kim, C. Kim, E. L. Ding, M. K. Townsend, and L. A. Lipsitz, "Adiponectin levels and the risk of hypertension: a systematic review and meta-analysis," *Hypertension*, vol. 62, no. 1, pp. 27–32, 2013.

[9] E. Hu, P. Liang, and B. M. Spiegelman, "AdipoQ is a novel adipose-specific gene dysregulated in obesity," *The Journal of Biological Chemistry*, vol. 271, no. 18, pp. 10697–10703, 1996.

[10] P. A. Kern, G. B. Di Gregorio, T. Lu, N. Rassouli, and G. Ranganathan, "Adiponectin expression from human adipose tissue: relation to obesity, insulin resistance, and tumor necrosis factor-α expression," *Diabetes*, vol. 52, no. 7, pp. 1779–1785, 2003.

[11] K. Maeda, K. Okubo, I. Shimomura, T. Funahashi, Y. Matsuzawa, and K. Matsubara, "cDNA cloning and expression of a novel adipose specific collagen-like factor, apM1 (AdiPose most abundant gene transcript 1)," *Biochemical and Biophysical Research Communications*, vol. 221, no. 2, pp. 286–289, 1996.

[12] H. Masuzaki, Y. Ogawa, N. Isse et al., "Human obese gene expression. Adipocyte-specific expression and regional

differences in the adipose tissue," *Diabetes*, vol. 44, no. 7, pp. 855–858, 1995.

[13] C. T. Montague, J. B. Prins, L. Sanders, J. E. Digby, and S. O'Rahilly, "Depot- and sex-specific differences in human leptin mRNA expression: implications for the control of regional fat distribution," *Diabetes*, vol. 46, no. 3, pp. 342–347, 1997.

[14] P. E. Scherer, S. Williams, M. Fogliano, G. Baldini, and H. F. Lodish, "A novel serum protein similar to C1q, produced exclusively in adipocytes," *The Journal of Biological Chemistry*, vol. 270, no. 45, pp. 26746–26749, 1995.

[15] M. E. Trujillo and P. E. Scherer, "Adiponectin–journey from an adipocyte secretory protein to biomarker of the metabolic syndrome," *Journal of Internal Medicine*, vol. 257, no. 2, pp. 167–175, 2005.

[16] R. H. Amin, S. T. Mathews, A. Alli, and T. Leff, "Endogenously produced adiponectin protects cardiomyocytes from hypertrophy by a PPARγ-dependent autocrine mechanism," *American Journal of Physiology-Heart and Circulatory Physiology*, vol. 299, no. 3, pp. H690–H698, 2010.

[17] H. Matsui, M. Motooka, H. Koike et al., "Ischemia/reperfusion in rat heart induces leptin and leptin receptor gene expression," *Life Sciences*, vol. 80, no. 7, pp. 672–680, 2007.

[18] J. Solarewicz, A. Manly, S. Kokoszka, N. Sleiman, T. Leff, and S. Cala, "Adiponectin secretion from cardiomyocytes produces canonical multimers and partial co-localization with calsequestrin in junctional SR," *Molecular and Cellular Biochemistry*, vol. 457, no. 1-2, pp. 201–214, 2019.

[19] N. Ekmen, A. Helvaci, M. Gunaldi, H. Sasani, and S. T. Yildirmak, "Leptin as an important link between obesity and cardiovascular risk factors in men with acute myocardial infarction," *Indian Heart Journal*, vol. 68, no. 2, pp. 132–137, 2016.

[20] H. A. Khafaji, A. B. Bener, N. M. Rizk, and J. Al Suwaidi, "Elevated serum leptin levels in patients with acute myocardial infarction; correlation with coronary angiographic and echocardiographic findings," *BMC Research Notes*, vol. 5, p. 262, 2012.

[21] B. B. Bell and K. Rahmouni, "Leptin as a mediator of obesity-induced hypertension," *Current Obesity Reports*, vol. 5, no. 4, pp. 397–404, 2016.

[22] C. M. Ghantous, F. H. Kobeissy, N. Soudani et al., "Mechanical stretch-induced vascular hypertrophy occurs through modulation of leptin synthesis-mediated ROS formation and GATA-4 nuclear translocation," *Frontiers in Pharmacology*, vol. 6, p. 240, 2015.

[23] A. Zeidan, D. M. Purdham, V. Rajapurohitam, S. Javadov, S. Chakrabarti, and M. Karmazyn, "Leptin induces vascular smooth muscle cell hypertrophy through angiotensin II- and endothelin-1-dependent mechanisms and mediates stretch-induced hypertrophy," *The Journal of Pharmacology and Experimental Therapeutics*, vol. 315, no. 3, pp. 1075–1084, 2005.

[24] N. Soudani, C. M. Ghantous, Z. Farhat, W. N. Shebaby, K. Zibara, and A. Zeidan, "Calcineurin/NFAT activation-dependence of leptin synthesis and vascular growth in response to mechanical stretch," *Frontiers in Physiology*, vol. 7, p. 433, 2016.

[25] A. Zeidan, B. Paylor, K. J. Steinhoff et al., "Actin cytoskeleton dynamics promotes leptin-induced vascular smooth muscle hypertrophy via RhoA/ROCK- and phosphatidylinositol 3-kinase/protein kinase B-dependent pathways," *Journal of Pharmacology and Experimental Therapeutics*, vol. 322, no. 3, pp. 1110–1116, 2007.

[26] Y. L. Hsieh, Y. L. Tsai, M. A. Shibu et al., "ZAK induces cardiomyocyte hypertrophy and brain natriuretic peptide expression via p38/JNK signaling and GATA4/c-Jun transcriptional factor activation," *Molecular and Cellular Biochemistry*, vol. 405, no. 1-2, pp. 1–9, 2015.

[27] D. Chen, Y. H. Zang, Y. Qiu et al., "BCL6 attenuates proliferation and oxidative stress of vascular smooth muscle cells in hypertension," *Oxidative Medicine and Cellular Longevity*, vol. 2019, Article ID 5018410, 9 pages, 2019.

[28] A. C. Montezano and R. M. Touyz, "Molecular mechanisms of hypertension—reactive oxygen species and antioxidants: a basic science update for the clinician," *Canadian Journal of Cardiology*, vol. 28, no. 3, pp. 288–295, 2012.

[29] T. Adachi, D. R. Pimentel, T. Heibeck et al., "S-glutathiolation of Ras mediates redox-sensitive signaling by angiotensin II in vascular smooth muscle cells," *The Journal of Biological Chemistry*, vol. 279, no. 28, pp. 29857–29862, 2004.

[30] H. D. Wang, S. Xu, D. G. Johns et al., "Role of NADPH oxidase in the vascular hypertrophic and oxidative stress response to angiotensin II in mice," *Circulation Research*, vol. 88, no. 9, pp. 947–953, 2001.

[31] F. Ianniello, L. Quagliozzi, A. Caruso, and G. Paradisi, "Low adiponectin in overweight/obese women: association with diabetes during pregnancy," *European Review for Medical and Pharmacological Sciences*, vol. 17, no. 23, pp. 3197–3205, 2013.

[32] C. Lara-Castro, N. Luo, P. Wallace, R. L. Klein, and W. T. Garvey, "Adiponectin multimeric complexes and the metabolic syndrome trait cluster," *Diabetes*, vol. 55, no. 1, pp. 249–259, 2006.

[33] R. Weiss, S. Dufour, A. Groszmann et al., "Low adiponectin levels in adolescent obesity: a marker of increased intramyocellular lipid accumulation," *The Journal of Clinical Endocrinology and Metabolism*, vol. 88, no. 5, pp. 2014–2018, 2003.

[34] S. Kojima, T. Funahashi, F. Otsuka et al., "Future adverse cardiac events can be predicted by persistently low plasma adiponectin concentrations in men and marked reductions of adiponectin in women after acute myocardial infarction," *Atherosclerosis*, vol. 194, no. 1, pp. 204–213, 2007.

[35] T. Pischon, C. J. Girman, G. S. Hotamisligil, N. Rifai, F. B. Hu, and E. B. Rimm, "Plasma adiponectin levels and risk of myocardial infarction in men," *JAMA*, vol. 291, no. 14, pp. 1730–1737, 2004.

[36] T. Imatoh, M. Miyazaki, Y. Momose, S. Tanihara, and H. Une, "Adiponectin levels associated with the development of hypertension: a prospective study," *Hypertension Research*, vol. 31, no. 2, pp. 229–233, 2008.

[37] A. T. Gonon, U. Widegren, A. Bulhak et al., "Adiponectin protects against myocardial ischaemia-reperfusion injury via AMP-activated protein kinase, Akt, and nitric oxide," *Cardiovascular Research*, vol. 78, no. 1, pp. 116–122, 2008.

[38] R. Shibata, K. Sato, D. R. Pimentel et al., "Adiponectin protects against myocardial ischemia-reperfusion injury through AMPK- and COX-2-dependent mechanisms," *Nature Medicine*, vol. 11, no. 10, pp. 1096–1103, 2005.

[39] S. Fukuda, S. Kita, Y. Obata et al., "The unique prodomain of T-cadherin plays a key role in adiponectin binding with the essential extracellular cadherin repeats 1 and 2," *The Journal of Biological Chemistry*, vol. 292, no. 19, pp. 7840–7849, 2017.

[40] T. Kadowaki and T. Yamauchi, "Adiponectin and adiponectin receptors," *Endocrine Reviews*, vol. 26, no. 3, pp. 439–451, 2005.

[41] T. Yamauchi, J. Kamon, Y. Ito et al., "Cloning of adiponectin receptors that mediate antidiabetic metabolic effects," *Nature*, vol. 423, no. 6941, pp. 762–769, 2003.

[42] T. Yamauchi, Y. Nio, T. Maki et al., "Targeted disruption of AdipoR1 and AdipoR2 causes abrogation of adiponectin binding and metabolic actions," *Nature Medicine*, vol. 13, no. 3, pp. 332–339, 2007.

[43] M. S. Denzel, M. C. Scimia, P. M. Zumstein, K. Walsh, P. Ruiz-Lozano, and B. Ranscht, "T-cadherin is critical for adiponectin-mediated cardioprotection in mice," *The Journal of Clinical Investigation*, vol. 120, no. 12, pp. 4342–4352, 2010.

[44] J. L. Parker-Duffen, K. Nakamura, M. Silver et al., "T-cadherin is essential for adiponectin-mediated revascularization," *The Journal of Biological Chemistry*, vol. 288, no. 34, pp. 24886–24897, 2013.

[45] T. Yamauchi, J. Kamon, Y. Minokoshi et al., "Adiponectin stimulates glucose utilization and fatty-acid oxidation by activating AMP-activated protein kinase," *Nature Medicine*, vol. 8, no. 11, pp. 1288–1295, 2002.

[46] A. Woods, S. R. Johnstone, K. Dickerson et al., "LKB1 is the upstream kinase in the AMP-activated protein kinase cascade," *Current Biology*, vol. 13, no. 22, pp. 2004–2008, 2003.

[47] Z. Xie, Y. Dong, R. Scholz, D. Neumann, and M. H. Zou, "Phosphorylation of LKB1 at serine 428 by protein kinase C-zeta is required for metformin-enhanced activation of the AMP-activated protein kinase in endothelial cells," *Circulation*, vol. 117, no. 7, pp. 952–962, 2008.

[48] R. J. Shaw, M. Kosmatka, N. Bardeesy et al., "The tumor suppressor LKB1 kinase directly activates AMP-activated kinase and regulates apoptosis in response to energy stress," *Proceedings of the National Academy of Sciences of the United States of America*, vol. 101, no. 10, pp. 3329–3335, 2004.

[49] L. Zhou, S. S. Deepa, J. C. Etzler et al., "Adiponectin activates AMP-activated protein kinase in muscle cells via APPL1/LKB1-dependent and phospholipase C/Ca^{2+}/Ca^{2+}/-calmodulin-dependent protein kinase kinase-dependent pathways," *The Journal of Biological Chemistry*, vol. 284, no. 33, pp. 22426–22435, 2009.

[50] M. Zhang, Y. Dong, J. Xu et al., "Thromboxane receptor activates the AMP-activated protein kinase in vascular smooth muscle cells via hydrogen peroxide," *Circulation Research*, vol. 102, no. 3, pp. 328–337, 2008.

[51] S. Wang, J. Xu, P. Song, B. Viollet, and M. H. Zou, "In vivo activation of AMP-activated protein kinase attenuates diabetes-enhanced degradation of GTP cyclohydrolase I," *Diabetes*, vol. 58, no. 8, pp. 1893–1901, 2009.

[52] S. Wang, B. Liang, B. Viollet, and M. H. Zou, "Inhibition of the AMP-activated protein kinase-α2 accentuates agonist-induced vascular smooth muscle contraction and high blood pressure in mice," *Hypertension*, vol. 57, no. 5, pp. 1010–1017, 2011.

[53] H. Chen, M. Montagnani, T. Funahashi, I. Shimomura, and M. J. Quon, "Adiponectin stimulates production of nitric oxide in vascular endothelial cells," *The Journal of Biological Chemistry*, vol. 278, no. 45, pp. 45021–45026, 2003.

[54] R. Li, W. B. Lau, and X. L. Ma, "Adiponectin resistance and vascular dysfunction in the hyperlipidemic state," *Acta Pharmacologica Sinica*, vol. 31, no. 10, pp. 1258–1266, 2010.

[55] S. Albinsson, A. Bhattachariya, and P. Hellstrand, "Stretch-dependent smooth muscle differentiation in the portal vein-role of actin polymerization, calcium signaling, and micro-RNAs," *Microcirculation*, vol. 21, no. 3, pp. 230–238, 2014.

[56] A. Zeidan, I. Nordstrom, S. Albinsson, U. Malmqvist, K. Sward, and P. Hellstrand, "Stretch-induced contractile differentiation of vascular smooth muscle: sensitivity to actin polymerization inhibitors," *American Journal of Physiology-Cell Physiology*, vol. 284, no. 6, pp. C1387–C1396, 2003.

[57] A. Zeidan, I. Nordstrom, K. Dreja, U. Malmqvist, and P. Hellstrand, "Stretch-dependent modulation of contractility and growth in smooth muscle of rat portal vein," *Circulation Research*, vol. 87, no. 3, pp. 228–234, 2000.

[58] M. C. Sutter, "The mesenteric-portal vein in research," *Pharmacological Reviews*, vol. 42, no. 4, pp. 287–325, 1990.

[59] A. Thievent and J. L. Connat, "Cytoskeletal features in longitudinal and circular smooth muscles during development of the rat portal vein," *Cell and Tissue Research*, vol. 279, no. 1, pp. 199–208, 1995.

[60] A. Zeidan, J. Broman, P. Hellstrand, and K. Sward, "Cholesterol dependence of vascular ERK1/2 activation and growth in response to Stretch," *Arteriosclerosis, Thrombosis, and Vascular Biology*, vol. 23, no. 9, pp. 1528–1534, 2003.

[61] B. Ljung, "Vascular selectivity of Felodipine," *Journal of Cardiovascular Pharmacology*, vol. 15, Supplement 4, pp. S11–S16, 1990.

[62] N. Ouchi, S. Kihara, Y. Arita et al., "Novel modulator for endothelial adhesion molecules: adipocyte-derived plasma protein adiponectin," *Circulation*, vol. 100, no. 25, pp. 2473–2476, 1999.

[63] W. Nour-Eldine, C. M. Ghantous, K. Zibara et al., "Adiponectin attenuates angiotensin II-induced vascular smooth muscle cell remodeling through nitric oxide and the RhoA/ROCK pathway," *Frontiers in Pharmacology*, vol. 7, p. 86, 2016.

[64] A. H. Berg, T. P. Combs, and P. E. Scherer, "ACRP30/adiponectin: an adipokine regulating glucose and lipid metabolism," *Trends in Endocrinology and Metabolism*, vol. 13, no. 2, pp. 84–89, 2002.

[65] C. N. A. Ayina, F. T. A. Endomba, S. H. Mandengue et al., "Association of the leptin-to-adiponectin ratio with metabolic syndrome in a sub-Saharan African population," *Diabetology and Metabolic Syndrome*, vol. 9, p. 66, 2017.

[66] G. Fruhbeck, V. Catalan, A. Rodriguez et al., "Adiponectin-leptin ratio is a functional biomarker of adipose tissue inflammation," *Nutrients*, vol. 11, no. 2, 2019.

[67] P. M. Bauer, D. Fulton, Y. C. Boo et al., "Compensatory phosphorylation and protein-protein interactions revealed by loss of function and gain of function mutants of multiple serine phosphorylation sites in endothelial nitric-oxide synthase," *The Journal of Biological Chemistry*, vol. 278, no. 17, pp. 14841–14849, 2003.

[68] A. Bouallegue, G. B. Daou, and A. K. Srivastava, "Nitric oxide attenuates endothelin-1-induced activation of ERK1/2, PKB, and Pyk2 in vascular smooth muscle cells by a cGMP-dependent pathway," *American Journal of Physiology-Heart and Circulatory Physiology*, vol. 293, no. 4, pp. H2072–H2079, 2007.

[69] T. D. Giles, G. E. Sander, B. D. Nossaman, and P. J. Kadowitz, "Impaired vasodilation in the pathogenesis of hypertension: focus on nitric oxide, endothelial-derived hyperpolarizing

factors, and prostaglandins," *Journal of Clinical Hypertension*, vol. 14, no. 4, pp. 198–205, 2012.

[70] Y. Zhang, K. K. Griendling, A. Dikalova, G. K. Owens, and W. R. Taylor, "Vascular hypertrophy in angiotensin II-induced hypertension is mediated by vascular smooth muscle cell-derived H_2O_2," *Hypertension*, vol. 46, no. 4, pp. 732–737, 2005.

[71] H. Kai, H. Kudo, N. Takayama, S. Yasuoka, H. Kajimoto, and T. Imaizumi, "Large blood pressure variability and hypertensive cardiac remodeling–role of cardiac inflammation," *Circulation Journal*, vol. 73, no. 12, pp. 2198–2203, 2009.

[72] M. L. Hixon, C. Muro-Cacho, M. W. Wagner et al., "Akt1/PKB upregulation leads to vascular smooth muscle cell hypertrophy and polyploidization," *The Journal of Clinical Investigation*, vol. 106, no. 8, pp. 1011–1020, 2000.

[73] A. Zeidan, K. Sward, I. Nordstrom et al., "Ablation of SM22α decreases contractility and actin contents of mouse vascular smooth muscle," *FEBS Letters*, vol. 562, no. 1-3, pp. 141–146, 2004.

[74] Y. Nakano, T. Tobe, N. H. Choi-Miura, T. Mazda, and M. Tomita, "Isolation and characterization of GBP28, a novel gelatin-binding protein purified from human plasma," *Journal of Biochemistry*, vol. 120, no. 4, pp. 803–812, 1996.

[75] J. Fruebis, T. S. Tsao, S. Javorschi et al., "Proteolytic cleavage product of 30-kDa adipocyte complement-related protein increases fatty acid oxidation in muscle and causes weight loss in mice," *Proceedings of the National Academy of Sciences of the United States of America*, vol. 98, no. 4, pp. 2005–2010, 2001.

[76] J. Ryu, C. A. Loza, H. Xu et al., "Potential roles of adiponectin isoforms in human obesity with delayed wound healing," *Cell*, vol. 8, no. 10, 2019.

[77] N. S. Salathia, J. Shi, J. Zhang, and R. J. Glynne, "An in vivo screen of secreted proteins identifies adiponectin as a regulator of murine cutaneous wound healing," *The Journal of Investigative Dermatology*, vol. 133, no. 3, pp. 812–821, 2013.

[78] E. Tomas, T. S. Tsao, A. K. Saha et al., "Enhanced muscle fat oxidation and glucose transport by ACRP30 globular domain: acetyl-CoA carboxylase inhibition and AMP-activated protein kinase activation," *Proceedings of the National Academy of Sciences of the United States of America*, vol. 99, no. 25, pp. 16309–16313, 2002.

[79] T. Yamauchi, J. Kamon, H. Waki et al., "The fat-derived hormone adiponectin reverses insulin resistance associated with both lipoatrophy and obesity," *Nature Medicine*, vol. 7, no. 8, pp. 941–946, 2001.

[80] M. Ding, Y. Xie, R. J. Wagner et al., "Adiponectin induces vascular smooth muscle cell differentiation via repression of mammalian target of rapamycin complex 1 and FoxO4," *Arteriosclerosis, Thrombosis, and Vascular Biology*, vol. 31, no. 6, pp. 1403–1410, 2011.

[81] Y. Hattori, Y. Nakano, S. Hattori, A. Tomizawa, K. Inukai, and K. Kasai, "High molecular weight adiponectin activates AMPK and suppresses cytokine-induced NF-κB activation in vascular endothelial cells," *FEBS Letters*, vol. 582, no. 12, pp. 1719–1724, 2008.

[82] Z. P. Chen, K. I. Mitchelhill, B. J. Michell et al., "AMP-activated protein kinase phosphorylation of endothelial NO synthase," *FEBS Letters*, vol. 443, no. 3, pp. 285–289, 1999.

[83] B. J. Davis, Z. Xie, B. Viollet, and M. H. Zou, "Activation of the AMP-activated kinase by antidiabetes drug metformin stimulates nitric oxide synthesis in vivo by promoting the association of heat shock protein 90 and endothelial nitric oxide synthase," *Diabetes*, vol. 55, no. 2, pp. 496–505, 2006.

[84] V. A. Morrow, F. Foufelle, J. M. Connell, J. R. Petrie, G. W. Gould, and I. P. Salt, "Direct activation of AMP-activated protein kinase stimulates nitric-oxide synthesis in human aortic endothelial cells," *The Journal of Biological Chemistry*, vol. 278, no. 34, pp. 31629–31639, 2003.

[85] S. Dimmeler, I. Fleming, B. Fisslthaler, C. Hermann, R. Busse, and A. M. Zeiher, "Activation of nitric oxide synthase in endothelial cells by Akt-dependent phosphorylation," *Nature*, vol. 399, no. 6736, pp. 601–605, 1999.

[86] D. Fulton, J. P. Gratton, T. J. McCabe et al., "Regulation of endothelium-derived nitric oxide production by the protein kinase Akt," *Nature*, vol. 399, no. 6736, pp. 597–601, 1999.

[87] I. B. Buchwalow, T. Podzuweit, W. Bocker et al., "Vascular smooth muscle and nitric oxide synthase," *The FASEB Journal*, vol. 16, no. 6, pp. 500–508, 2002.

[88] I. B. Buchwalow, T. Podzuweit, V. E. Samoilova et al., "An in situ evidence for autocrine function of NO in the vasculature," *Nitric Oxide*, vol. 10, no. 4, pp. 203–212, 2004.

[89] T. Oka, M. Maillet, A. J. Watt et al., "Cardiac-specific deletion of Gata4 reveals its requirement for hypertrophy, compensation, and myocyte viability," *Circulation Research*, vol. 98, no. 6, pp. 837–845, 2006.

[90] N. Saadane, L. Alpert, and L. E. Chalifour, "Expression of immediate early genes, GATA-4, and Nkx-2.5 in adrenergic-induced cardiac hypertrophy and during regression in adult mice," *British Journal of Pharmacology*, vol. 127, no. 5, pp. 1165–1176, 1999.

[91] A. Zeidan, J. C. Hunter, S. Javadov, and M. Karmazyn, "mTOR mediates RhoA-dependent leptin-induced cardiomyocyte hypertrophy," *Molecular and Cellular Biochemistry*, vol. 352, no. 1-2, pp. 99–108, 2011.

Hindawi
Oxidative Medicine and Cellular Longevity
Volume 2020, Article ID 3145182, 19 pages
https://doi.org/10.1155/2020/3145182

Research Article

Apatinib, a Novel Tyrosine Kinase Inhibitor, Promotes ROS-Dependent Apoptosis and Autophagy via the Nrf2/HO-1 Pathway in Ovarian Cancer Cells

Xiaodan Sun,[1,2] **Ji Li**,[1] **Yizhuo Li**,[1] **Shouhan Wang**,[3] **and Qingchang Li**[1,4]

[1]*Department of Pathology, College of Basic Medical Sciences, China Medical University, Shenyang 110122, China*
[2]*Department of 2nd Gynecologic Oncology Surgery, Jilin Cancer Hospital, Changchun 130012, China*
[3]*Department of Hepatopancreatobiliary Surgery, Jilin Cancer Hospital, Changchun 130012, China*
[4]*Department of Pathology, China Medical University, Shenyang 110122, China*

Correspondence should be addressed to Shouhan Wang; 15640584861@163.com and Qingchang Li; qcli@cmu.edu.cn

Received 6 December 2019; Revised 9 March 2020; Accepted 20 April 2020; Published 14 May 2020

Guest Editor: Raffaele Strippoli

Apatinib, a new-generation oral tyrosine kinase inhibitor targeting the vascular endothelial growth factor receptor 2 (VEGFR2) signaling pathway, shows favorable therapeutic effects in various malignant tumors. However, its effect on ovarian cancer has not yet been characterized. Here, we demonstrated that apatinib inhibited ovarian cancer cell growth and migration in a concentration-dependent manner. Further, we found that apatinib could directly act on tumor cells and promote ROS-dependent apoptosis and autophagy. Mechanistically, we showed that apatinib suppressed glutathione to generate ROS via the downregulation of the nuclear factor erythroid 2-related factor 2 (Nrf2)/heme oxygenase 1 (HO-1) pathway and maintained an antitumor effect at a low level of VEGFR2 in ovarian cancer, suggesting that combination of apatinib with Nrf2 inhibitor may be a promising therapy strategy for patients with ovarian cancer.

1. Introduction

Ovarian cancer (OC) ranked eighth in incidence and seventh in mortality rates globally among all cancers in women in 2018 (WHO, http://gco.iarc.fr/today/home); it has become the leading malignancy in gynecological cancers in China, with an estimated 52,100 new cases and 22,500 deaths in 2015 [1]. The standard regimen for advanced OC is platinum-based chemotherapy following debulking surgery. However, approximately 75% of patients with advanced stages will eventually experience recurrence [2], and almost all patients with recurrent disease ultimately develop platinum resistance, resulting in poor prognosis with only 40% of patients surviving for 5 years [3]. As such, improved treatment options for OC are urgently needed.

Angiogenesis is universally considered a cancer hallmark and is responsible for tumor proliferation, progression, and metastasis [4], making its interruption an attractive therapeutic strategy for OC. The vascular endothelial growth factor (VEGF)/VEGF-receptor (VEGFR) signaling pathway is a key regulator of angiogenesis; emerging studies have demonstrated the potent efficacy of anti-VEGF antibodies and VEGFR inhibitors in the treatment of OC [5]. Bevacizumab, a monoclonal antibody against VEGF, is one of the most studied angiogenesis inhibitors; it is approved for the first- and second-line treatments of advanced epithelial OC according to the National Comprehensive Cancer Network Guidelines [6]. Unfortunately, this is an inconvenient and costly treatment that is not attainable for all patients with OC in China.

Apatinib, also known as YN968D1, is a novel oral small-molecule tyrosine kinase inhibitor developed in China. It can block the migration and proliferation of VEGFR-induced endothelial cells and reduce tumor microvascular density via highly selective targeting of VEGFR-2 [7]; it was approved by the Chinese Food and Drug Administration in 2014 as a third-line treatment for patients with advanced gastric or gastroesophageal adenocarcinoma. Increasing evidence indicates

that apatinib exerts favorable antitumor effects with tolerable toxicities in other human cancers, including breast cancer [8], non-small-cell lung cancer (NSCLC) [9], colon cancer [10], hepatocellular carcinoma [11], pancreatic cancer [12], anaplastic thyroid cancer [13, 14], and osteosarcoma [15].

To date, there have been limited studies on the therapeutic efficacy of apatinib in patients with OC, and its molecular mechanism in this application has not been characterized. In the present study, we investigated the effect of apatinib in OC and observed that a novel regulatory mechanism could underlie its antitumor effect.

2. Materials and Methods

2.1. Antibodies and Reagents. The following primary antibodies were purchased from Cell Signaling Technology (Danvers, MA, USA): GAPDH, histone H3, β-actin, E-cadherin, N-cadherin, vimentin, matrix metalloproteinase 9 (MMP9), PARP, Bax, Bcl2, P62, light chain 3B (LC3B), VEGFR2, nuclear factor erythroid 2-related factor 2 (Nrf2), heme oxygenase 1 (HO-1), and SOD2. The following secondary antibodies were provided by Proteintech (Wuhan, China): goat anti-rabbit IgG, goat anti-mouse IgG, and FITC-conjugated secondary antibody. Apatinib and TBHQ (an Nrf2-specific activator) were purchased from MCE, China. N-acetyl-L-cysteine (NAC), a reactive oxygen species (ROS) scavenger, was purchased from Selleck, China.

2.2. Cell Culture and Treatments. A2780, SKOV-3, and CAOV-3 human OC cell lines were purchased from the China Center for Type Culture Collection (Wuhan, China). A2780 and CAOV-3 cells were cultured in DMEM supplemented with 10% fetal bovine serum (FBS). SKOV-3 cells were cultured in RPMI-1640 medium supplemented with 10% FBS. The cells were grown at 37°C in a humidified atmosphere with 5% CO_2.

Transient transfection was carried out using Lipofectamine 3000 reagent (Invitrogen, Carlsbad, CA) according to the manufacturer's instructions. A VEGFR2 expression plasmid and the corresponding empty plasmid (OriGene, Rockville, MD, USA) were used for VEGFR2 overexpression and as a negative control, respectively. Cells were transfected with VEGFR2-siRNA and negative control siRNA (GenePharma, Shanghai, China) for VEGFR2 knockdown experiments.

2.3. Cell Proliferation and Colony Formation Assays. To evaluate cell proliferation, Cell Counting Kit-8 (CCK-8, Beyotime, Shanghai, China) assay was performed. After seeding in 96-well plates at a density of 5000 cells/well with 100 μl culture medium, the cells were treated with different concentrations of apatinib (0, 1, 5, 10, 20, and 40 μM) for an indicated time (24, 48, 72, and 96 h), changing the apatinib-containing medium every 48 h. At the end of the experiments, 10 μl of CCK-8 reagent was mixed into each well, and the cells were incubated at 37°C for 2 h. The absorbance (OD) of each well was measured at 450 nm using a microplate reader. The percentage of cell viability was calculated as (experimental group OD − blank well OD)/(control group OD − blank well OD) × 100%. GraphPad Prism 7.0 software was used to calculate values indicating 50% inhibition of surviving fraction (IC50).

For the colony formation assays, 500 cells per well were plated in 6-well plates. After coincubation with 0, 1, 5, and 10 μM apatinib for 14 days, the cells were washed three times with PBS, fixed with 4% paraformaldehyde, and stained with Giemsa solution. The number of colonies containing more than 50 cells was counted by using a microscope. Colony formation efficiency was calculated as (colony numbers/500) × 100%.

2.4. Transwell and Wound Healing Assay. Twenty-four-well transwell chambers (8 μm pore size, 6.5 mm diameter; Millipore, USA) coated with Matrigel (BD Biosciences, San Jose, CA, USA) were used to perform a cell migration assay. First, 500 μl of medium containing 10% FBS was added to the bottom of the chamber. Next, 100 μl of the OC cell suspensions at a density of 10×10^4 cells/ml in a serum-free medium, treated with different concentrations of apatinib (0, 10, and 20 μM), was seeded into the upper chambers. After 24 h, the cells that adhered to the upper surfaces of the transwell membranes were removed using cotton swabs, and those on the lower surfaces were fixed with 4% paraformaldehyde and stained with a 0.1% crystal violet dye. The migrated cells were photographed and counted in five random fields using an inverted microscope.

To assess wound healing, cells were plated in six-well plates and the confluent monolayer cell plate was wounded using the tip of a 250 μl pipette. PBS was used to remove floating cells, and the cells were cultured in a serum-free medium in the presence or absence of apatinib for 24 h. Images of the same position of the wounded monolayer were obtained by using a microscope. ImageJ software was used to quantitatively measure wound distance.

2.5. Analysis of Apoptosis. Annexin V-FITC/PI Apoptosis Detection Kit (BD, Biosciences, China) was used to detect apoptosis. After treatment with the indicated concentrations of apatinib (0, 10, and 20 μM), the harvested cells were resuspended in Annexin V-binding buffer, then stained with FITC-conjugated Annexin V and PI according to the manufacturer's protocol. The degree of apoptosis was analyzed using a flow cytometer (LSRFortessa, BD Biosciences).

2.6. ROS Detection and Measurement of Intracellular Glutathione (GSH). ROS induced by apatinib was determined using a ROS Assay Kit (Beyotime, Shanghai, China) according to the manufacturer's protocol as previously described [16]. Briefly, after exposure to apatinib (0, 10, and 20 μM) for 24 h, the cells were incubated with 10 μM 2′-7′ dichlorofluorescin diacetate (DCFH-DA) in the dark for 20 min at 37°C in a humidified atmosphere at 5% CO_2. Next, the cells were washed three times with cold PBS to remove excess fluorescent probe. The cells were then observed using a fluorescence microscope or resuspended in 300 μl of PBS and assessed for fluorescence intensity using a flow cytometer (LSRFortessa). The data were analyzed using FlowJo X 10.0.7 Software.

A Total Glutathione Assay Kit (Beyotime) was used to measure intracellular GSH levels according to the manufacturer's instructions as previously described [16]. Briefly, after being cocultured with or without apatinib for 24 h and/or pretreated with 200 μM TBHQ for 4 h to activate the Nrf2 pathway, cells were harvested and lysed in the protein removal solution S provided in the kit. After incubation for 5 min at 4°C, the samples were centrifuged at 12,000 rpm for 10 min at 4°C. The supernatant was treated with assay solution for 25 min at 25°C, and the absorbance at 412 nm was measured using a microplate reader (SpectraMax i3x, Molecular Devices, Sunnyvale, CA). Relative intracellular GSH levels were calculated by normalization to the values of the control group.

2.7. Immunofluorescence Staining. Cells were seeded in 20 mm culture plates and cocultured with 20 μM apatinib for 24 h or pretreated with 5 mM NAC for 2 h to inhibit ROS generation, then washed with PBS, fixed with 4% paraformaldehyde for 15 min, and permeabilized in 0.1% Triton X-100 for 5 min. After blocking with 5% bovine serum albumin for 1 h at room temperature, the cells were incubated with primary antibody against LC3B (dilution 1 : 100) overnight at 4°C. Then, FITC-conjugated secondary antibody (dilution 1 : 200) was incubated with the cells for 1 h in the dark at room temperature, and the cells were stained with 4′,6-diamidino-2-phenylindole (DAPI) for 5 min to visualize the nuclei. Images were captured using a fluorescence microscope.

2.8. Transmission Electron Microscopy (TEM). After 24 h apatinib treatment (20 μM) or 2 h NAC pretreatment (5 mM), the cells were washed lightly with PBS, digested with 0.25% trypsin, and centrifuged at 3000 rpm for 10 min at 4°C. The samples were fixed in 3% glutaraldehyde overnight at 4°C for fixation. Then, ultrathin sections (100 nm) were stained with 5% uranyl acetate and Reynold's lead citrate and detected using a TEM (H-7650, Hitachi, Tokyo, Japan).

2.9. Western Blotting and Nuclear and Cytoplasm Isolation. Total proteins were isolated from OC cells with or without apatinib treatment. After washing with ice-cold PBS three times, cells were lysed in a lysis buffer supplemented with a cocktail of proteinase inhibitors. Equal amounts of protein (40 μg) from cell extracts were separated using 10% SDS-PAGE and transferred onto 0.45 μm polyvinylidene fluoride (PVDF) membranes (Millipore, Billerica, MA, USA) as previously described [16]. ImageJ software was used to evaluate the gray value of each band.

A Nuclear and Cytoplasmic Protein Extraction kit (Beyotime) was used to isolate the cytosolic and nuclear cell fractions, following the manufacturer's instructions as previously described [16]. Briefly, the collected cells were suspended in ice-cold hypotonic buffer and incubated on ice for 20 min. The extracts were then centrifuged at 12,000 × g for 5 min, and the supernatants were collected as cytosolic fractions. The pellets were washed with ice-cold PBS and resuspended in the lysis buffer, followed by vortexing at the highest speed. These extracts were centrifuged at 12,000 × g for 10 min, and the supernatants were collected as the nuclear fractions.

2.10. Quantitative Real-Time PCR Analysis (qRT-PCR). TRIzol (Invitrogen) was used to extract total RNA from ovarian cancer cells. Reverse transcription was performed as preciously described [17] using PrimeScript RT Master Mix (Takara, Otsu, Japan). qRT-PCR was performed as preciously described using Applied Biosystems Power SYBR Green on a qTOWER2.0 [17], briefly, 10 seconds at 95°C, then 40 cycles at 95°C for 5 seconds and 65°C for 34 seconds. The mRNA ratio of the target genes to GAPDH was calculated using the $2^{-\Delta\Delta Ct}$ formula. The specific primer sequences are performed as follows:

GAPDH, Forward 5′-CCACCCATGGCAAATTCC-3′, Reverse 5′-GATGGGATTTCCATTGATGACA-3′; VEGFR2, Forward-5′GGACTCTCTCTGCCTACCTCAC-3′, Reverse 5′-GGCTCTTTCGCTTACTGTTCTG-3′; Nrf2, Forward 5′-TCATGATGGACTTGGAGCTG-3′, Reverse 5′-CATA CTCTTTCCGTCGCTGA-3′; HO-1, Forward 5′-CCAGGC AGAGAATGCTGAGT-3′, Reverse 5′-GGCGAAGACTG GGCTCTC-3′; GCLC, Forward 5′-ACATCTACCACGCC GTCAAG-3′, Reverse 5′-ACAGGACCAACCGGACTTTT-3′; and GCLM, Forward 5′-GGGGAACCTGCTGAACTG-3′, Reverse 5′-TCTGGGTTGATTTGGGAACT-3′.

2.11. Online Database. A series of online databases were implemented as previously described [17]. Briefly, the GEPIA database (http://gepia.cancer-pku.cn/), the Oncomine database (http://www.oncomine.org/), and the Human Protein Atlas database (https://www.proteinatlas.org/) were used to analyze mRNA or protein expression of VEGFR2 in OC and normal tissues, respectively.

2.12. Statistical Analysis. All experiments were repeated at least three times, and all results are presented as the means ± standard deviations. Statistical analysis was performed using GraphPad Prism 7.0 software. Statistical significance was determined based on Student's *t*-test or one-way ANOVA; P values < 0.05 were considered statistically significant.

3. Results

3.1. Apatinib Suppressed the Growth of OC Cells. First, the cell viability of the A2780, SKOV-3, and CAOV-3 cell lines decreased as the drug concentration increased (Figure 1(a)), with IC50 values of 18.89 ± 5.6, 25.61 ± 2.1, and 20.46 ± 0.5 μM, respectively (Figure 1(b)). These results suggested that apatinib reduced OC cell growth in a concentration-dependent manner. Following this, 50% of the IC50 dose and the IC50 dose, i.e., approximately 10 μM and 20 μM doses of apatinib, were used for the subsequent experiments. Next, we found that the growth of OC cells was suppressed by apatinib in a time-dependent manner as well (Figure 1(c)). In addition, we observed cell morphology changes induced by apatinib. In the control group, A2780 was round, SKOV-3 was epithelial-like, and CAOV-3 was spindle-shaped, in line with previous descriptions of these three OC cell lines [18].

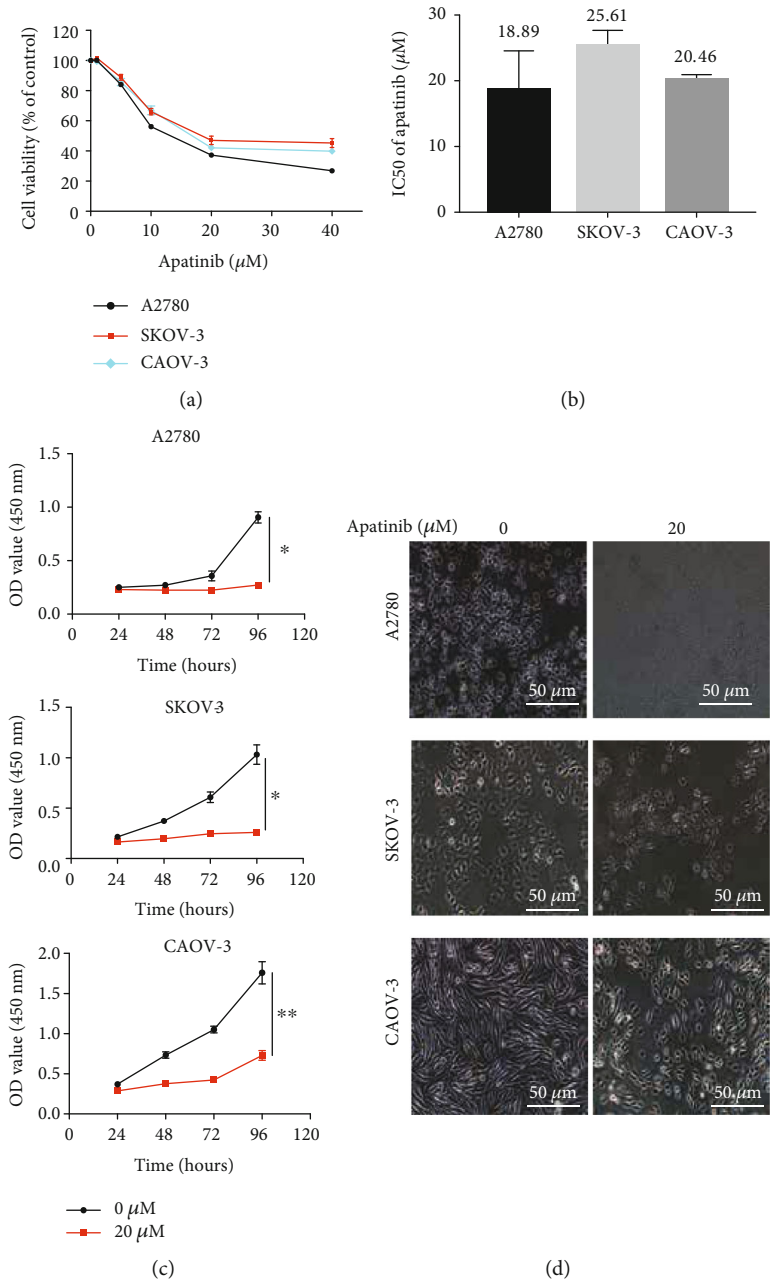

Figure 1: Continued.

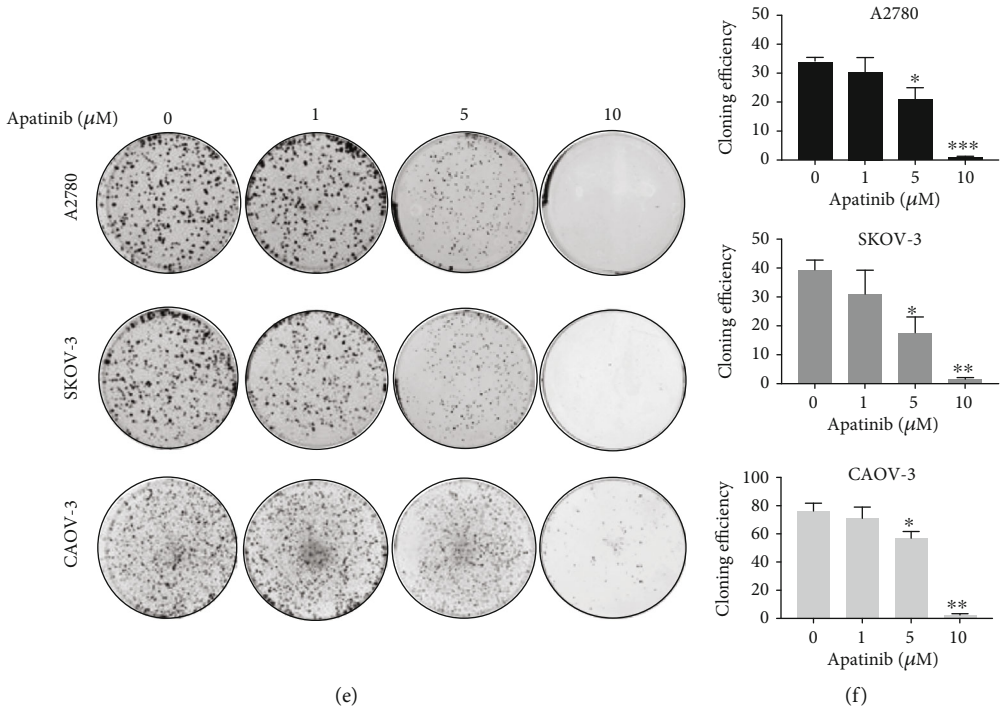

Figure 1: Apatinib suppressed growth of OC cells. (a) Cell viability assays of A2780, SKOV-3, and CAOV-3 cells treated with low-to-high concentrations of apatinib for 48 h. (b) The IC50 values of apatinib for 48 h in three OC cells. (c) The OC cells were treated with 20 μM apatinib for different time intervals (24, 48, 72, and 96 h). The cell viability was detected by CCK-8 and expressed as absorbance value (OD). (d) The effects of 20 μM apatinib on the morphology of OC cells were observed using light microscope (20x). Scale bar = 50 μm. (e, f) Colony formation assay of three OC cells. Colony numbers were counted using the microscope, and the colony formation efficiency was calculated. Data are presented as the mean ± SD of three independent experiments. $^{*}P < 0.05$, $^{**}P < 0.01$, and $^{***}P < 0.001$, compared with the control groups.

After treatment with apatinib, the number of cells was reduced, and the cells were observed to be smaller and irregular in shape; moreover, they took on indistinct margins, with looser intercellular connections, compared to the cells in the control group (Figure 1(d)). The apatinib-treated cells had a lower colony formation ability than the cells in the control group, especially when 10 μM apatinib was applied ($P < 0.05$; Figures 1(e) and 1(f)). Collectively, these results suggest that apatinib suppressed the proliferation of OC cells in both a concentration- and time-dependent manner.

3.2. Apatinib Inhibited OC Cell Migration. Apatinib is known to specifically inhibit VEGFR2 to suppress tumor angiogenesis, which plays an important role in tumor metastasis. Therefore, we explored the role of apatinib in OC migration using the transwell assay. Cell migration was significantly delayed under apatinib treatment in a concentration-dependent manner, especially at 20 μM (Figures 2(a) and 2(b)). Consistently, the wound healing abilities of OC cells were also significantly decreased in a concentration-dependent manner (Figures 2(c) and 2(d)). Furthermore, we performed western blotting to explore whether apatinib suppresses the levels of epithelial-mesenchymal transition-(EMT-) associated markers in OC cells since EMT is closely related to tumor metastasis. Under apatinib treatment, the level of the epithelial marker E-cadherin increased, whereas the levels of the mesenchymal markers vimentin and N-cadherin decreased. The level of another metastasis-associated protein, MMP9, also decreased under apatinib treatment (Figures 2(e) and 2(f)). Thus, apatinib inhibited OC cell migration mainly via suppressing EMT.

3.3. Apatinib Induced Apoptosis and Autophagy in OC Cells. We attempted to identify the potential mechanism underlying the antitumor effect of apatinib. In addition to inhibiting VEGFR2 signal transduction, many studies have shown that apatinib can directly act on tumor cells [10, 12, 14, 15, 19]. Accordingly, we evaluated whether apatinib could induce apoptosis in OC cells. After treatment with 10 and 20 μM of apatinib for 24 h, the percentage of apoptotic cells was significantly higher than that in the control group ($P < 0.05$); this effect was observed to be concentration dependent (Figures 3(a) and 3(b)). In addition to apoptosis, we also tested whether apatinib caused autophagy. After exposure to 20 μM apatinib for 24 h, more autophagosomes with a double membrane containing damaged proteins and organelles and more autolysosomes with a single membrane and degraded contents were observed in the treated group than in the control group using TEM (Figure 3(c)). Next, we evaluated the level of LC3-II, a key marker in the initial stages of autophagy, in OC cells by immunofluorescence. Apatinib-treated cells presented a dot pattern of LC3-II fluorescence, indicating a higher number of autophagosomes than in the control group (Figure 3(d)). In addition, we explored changes

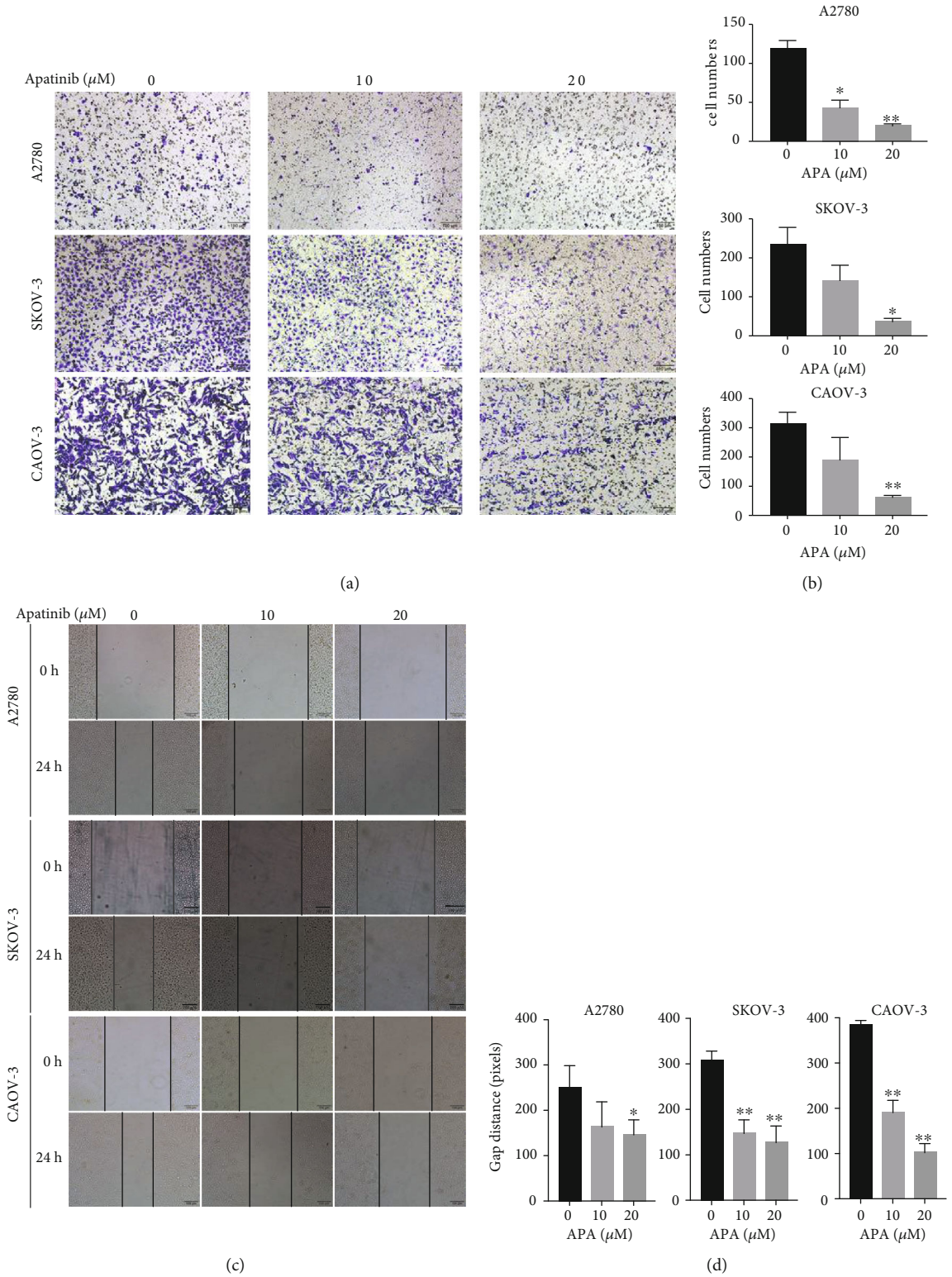

Figure 2: Continued.

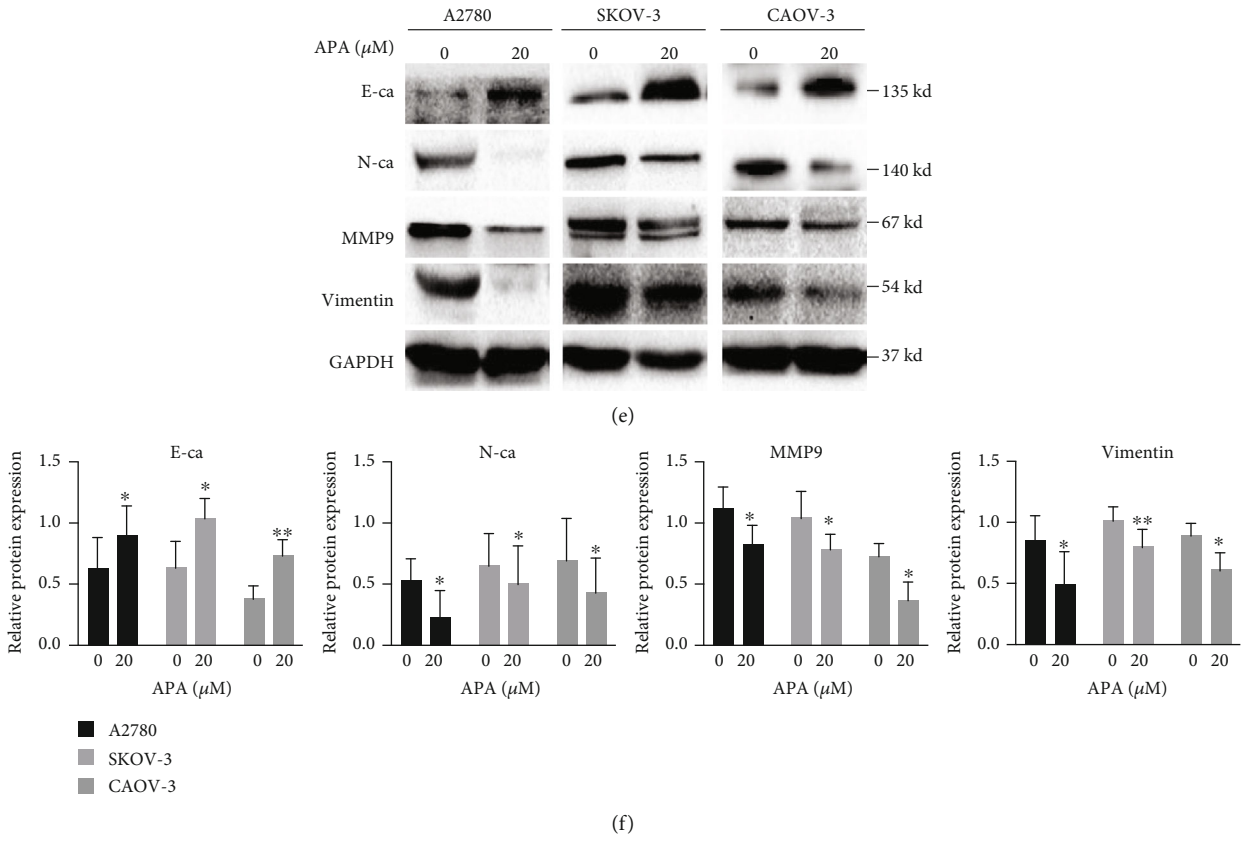

Figure 2: Apatinib inhibited OC cell migration. (a, b) The migration of A2780, SKOV-3, and CAOV-3 cells after treatment with apatinib (0, 10, and 20 μM) for 24 h was assessed using the transwell assay. The invaded cells on the bottom surface of the filters were stained, and the cell numbers were counted by ImageJ software. (c, d) The movement ability of three OC cells after treatment with apatinib (0, 10, and 20 μM) for 24 h was detected using wound healing assays. The gap distance that was calculated by ImageJ software was used to measure the movement ability. (e) After treatment with 20 μM apatinib for 24 h, protein levels of the EMT markers E-cadherin, N-cadherin, vimentin, and metastasis-associated protein, MMP9, in three OC cells were determined by western blotting. (f) The relative western blot gray values are shown in the histogram. Data are presented as the mean ± SD of three independent experiments. APA: apatinib. $^{*}P < 0.05$, $^{**}P < 0.01$, compared with the control groups.

in the key indicators of apoptosis and autophagy by western blotting. The levels of cleaved PARP and Bax increased after treatment with 20 μM apatinib, whereas the expression of Bcl-2 decreased. An increase in the conversion of LC3-I to LC3-II, a specific process of autophagy, and a decrease in p62, which is degraded during autophagy, were also detected in apatinib-treated OC cells (Figures 3(e) and 3(f)). These findings suggest that apatinib promoted apoptosis and autophagy in OC cells.

3.4. The Generation of ROS Is Crucial for Apatinib-Induced Apoptosis and Autophagy. We further investigated the mechanism by which apatinib promoted apoptosis and autophagy. Since apatinib has been reported to induce ROS in pancreatic cancer and cervical cancer [12, 19] and excessive intracellular levels of ROS may lead to mitochondrial dysfunction to promote apoptosis and autophagy [20, 21], we hypothesized that apatinib induced apoptosis and autophagy by promoting ROS generation. A concentration-dependent increase in the fluorescence intensity of DCFH-DA was observed using a fluorescence microscope in apatinib-treated OC cells compared with the controls (Figure 4(a)); the results were validated by measuring the ROS level using a flow cytometer (Figures 4(b) and 4(c)). As expected, the promotion of apoptosis and autophagy by apatinib was reversed by the administration of NAC (5 mM), a ROS scavenger (Figures 4(d)–4(g)). Collectively, these results indicate that apatinib induced apoptosis and autophagy in a ROS-dependent manner in OC cells.

3.5. Apatinib Suppressed GSH to Generate ROS via the Downregulation of Nrf2/HO-1. We subsequently identified the potential molecular mechanisms involved in the generation of ROS by apatinib. First, we measured the levels of GSH, a well-known ROS scavenger [22, 23], in OC cells treated with or without apatinib. As expected, apatinib treatment decreased the level of GSH (Figure 5(a)). Next, we investigated whether apatinib regulates the Nrf2/HO-1 pathway, which is also known to eliminate ROS [24] and is reported to be involved in the regulation of GSH abundance [22]. We found that apatinib decreased the level of Nrf2 and HO-1, whereas SOD2 expression was not significantly

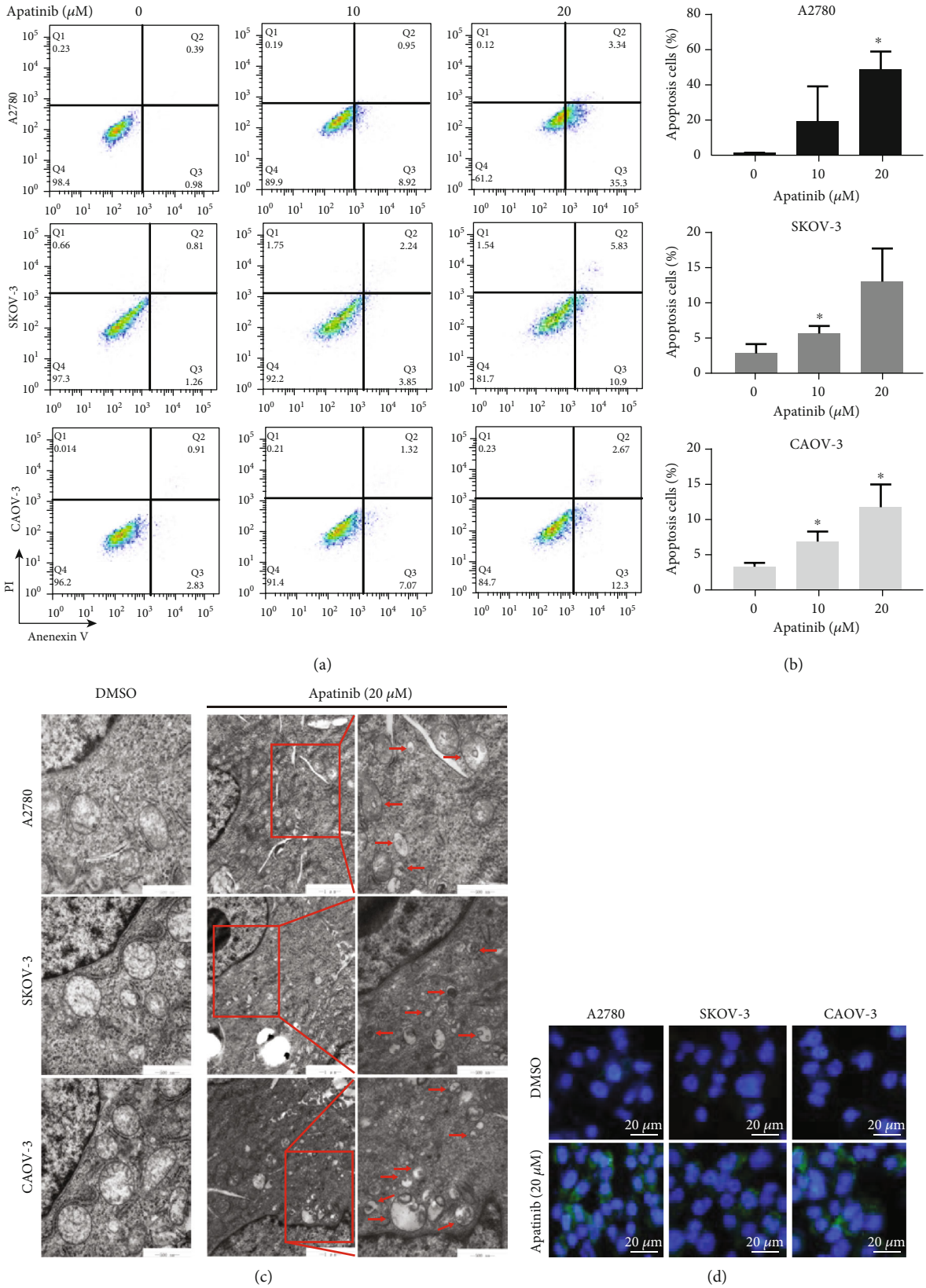

Figure 3: Continued.

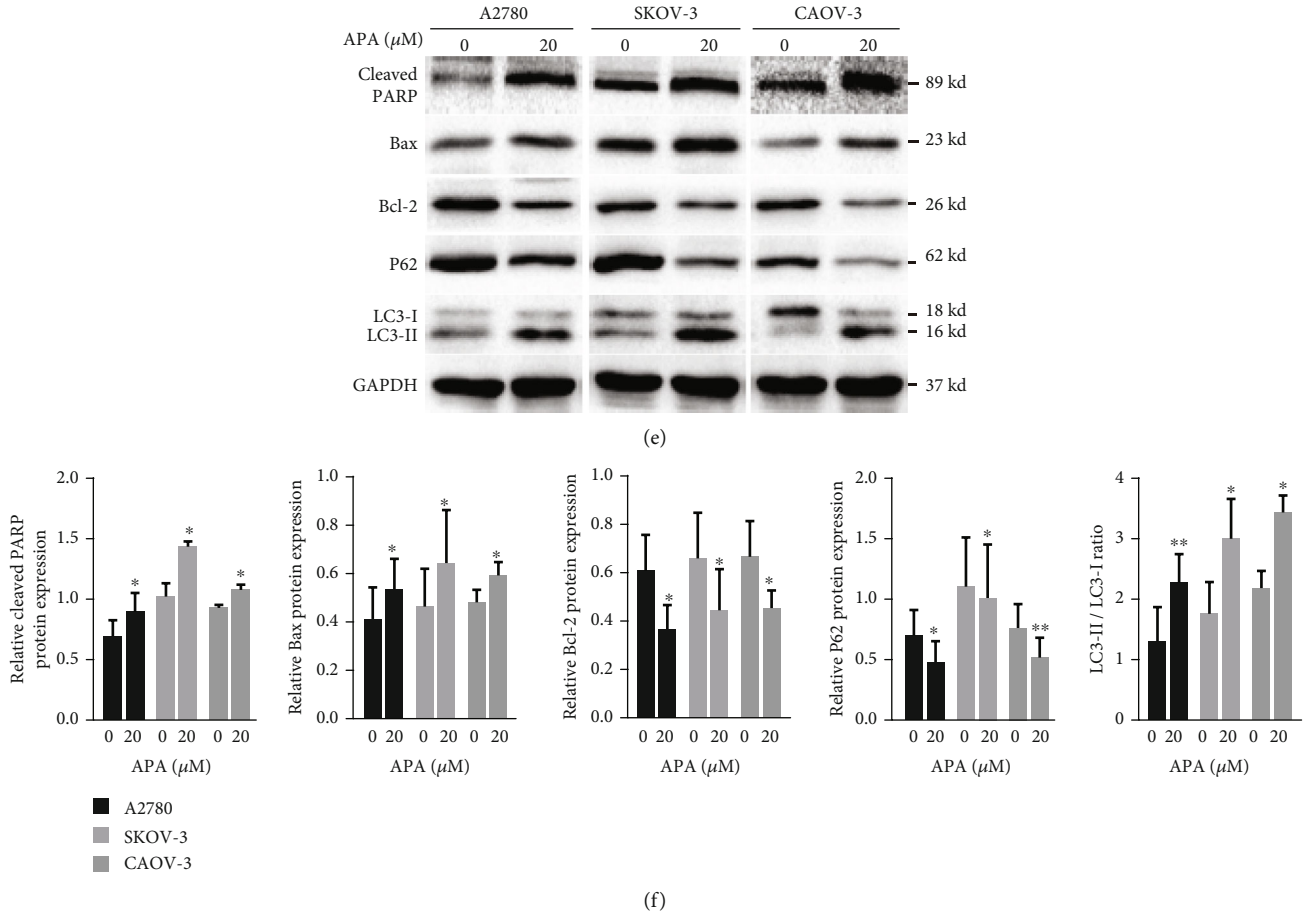

Figure 3: Apatinib induced apoptosis and autophagy in OC cells. (a) After treatment of A2780, SKOV-3, and CAOV-3 cells with apatinib (0, 10, and 20 μM) for 24 h, these cells were stained with Annexin V-FITC/PI and analyzed by a flow cytometer. (b) The quantitative analysis of the apoptotic cell percentages is shown. (c) The representative images of TEM: more autophagic vacuoles (red arrows) are shown in the three apatinib-treated (20 μM) OC cell lines for 24 h compared with the DMSO-treated control groups. Scale bar = 1 μm (the middle panel)/500 nm (the left and right panels). (d) The representative images of immunofluorescence: a dot pattern of LC3-II fluorescence is presented in the apatinib-treated (20 μM) OC cells (40x). Scale bar = 20 μm. (e) After treatment with 20 μM apatinib for 24 h, the protein levels of cleaved PARP, Bcl-2, Bax, p62, and LC3B (LC3 II/LC3 I) were determined by western blotting. (f) The relative western blot gray values are shown in the histogram. Data are presented as the mean ± SD of three independent experiments. APA: apatinib. $^{*}P < 0.05$, $^{**}P < 0.01$, compared with the control groups.

changed in apatinib-treated cells as observed by western blotting (Figure 5(b)). These results suggest that apatinib could inhibit the levels of GSH, Nrf2, and HO-1 in OC cells.

To provide further supporting evidence, TBHQ, a specific activator of Nrf2, was utilized. The levels of nuclear and total Nrf2 and HO-1 were significantly upregulated upon the administration of TBHQ, which confirmed the activating effect of TBHQ on Nrf2. (Figures 5(c) and 5(d)). GSH levels were then measured after treating the cells in the absence or presence of TBHQ and apatinib. The results confirmed that the activation of the Nrf2 pathway could upregulate the GSH levels in the cells without apatinib treatment and that the inhibition of GSH by apatinib was reversed by TBHQ treatment (Figure 5(e)). Thus, apatinib could suppress GSH to generate ROS by negatively regulating the Nrf2/HO-1 pathway.

3.6. VEGFR2 Regulates Nrf2 Pathway and Apatinib Remains Effective at Low Level of VEGFR2 in OC. As apatinib is a specific VEGFR2 inhibitor, we wondered about the relationship between VEGFR2 and the Nrf2 pathway. Firstly, we found that there was a significant positive correlation between the *Nrf2* and *VEGFR2* mRNA levels based on the GEPIA database ($R = 0.2$, $P = 4.1e-05$; Figure 6(a)). Then, the protein and mRNA levels of VEGFR2 were examined in three ovarian cancer cell lines. A2780 cell line showed the lowest level among these cell lines while SKOV-3 showed the highest level (Figures 6(b) and 6(c)). These two cell lines were used for further experiments. Overexpression of VEGFR2 in the A2780 cell line resulted in upregulated both mRNA and protein levels of Nrf2, indicating that VEGFR2 regulated Nrf2 at the transcription level. In addition, we found that upregulated VEGFR2 could significantly increase the levels of Nrf2 downstream antioxidant genes HO-1, heavy and light subunits of γ-glutamyl cysteine synthetase (GCLC and GCLM, which are important rate-limiting enzymes for GSH synthesis) (Figures 6(d) and 6(e)). The opposite results were observed in the SKOV-3 cell line upon downregulation of

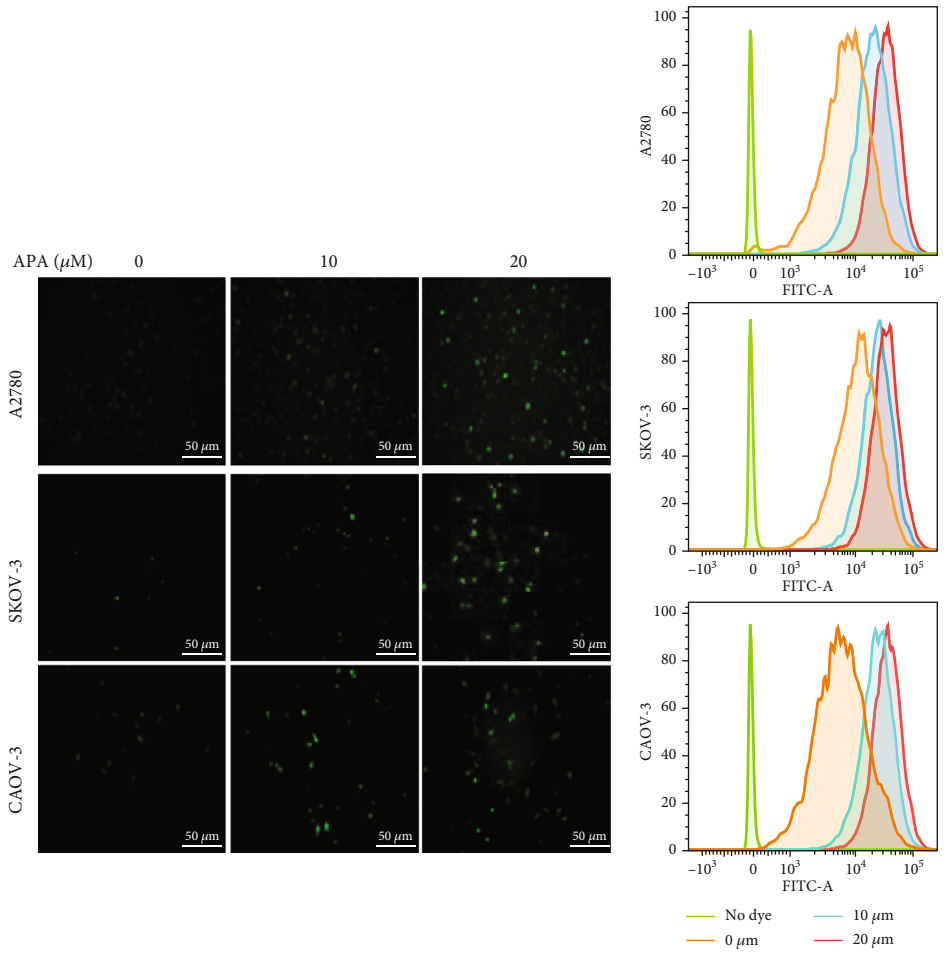

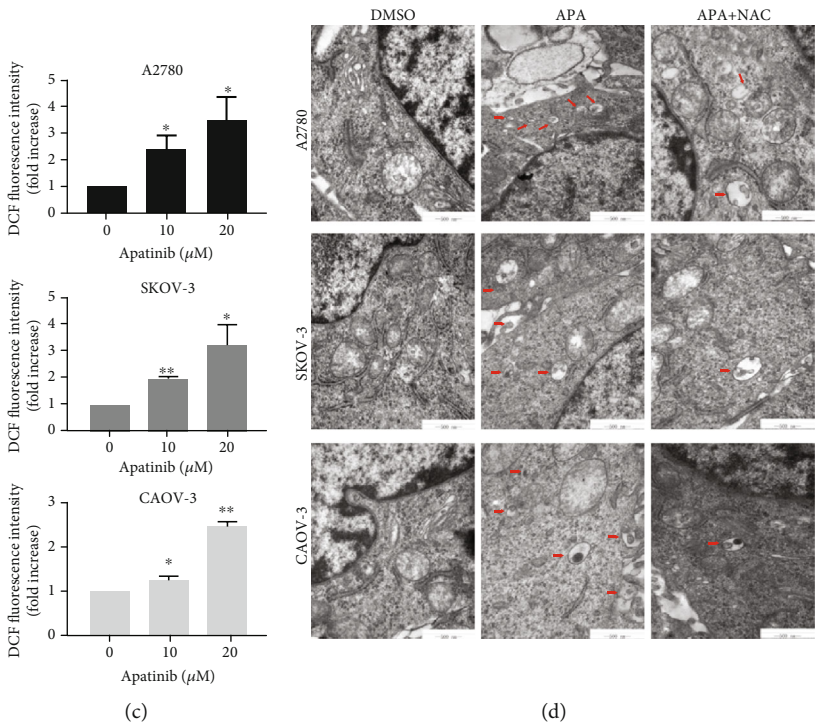

Figure 4: Continued.

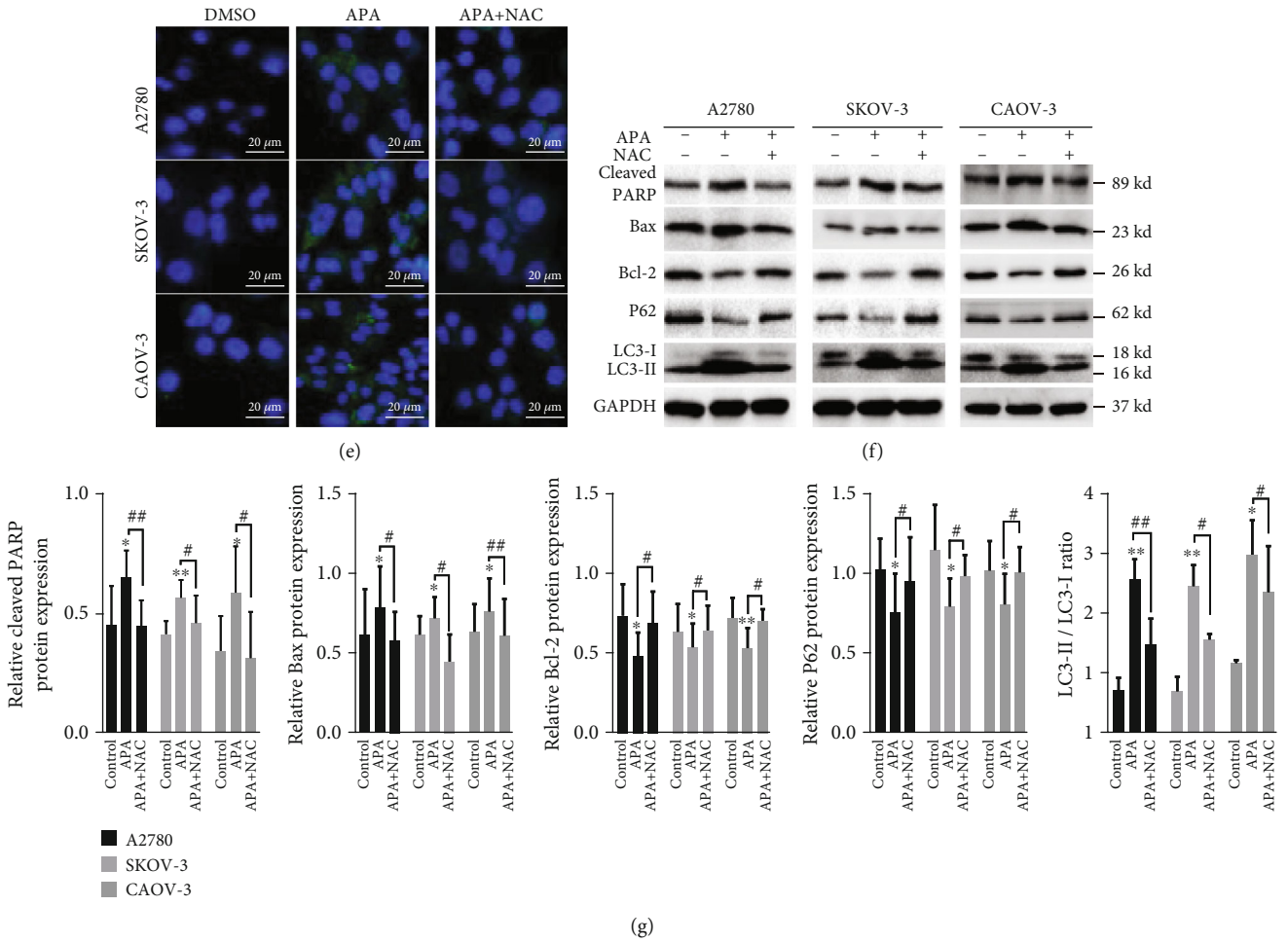

Figure 4: The generation of ROS is crucial for apatinib-induced apoptosis and autophagy. (a) The representative images of fluorescence intensity of DCFH-DA in apatinib-treated (0, 10, and 20 μM) A2780, SKOV-3, and CAOV-3 cells observed by a fluorescence microscope (20x). Scale bar = 50 μm. (b, c) The fluorescence intensity of DCFH-DA was detected by a flow cytometer, and the results were analyzed by FlowJo software. (d, e) The representative images of TEM and fluorescence microscopy after apatinib incubation (20 μM) without or with NAC (5 mM). Scale bar = 20 μm (fluorescence images)/500 nm (TEM images). (f) The expression of apoptosis- and autophagy-related proteins was tested by western blotting after apatinib incubation without or with NAC (5 mM). (g) The relative western blot gray values are shown in the histogram. Data are presented as the mean ± SD of three independent experiments. APA: apatinib. $^{*}P < 0.05$, $^{**}P < 0.01$, compared with the control groups. $^{\#}P < 0.05$, $^{\#\#}P < 0.01$.

VEGFR2 by siRNA (Figures 6(f) and 6(g)). These results suggest that VEGFR2 was a positive regulator of Nrf2 pathway.

Next, we investigated VEGFR2 expression in OC tissues based on a series of online databases since bioinformatics analysis has become a hot research focus. The data from the Oncomine database indicated that *VEGFR2* mRNA expression was lower in OC than in normal tissue. In comparison with 10 samples of normal ovarian surface epithelium, the mRNA levels of *VEGFR2* were significantly lower in 185 cases of ovarian carcinoma ($P = 1.8e-08$; Figure 6(h)), and *VEGFR2* was significantly downregulated in different pathological subtypes of OC (serous, mucinous, endometrioid, and clear cell), especially in the serous type (Table 1). The GEPIA database validated the aforementioned results (Figure 6(i)). In addition, the representative immunochemistry images from the HPA database showed that no significantly positive VEGFR2 staining could be detected in any pathological subtype of OC compared with normal tissues (Figure 6(j)). These findings attracted our interest that whether apatinib could function through a low level of VEGFR2 in OC. We confirmed that apatinib could still reduce the level of VEGFR2 in the SKOV-3 cell line when VEGFR2 was downregulated by siRNA (Figure 6(k)). In addition, compared to the control groups, apatinib still exerted inhibitory effect on cell viability and migration although VEGFR2 level was reduced in OC cells (Figures 6(l) and 6(m)). Besides, we previously observed the antitumor effect of apatinib on the A2780 cell line, which expressed a relative low level of VEGFR2 originally. These findings indicate that apatinib remained effective at low level of VEGFR2 in OC.

4. Discussion

Apatinib, a small-molecule selective tyrosine kinase inhibitor of VEGFR-2, is considered a new-generation oral

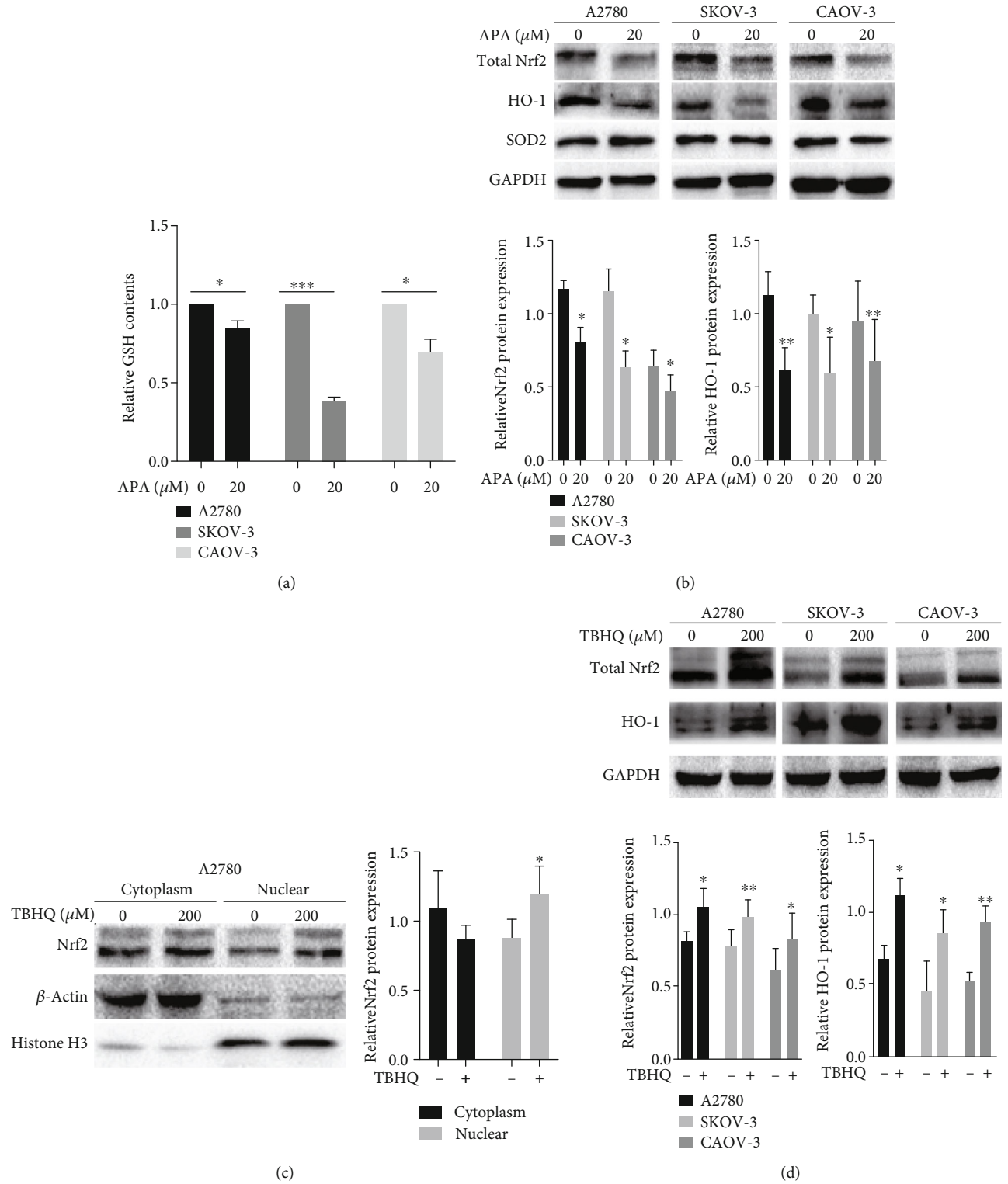

Figure 5: Continued.

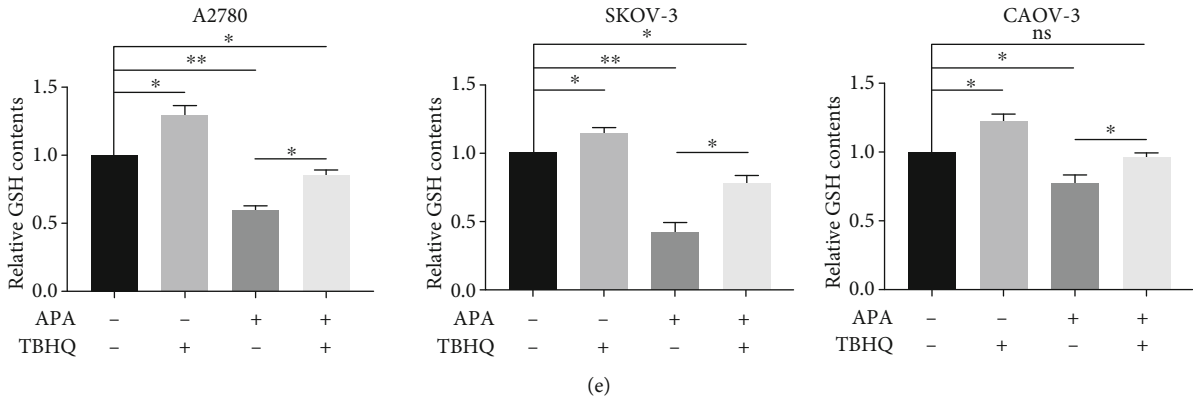

Figure 5: Apatinib suppressed GSH to generate ROS via the downregulation of Nrf2/HO-1. (a) The relative GSH levels in A2780, SKOV-3, and CAOV-3 cells after apatinib treatment (20 μM). (b) The protein expression of Nrf2, HO-1, and SOD2 was tested by western blotting after incubation with apatinib. The relative western blot gray values are shown in the histogram. (c, d) The upregulated protein expression of total Nrf2, nuclear Nrf2, and HO-1 was determined by western blotting and nuclear and cytoplasm isolation after the application of TBHQ (200 μM). The relative western blot gray values are shown in the histogram. (e) The relative GSH levels were detected in the three OC cell lines after incubation in the absence or presence of TBHQ and apatinib. Data are presented as the mean ± SD of three independent experiments. APA: apatinib; ns: not significant. $^{*}P < 0.05$, $^{**}P < 0.01$, and $^{***}P < 0.001$, compared with the control groups.

antiangiogenesis drug in China; it has been reported to be effective in various solid tumors. In line with previous case reports that apatinib has potential antitumor activity in patients with OC [25–30], we found it to be effective against OC cell proliferation in both a time- and concentration-dependent manner in vitro. Similarly, apatinib has been found to inhibit cell growth in breast cancer [8], NSCLC [9], colon cancer [10], hepatocellular carcinoma [11], pancreatic cancer [12], anaplastic thyroid cancer [13, 14], osteosarcoma [15], and OC [31]. Interestingly, apatinib shows contrasting effects on OC cell proliferation, with no cytotoxic effects on OC cells and no alteration of the cell cycle or apoptosis in vitro. However, it inhibits EMT in OC cells by inhibiting the JAK/STAT3 and PI3K/Akt signaling pathways, resulting in the suppression of tumor volume in vivo by inhibiting tumor angiogenesis [32]. Consistently, we found that apatinib substantially inhibited the migration of OC cells in a concentration-dependent manner by the negative regulation of EMT. This antimetastatic effect of apatinib has also been observed in other cancers, such as breast cancer, colon cancer, pancreatic cancer, and anaplastic thyroid cancer [8, 10, 12, 14]. Thus, apatinib exerts favorable antitumor efficacy and could be a promising therapeutic strategy for patients with OC.

With regard to the antitumor mechanism of apatinib, recent studies have shown that apatinib could act directly on tumor cells by inducing apoptosis and cell cycle arrest [10, 12, 14, 15, 19]. Our results showed that it induced apoptosis in OC cells in a concentration-dependent manner. Likewise, autophagy appears to be involved as more autophagosomes and autolysosomes were present in the treated groups than in the controls. The dot pattern of LC3-II fluorescence, the increased LC3-II/LC-I expression ratio, and a decrease in p62 levels were observed in apatinib-treated OC cells indicating that apatinib can induce autophagy. Interestingly, the contrary roles of apatinib-induced autophagy have been reported. In colon cancer and pancreatic cancer, apatinib promotes tumor cell death and suppresses tumor growth by inducing autophagy [10, 12]. Conversely, apatinib promotes protective autophagy in anaplastic thyroid cancer and osteosarcoma. Moreover, the inhibition of autophagy sensitizes these tumor cells to apatinib-induced apoptosis in vitro and enhances the effect of apatinib-induced growth inhibition in anaplastic thyroid cancer cells in vivo [13, 15]. Therefore, the role of apatinib-induced autophagy may be context specific and should be further explored in OC.

Increasing evidence has shown that ROS plays an important role in tumors [33]; the interplay between ROS, apoptosis, and autophagy has attracted research attention [20, 21, 34, 35]. Treatment with apatinib may increase ROS in pancreatic cancer and cervical cancer [12, 19]. We likewise observed that apatinib promoted ROS generation in a concentration-dependent manner. In addition, apatinib-induced apoptosis and autophagy were ROS-dependent in OC cells, since treatment with a ROS scavenger reversed the promotion effect. Therefore, the promotion of ROS may be the novel cytotoxic effect of apatinib.

Among ROS regulators, GSH is remarkable as it is a ROS scavenger and is involved in multiple processes during tumor development, including cellular proliferation and the development of chemotherapy resistance [22, 23]. The Nrf2/HO-1 pathway, which is well known to eliminate ROS [24], is reported to be involved in the regulation of GSH abundance [22, 36]; moreover, upregulated protein levels of Nrf2 and HO-1 have been found in many tumors, including OC [37, 38]. In our study, the levels of GSH, Nrf2, and HO-1 were significantly inhibited by apatinib and the activation of the Nrf2 pathway upregulated the levels of GSH. The reversal of the apatinib-mediated GSH inhibition by TBHQ indicated that apatinib suppressed GSH to generate ROS by negatively regulating the Nrf2/HO-1 pathway.

In addition, a significant positive correlation was indicated between Nrf2 and VEGFR2 in OC based on the GEPIA database. We confirmed that the levels of Nrf2 and its

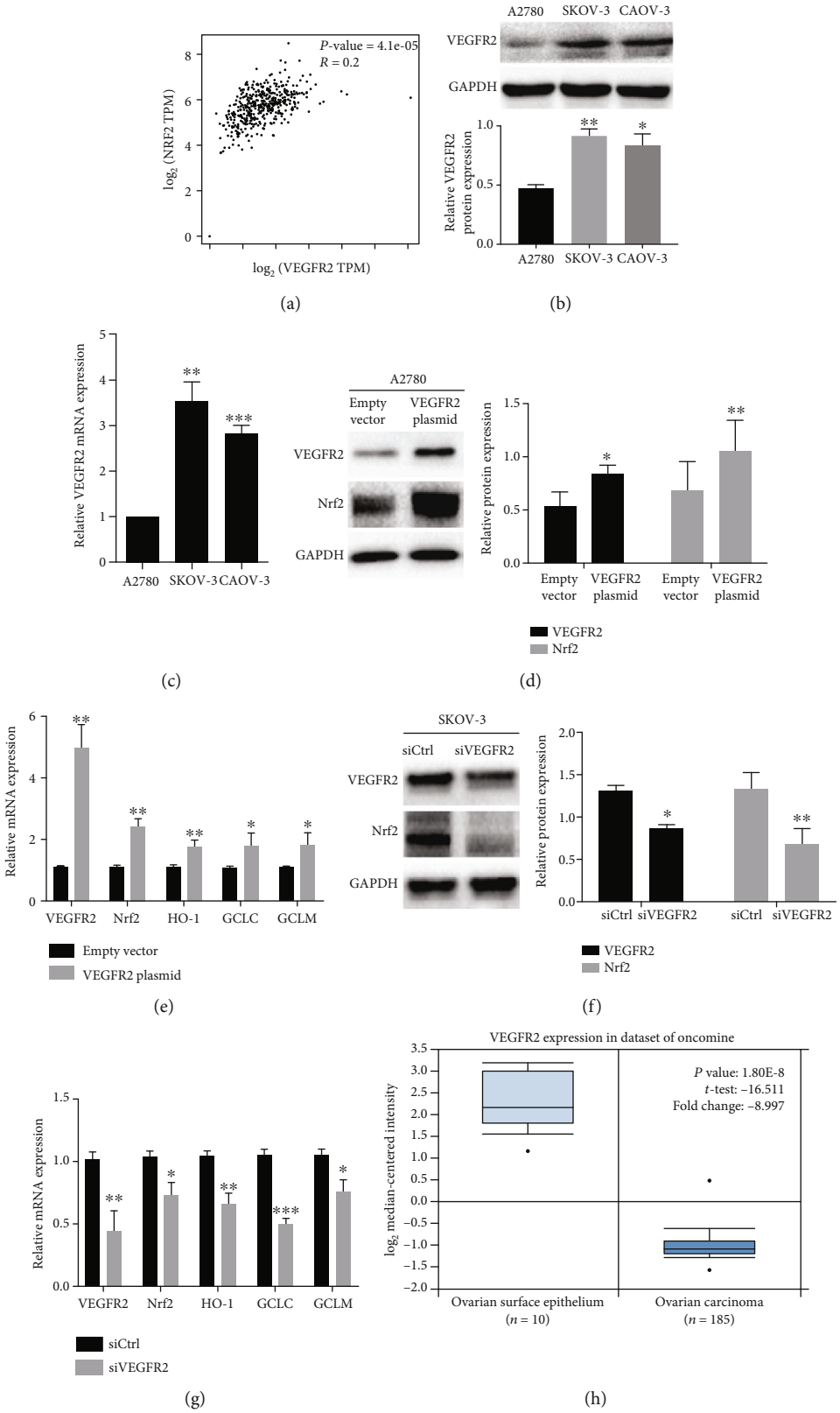

Figure 6: Continued.

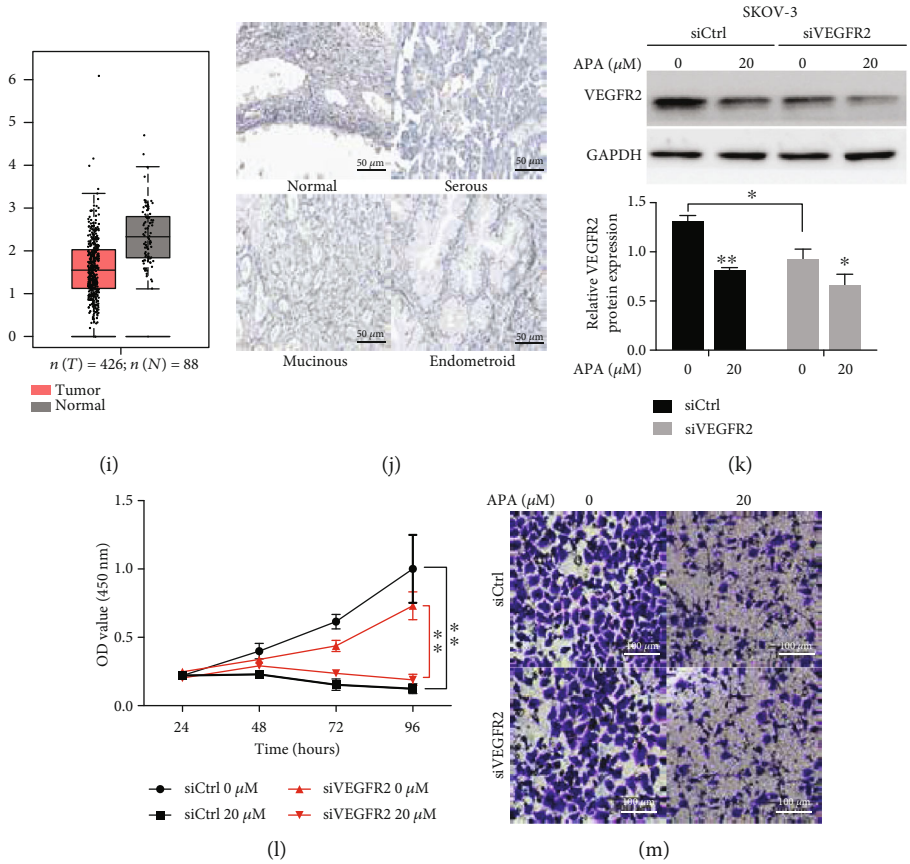

Figure 6: VEGFR2 regulates the Nrf2 pathway, and apatinib remains effective at a low level of VEGFR2 in OC. (a) *Nrf2* had a significant positive relationship with *VEGFR2* based on the GEPIA database. (b, c) The protein and mRNA levels of VEGFR2 were examined in three ovarian cancer cell lines by western blotting and qRT-PCR, respectively. A2780 cells were transfected with VEGFR2 or empty plasmid. (d) The protein levels of VEGFR2 and Nrf2 were tested by western blotting and (e) the increased mRNA levels of VEGFR2, Nrf2, HO-1, GCLC, and GCLM were determined by qRT-PCR. SKOV-3 cells were transfected with VEGFR2 or control siRNA. (f) The protein levels of VEGFR2 and Nrf2 were tested by western blotting and (g) the decreased mRNA levels of VEGFR2, Nrf2, HO-1, GCLC, and GCLM were tested by qRT-PCR. (h) The mRNA levels of VEGFR2 significantly decreased in OC compared with normal ovarian surface epithelium based on the dataset of Oncomine. (i) VEGFR2 mRNA expression was decreased in OC compared with normal tissues based on GEPIA database. (j) Representative immunohistochemical staining images of VEGFR2 in different pathological subtypes of OC and normal tissues based on the HPA database. Scale bar = 50 μm. SKOV-3 cells were transfected with VEGFR2 or control siRNA. (k) The protein levels of VEGFR2 were reduced after incubation with 20 μM apatinib. (l) The cell viability and (m) the migration of transfected SKOV-3 cells were suppressed by apatinib. Scale bar = 100 μm. The relative western blot gray values are shown in the histogram. Data are presented as the *mean* ± *SD* of three independent experiments. APA: apatinib; TPM: transcripts per million.". $^{*}P < 0.05$, $^{**}P < 0.01$, and $^{***}P < 0.001$, compared with the control groups.

downstream genes could be significantly regulated by VEGFR2. Among these downstream genes, GCLC and GCLM are two catalytic subunits of glutamate cysteine ligase (GCL), whose level and enzymatic activity constitute rate-limiting steps for GSH synthesis and can also be controlled by Nrf2 [39]. Considering the fact that high GCLC or GCLM levels are found in patients with various cancers [40, 41] and that the reduction of GSH production by the irreversible GCL inhibitor promotes apoptosis and attenuates cell growth in cancer cells [42], we speculate that apatinib may also function as a ROS inducer by suppressing the VEGFR2-Nrf2 path, leading to decreased GCLC and GCLM levels, resulting in the reduction of GSH.

Recent studies have mostly focused on apatinib inhibiting VEGFR2 and its downstream pathway as antiangiogenesis and antitumorigenesis targets [14, 43, 44] owing to the fact that VEGFR2 expression is upregulated in the vasculature of some tumors compared to the normal vascular system [45–47]. For instance, VEGFR2 expression is elevated in osteosarcoma and cervical cancer tissues [15, 19]. Apatinib can inhibit tumor cell growth by blocking the VEGFR2/-STAT3/Bcl-2 or Akt/GSK3β/angiogenin signaling pathways, suppressing tumor angiogenesis in osteosarcoma and anaplastic thyroid cancer, respectively [14, 15]. Interestingly, in our study, we found that both the mRNA and protein levels of VEGFR2 were lower in OC than in normal tissue based on a series of online databases. Similarly, VEGFR2 was reported to be negatively expressed in breast cancer [48]. However, even though we downregulated the level of VEGFR2 in the SKOV-3 cell line, which showed a relatively high level of VEGFR2, apatinib still exerted effective inhibition on VEGFR2 and antitumor effect on OC cells. Besides,

Table 1: VEGFR2 expression (cancer vs. normal) in other datasets of Oncomine.

Datasets	Subtype	*P* value	*t*-test	Fold change	*N*
Lu ovarian	Serous	**0.007**	-3.921	-1.622	20
	Mucinous	**0.007**	-3.453	-1.592	9
	Endometrioid	**0.009**	-3.514	-1.562	9
	Clear cell	**0.013**	-2.902	-1.480	7
TCGA ovarian	Serous	**0.002**	-3.997	-1.708	586
Yoshihara ovarian	Serous	**8.33E-4**	-3.460	-2.572	22
Adib ovarian	Serous	**0.015**	-3.044	-1.406	6
Hendrix ovarian	Serous	**0.033**	-2.580	-1.137	41
	Mucinous	0.118	-1.313	-1.078	13
	Endometrioid	0.058	-2.075	-1.107	37
	Clear cell	0.157	-1.095	-1.065	8

Notes: the bold font indicates the difference was significant statistically. The negative value of fold change represents that VEGFR2 expression was downregulated. *N*: number of patients.

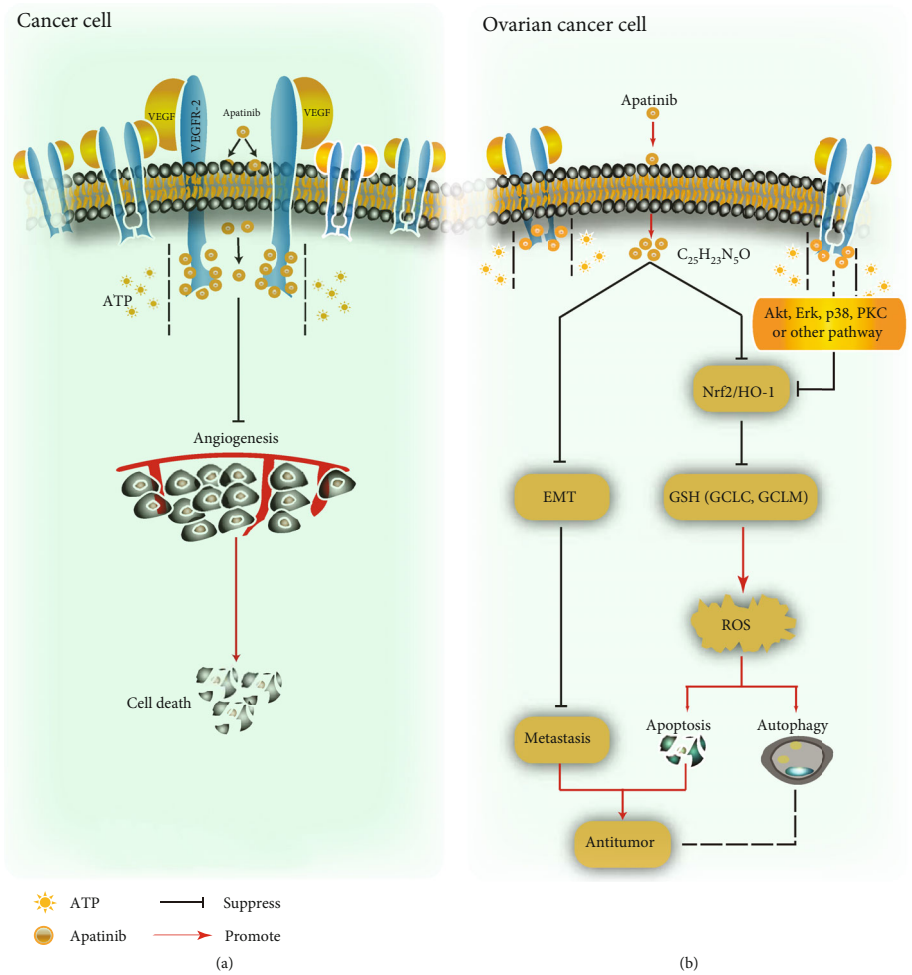

Figure 7: Schematic representation of the antitumor effect of apatinib in cancer cells. (a) After entering the tumor cell, apatinib competes with adenosine triphosphate (ATP) for binding to the ATP site of VEGFR2, inhibiting angiogenesis by blocking downstream signal transduction, resulting in tumor cell death. (b) Apatinib inhibits OC cell migration by suppressing EMT and promotes ROS-dependent apoptosis and autophagy through negatively regulating the VEGFR2/Nrf2/HO-1-GSH pathway in OC cells. PKC: protein kinase C.

apatinib showed favorable antitumor efficacy on the A2780 cell line, which expressed a relatively low level of VEGFR2 originally. Taken these findings together, we concluded that apatinib could function through a low level of VEGFR2 in OC.

Preclinical research has suggested that apatinib may reverse multidrug resistance by inhibiting some proteins associated with its development [49–51]. In two recent phase 2 clinical trials, patients with platinum-resistant and platinum-refractory OC benefited from treatment with apatinib alone or in combination with oral etoposide [52, 53]. Our previous study indicated that GSH, Nrf2, and HO-1 were upregulated in cisplatin-resistant OC cell lines [16]. Therefore, we speculate that apatinib may increase the sensitivity of OC cells to cisplatin by inhibiting the Nrf2 pathway as well. However, this hypothesis needs to be tested further.

Unfortunately, there is a lack of clarity on the precise mechanism of the relationship between Nrf2 and VEGFR2, although the GEPIA database indicated a significant positive correlation between them. In addition to the direct suppression of Nrf2 as discussed above, another possibility is that Nrf2 could be regulated by apatinib via downstream signaling of VEGFR2, such as Akt [54], Erk, p38, and protein kinase C [55]. However, this hypothesis will also need to be investigated in future experiments.

5. Conclusions

In conclusion, we found that apatinib inhibited the proliferation and metastasis of OC cells. Notably, apatinib promoted ROS-dependent apoptosis and autophagy mainly via the inhibition of the Nrf2/HO-1-GSH signaling pathway (Figure 7). This novel regulatory mechanism provides a new perspective for the antitumor effect of apatinib in OC treatment; moreover, the combination of this drug with an Nrf2 inhibitor may be a promising treatment strategy for patients with OC. However, further animal studies or clinical trials need to be performed to confirm this.

Data Availability

The data used to support the findings of this study are available from the corresponding author upon request.

Conflicts of Interest

The authors declare that there is no conflict of interest regarding the publication of this paper.

Authors' Contributions

QL, SW, and XS contributed to the conception and design of the study. XS, JL, and YL performed the experiments and the statistical analysis. XS and SW wrote the first draft of the manuscript. All authors contributed to manuscript revision and have read and approved the submitted version.

Acknowledgments

We would like to thank Editage (https://www.editage.cn) for English language editing and Mr. Yifu Song for the technological support. This research was funded by the National Natural Science Foundation of China, grant numbers 81672964, 81874214, and 81702269.

References

[1] W. Chen, R. Zheng, P. D. Baade et al., "Cancer statistics in China, 2015," *CA: A Cancer Journal for Clinicians*, vol. 66, no. 2, pp. 115–132, 2016.

[2] R. F. Ozols, B. N. Bundy, B. E. Greer et al., "Phase III trial of carboplatin and paclitaxel compared with cisplatin and paclitaxel in patients with optimally resected stage III ovarian cancer: a Gynecologic Oncology Group study," *Journal of Clinical Oncology*, vol. 21, no. 17, pp. 3194–3200, 2003.

[3] I. J. Jacobs, U. Menon, A. Ryan et al., "Ovarian cancer screening and mortality in the UK Collaborative Trial of Ovarian Cancer Screening (UKCTOCS): a randomised controlled trial," *The Lancet*, vol. 387, no. 10022, pp. 945–956, 2016.

[4] D. Hanahan and R. A. Weinberg, "Hallmarks of cancer: the next generation," *Cell*, vol. 144, no. 5, pp. 646–674, 2011.

[5] A. L. Jackson, E. L. Eisenhauer, and T. J. Herzog, "Emerging therapies: angiogenesis inhibitors for ovarian cancer," *Expert Opinion on Emerging Drugs*, vol. 20, no. 2, pp. 331–346, 2015.

[6] U. A. Matulonis, "Bevacizumab and its use in epithelial ovarian cancer," *Future Oncology*, vol. 7, no. 3, pp. 365–379, 2011.

[7] S. Tian, H. Quan, C. Xie et al., "YN968D1 is a novel and selective inhibitor of vascular endothelial growth factor receptor-2 tyrosine kinase with potent activity in vitro and in vivo," *Cancer Science*, vol. 102, no. 7, pp. 1374–1380, 2011.

[8] H. Zhang, J. Sun, W. Ju et al., "Apatinib suppresses breast cancer cells proliferation and invasion via angiomotin inhibition," *American Journal of Translational Research*, vol. 11, no. 7, pp. 4460–4469, 2019.

[9] Z. L. Liu, B. J. Jin, C. G. Cheng et al., "Apatinib resensitizes cisplatin-resistant non-small cell lung carcinoma A549 cell through reversing multidrug resistance and suppressing ERK signaling pathway," *European Review for Medical and Pharmacological Sciences*, vol. 21, no. 23, pp. 5370–5377, 2017.

[10] W. Lu, H. Ke, D. Qianshan, W. Zhen, X. Guoan, and Y. Honggang, "Apatinib has anti-tumor effects and induces autophagy in colon cancer cells," *Iranian Journal of Basic Medical Sciences*, vol. 20, no. 9, pp. 990–995, 2017.

[11] H. Zhang, Y. Cao, Y. Chen, G. Li, and H. Yu, "Apatinib promotes apoptosis of the SMMc-7721 hepatocellular carcinoma cell line via the PI3K/Akt pathway," *Oncology Letters*, vol. 15, no. 4, pp. 5739–5743, 2018.

[12] K. He, L. Wu, Q. Ding et al., "Apatinib promotes apoptosis of pancreatic cancer cells through downregulation of hypoxia-inducible factor-1α and increased levels of reactive oxygen species," *Oxidative Medicine and Cellular Longevity*, vol. 2019, Article ID 5152072, 9 pages, 2019.

[13] H. Feng, X. Cheng, J. Kuang et al., "Apatinib-induced protective autophagy and apoptosis through the AKT-mTOR pathway in anaplastic thyroid cancer," *Cell Death and Disease*, vol. 9, no. 10, p. 1030, 2018.

[14] Z. Jin, X. Cheng, H. Feng et al., "Apatinib inhibits angiogenesis via suppressing Akt/GSK3β/ANG signaling pathway in anaplastic thyroid cancer," *Cellular Physiology and Biochemistry*, vol. 44, no. 4, pp. 1471–1484, 2017.

[15] K. Liu, T. Ren, Y. Huang et al., "Apatinib promotes autophagy and apoptosis through VEGFR2/STAT3/BCL-2 signaling in osteosarcoma," *Cell Death & Disease*, vol. 8, no. 8, article e3015, 2017.

[16] X. Sun, S. Wang, J. Gai et al., "SIRT5 promotes cisplatin resistance in ovarian cancer by suppressing DNA damage in a ROS-dependent manner via regulation of the Nrf2/HO-1 pathway," *Frontiers in Oncology*, vol. 9, p. 754, 2019.

[17] X. Sun, S. Wang, and Q. Li, "Comprehensive analysis of expression and prognostic value of sirtuins in ovarian cancer," *Frontiers in Genetics*, vol. 10, p. 879, 2019.

[18] C. M. Beaufort, J. C. A. Helmijr, A. M. Piskorz et al., "Ovarian cancer cell line panel (OCCP): clinical importance of in vitro morphological subtypes," *PLoS One*, vol. 9, no. 9, p. e103988, 2014.

[19] H. Qiu, J. Li, Q. Liu, M. Tang, and Y. Wang, "Apatinib, a novel tyrosine kinase inhibitor, suppresses tumor growth in cervical cancer and synergizes with paclitaxel," *Cell Cycle*, vol. 17, no. 10, pp. 1235–1244, 2018.

[20] L. Li, J. Tan, Y. Miao, P. Lei, and Q. Zhang, "ROS and autophagy: interactions and molecular regulatory mechanisms," *Cellular and Molecular Neurobiology*, vol. 35, no. 5, pp. 615–621, 2015.

[21] M. Redza-Dutordoir and D. A. Averill-Bates, "Activation of apoptosis signalling pathways by reactive oxygen species," *Biochimica et Biophysica Acta (BBA) - Molecular Cell Research*, vol. 1863, no. 12, pp. 2977–2992, 2016.

[22] A. Bansal and M. C. Simon, "Glutathione metabolism in cancer progression and treatment resistance," *Journal of Cell Biology*, vol. 217, no. 7, pp. 2291–2298, 2018.

[23] S. C. Nunes and J. Serpa, "Glutathione in ovarian cancer: a double-edged sword," *International Journal of Molecular Sciences*, vol. 19, no. 7, p. 1882, 2018.

[24] A. L. Furfaro, N. Traverso, C. Domenicotti et al., "The Nrf2/HO-1 axis in cancer cell growth and chemoresistance," *Oxidative Medicine and Cellular Longevity*, vol. 2016, Article ID 1958174, 14 pages, 2016.

[25] Y. Cheng, J. Zhang, H. Geng, S. Qin, and H. Hua, "Multiline treatment combining apatinib with toptecan for platinum-resistant recurrent ovarian cancer patients: a report of three cases," *OncoTargets and Therapy*, vol. 11, pp. 1989–1995, 2018.

[26] H. Sun, M. Xiao, S. Liu, and R. Shi, "Use of apatinib combined with pemetrexed for advanced ovarian cancer," *Medicine*, vol. 97, no. 27, pp. e11036–e11036, 2018.

[27] M. Jin, J. Cai, X. Wang, T. Zhang, and Y. Zhao, "Successful maintenance therapy with apatinib inplatinum-resistant advanced ovarian cancer and literature review," *Cancer Biology and Therapy*, vol. 19, no. 12, pp. 1088–1092, 2018.

[28] D. Zhang, J. Huang, Y. Sun, and Q. Guo, "Long-term progression-free survival of apatinib monotherapy for relapsed ovarian cancer: a case report and literature review," *OncoTargets and Therapy*, vol. 12, pp. 3635–3644, 2019.

[29] L. Deng, Y. Wang, W. Lu, Q. Liu, J. Wu, and J. Jin, "Apatinib treatment combined with chemotherapy for advanced epithelial ovarian cancer: a case report," *OncoTargets and Therapy*, vol. 10, pp. 1521–1525, 2017.

[30] M. Zhang, Z. Tian, and Y. Sun, "Successful treatment of ovarian cancer with apatinib combined with chemotherapy," *Medicine*, vol. 96, no. 45, article e8570, 2017.

[31] L. Chen, X. Cheng, W. Tu et al., "Apatinib inhibits glycolysis by suppressing the VEGFR2/AKT1/SOX5/GLUT4 signaling pathway in ovarian cancer cells," *Cellular Oncology*, vol. 42, no. 5, pp. 679–690, 2019.

[32] J. Ding, X. Y. Cheng, S. Liu et al., "Apatinib exerts anti-tumour effects on ovarian cancer cells," *Gynecologic Oncology*, vol. 153, no. 1, pp. 165–174, 2019.

[33] S. S. Sabharwal and P. T. Schumacker, "Mitochondrial ROS in cancer: initiators, amplifiers or an Achilles' heel?," *Nature Reviews Cancer*, vol. 14, no. 11, pp. 709–721, 2014.

[34] L. Poillet-perez, G. Despouy, R. Delage-mourroux, and M. Boyer-guittaut, "Interplay between ROS and autophagy in cancer cells, from tumor initiation to cancer therapy," *Redox Biology*, vol. 4, pp. 184–192, 2015.

[35] R. Scherz-shouval and Z. Elazar, "Regulation of autophagy by ROS : physiology and pathology," *Trends in Biochemical Sciences*, vol. 36, no. 1, pp. 30–38, 2011.

[36] I. H. Kankia, H. S. Khalil, S. P. Langdon, P. R. Moult, J. L. Bown, and Y. Y. Deeni, "NRF2 regulates HER1 signaling pathway to modulate the sensitivity of ovarian cancer cells to lapatinib and erlotinib," *Oxidative Medicine and Cellular Longevity*, vol. 2017, Article ID 1864578, 19 pages, 2017.

[37] G. Shim, S. Manandhar, D. Shin, T.-H. Kim, and M.-K. Kwak, "Acquisition of doxorubicin resistance in ovarian carcinoma cells accompanies activation of the NRF2 pathway," *Free Radical Biology & Medicine*, vol. 47, no. 11, pp. 1619–1631, 2009.

[38] L.-J. Bao, M. C. Jaramillo, Z.-B. Zhang et al., "Nrf2 induces cisplatin resistance through activation of autophagy in ovarian carcinoma," *International Journal of Clinical and Experimental Pathology*, vol. 7, no. 4, pp. 1502–1513, 2014.

[39] S. C. Lu, "Glutathione synthesis," *Biochimica et Biophysica Acta (BBA) - General Subjects*, vol. 1830, no. 5, pp. 3143–3153, 2013.

[40] S. Fujimori, Y. Abe, M. Nishi et al., "The subunits of glutamate cysteine ligase enhance cisplatin resistance in human non-small cell lung cancer xenografts in vivo," *International Journal of Oncology*, vol. 25, no. 2, pp. 413–418, 2004.

[41] S. C. Lu, "Regulation of glutathione synthesis," *Molecular Aspects of Medicine*, vol. 30, no. 1–2, pp. 42–59, 2009.

[42] K. K. Andringa, M. C. Coleman, N. Aykin-Burns et al., "Inhibition of glutamate cysteine ligase activity sensitizes human breast cancer cells to the toxicity of 2-deoxy-D-glucose," *Cancer Research*, vol. 66, no. 3, pp. 1605–1610, 2006.

[43] L. Fornaro, E. Vasile, and A. Falcone, "Apatinib in advanced gastric cancer: a doubtful step forward," *Journal of Clinical Oncology*, vol. 34, no. 31, pp. 3822-3823, 2016.

[44] D. Zhao, H. Hou, and X. Zhang, "Progress in the treatment of solid tumors with apatinib: a systematic review," *OncoTargets and Therapy*, vol. 11, pp. 4137–4147, 2018.

[45] K. H. Plate, G. Breier, B. Millauer, A. Ullrich, and W. Risau, "Up-regulation of vascular endothelial growth factor and its cognate receptors in a rat glioma model of tumor angiogenesis," *Cancer Research*, vol. 53, no. 23, pp. 5822–5827, 1993.

[46] K. Holmes, O. L. Roberts, A. M. Thomas, and M. J. Cross, "Vascular endothelial growth factor receptor-2: structure, function, intracellular signalling and therapeutic inhibition," *Cellular Signalling*, vol. 19, no. 10, pp. 2003–2012, 2007.

[47] N. R. Smith, D. Baker, N. H. James et al., "Vascular endothelial growth factor receptors VEGFR-2 and VEGFR-3 are localized primarily to the vasculature in human primary solid cancers," *Clinical Cancer Research*, vol. 16, no. 14, pp. 3548–3561, 2010.

[48] T. R. Holzer, A. D. Fulford, D. M. Nedderman et al., "Tumor cell expression of vascular endothelial growth factor receptor 2 is an adverse prognostic factor in patients with squamous cell carcinoma of the lung," *PLoS One*, vol. 8, no. 11, p. e80292, 2013.

[49] F. Li, Z. Liao, C. Zhang et al., "Apatinib as targeted therapy for sarcoma," *Oncotarget*, vol. 9, no. 36, pp. 24548–24560, 2018.

[50] X. Tong, F. Wang, S. Liang et al., "Apatinib (YN968D1) enhances the efficacy of conventional chemotherapeutical drugs in side population cells and ABCB1-overexpressing leukemia cells," *Biochemical Pharmacology*, vol. 83, no. 5, pp. 586–597, 2012.

[51] Y.-J. Mi, Y.-J. Liang, H.-B. Huang et al., "Apatinib (YN968D1) reverses multidrug resistance by inhibiting the efflux function of multiple ATP-binding cassette transporters," *Cancer Research*, vol. 70, no. 20, pp. 7981–7991, 2010.

[52] C. Y. Lan, Y. Wang, Y. Xiong et al., "Apatinib combined with oral etoposide in patients with platinum-resistant or platinum-refractory ovarian cancer (AEROC): a phase 2, single-arm, prospective study," *The Lancet Oncology*, vol. 19, no. 9, pp. 1239–1246, 2018.

[53] M. Miao, G. Deng, S. Luo et al., "A phase II study of apatinib in patients with recurrent epithelial ovarian cancer," *Gynecologic Oncology*, vol. 148, no. 2, pp. 286–290, 2018.

[54] C. Ji, J.-w. Huang, Q.-y. Xu et al., "Gremlin inhibits UV-induced skin cell damages via activating VEGFR2-Nrf2 signaling," *Oncotarget*, vol. 7, no. 51, pp. 84748–84757, 2016.

[55] T. Nguyen, C. S. Yang, and C. B. Pickett, "The pathways and molecular mechanisms regulating Nrf2 activation in response to chemical stress," *Free Radical Biology & Medicine*, vol. 37, no. 4, pp. 433–441, 2004.

Hindawi
Oxidative Medicine and Cellular Longevity
Volume 2020, Article ID 2908108, 12 pages
https://doi.org/10.1155/2020/2908108

Research Article

Fernblock® Upregulates NRF2 Antioxidant Pathway and Protects Keratinocytes from $PM_{2.5}$-Induced Xenotoxic Stress

Pablo Delgado-Wicke,[1] **Azahara Rodríguez-Luna**,[2] **Yoshifumi Ikeyama**,[3] **Yoichi Honma**,[3] **Toshiaki Kume**,[4] **María Gutierrez**,[1] **Silvia Lorrio**,[1] **Ángeles Juarranz**,[1,5] **and Salvador González**[5,6]

[1]*Department of Biology, Faculty of Sciences, Autónoma University of Madrid (UAM) 28049, Madrid, Spain*
[2]*Medical Affairs Department, Cantabria Labs, 28043 Madrid, Spain*
[3]*Rohto Basic Research Development Division, Tokyo, Japan*
[4]*Department of Applied Pharmacology, Graduate School of Medicine and Pharmaceutical Sciences, University of Toyama, Sugitani, Toyama, Japan*
[5]*Instituto Ramón y Cajal de Investigación Sanitaria (IRYCIS), Madrid, Spain*
[6]*Department of Medicine and Medical Specialties, Alcalá de Henares University, 28805 Madrid, Spain*

Correspondence should be addressed to Ángeles Juarranz; angeles.juarranz@uam.es
and Salvador González; salvagonrod@gmail.com

Pablo Delgado-Wicke and Azahara Rodríguez-Luna contributed equally to this work.

Received 4 January 2020; Accepted 7 February 2020; Published 15 April 2020

Guest Editor: Miguel Sánchez-Álvarez

Humans in modern industrial and postindustrial societies face sustained challenges from environmental pollutants, which can trigger tissue damage from xenotoxic stress through different mechanisms. Thus, the identification and characterization of compounds capable of conferring antioxidant effects and protection against these xenotoxins are warranted. Here, we report that the natural extract of *Polypodium leucotomos* named Fernblock®, known to reduce aging and oxidative stress induced by solar radiations, upregulates the NRF2 transcription factor and its downstream antioxidant targets, and this correlates with its ability to reduce inflammation, melanogenesis, and general cell damage in cultured keratinocytes upon exposure to an experimental model of fine pollutant particles ($PM_{2.5}$). Our results provide evidence for a specific molecular mechanism underpinning the protective activity of Fernblock® against environmental pollutants and potentially other sources of oxidative stress and damage-induced aging.

1. Introduction

Air pollution is a growing challenge to public health worldwide and constitutes an emerging focus of research and surveillance for the World Health Organization [1]. Because of the role of the skin as a primary barrier against external sources of tissue damage, continuous exposure to these pollutants has a substantial negative impact on this organ and is precursory of premature skin aging, pigmentation, acne disorders, and psoriasis exacerbation, among others [2]. Specifically, $PM_{2.5}$ provokes increased ROS and loss of organelle homeostasis in keratinocytes [3], has been associated with aggravated allergic dermatitis and eczema in children [4], and is precursory to inflammation, aging, androgenic alopecia, and skin cancer [5]. Thus, air pollution, solar radiation, and tobacco smoke constitute extrinsic skin-aging factors, leading to ROS production and the subsequent activation of oxidative stress responses. Skin antioxidant defense responses are effective against these exogenous sources of damage; however, chronic exposure, aging, or several

concomitant pathologies can lead to decreased activation and increased oxidative damage, accelerating skin aging and skin cancer [6]. Prevention strategies including sun protection, skin barrier improvement, aryl hydrocarbon receptor (AhR) modulation [7], and increased skin tissue resistance through potentiation of natural detoxification pathways are target opportunities for skin protection [8]. Fully understanding mechanisms by which tissues confront these sources of xenotoxic stress and potential pharmacological opportunities to leverage on them are warranted.

Nuclear factor erythroid 2-related factor 2 (NRF2; also known as nuclear factor erythroid-derived 2-like 2, NFE2L2) is a basic leucine zipper transcription factor highly conserved in metazoans [9]. In nonstressed cells, the NRF2 protein is bound in the cytoplasm, ubiquitinated and rapidly degraded to low levels by the Kelch-like ECH-associated protein 1- (KEAP1-) Cullin 3 ubiquitin ligase complex. Generic insults provoking oxidative or electrophilic stress in cells inactivate the KEAP1/CUL3 complex, promoting nuclear translocation of accumulating NRF2, which in turn orchestrates the expression of different antioxidant enzymes (including most components of the glutathione de novo synthesis pathway and glutathione transferases and peroxidases) and detoxifying effectors (NAD(P)H Quinone Dehydrogenase 1 (NQO1), heme oxygenase 1 (HO-1), or Multidrug Resistant Proteins (MRPs)) in most cell types [10]. NRF2 constitutes an emerging, appealing target for therapeutic modulation in multiple pathologies [11]. Of note, NRF2 activity has been specifically associated with response to various environmental pollutants that potentially act as xenotoxins, including air $PM_{2.5}$ [12, 13].

Fernblock® is a natural standardized aqueous extract from the leaves of *Polypodium leucotomos* [14]. The use of decoctions of this fern was widespread in traditional medicine amongst local indigenous populations in Central America against numerous ailments, and modern medicine has confirmed its notable potential as an active conferring skin-specific antioxidant activity and protection against sun radiation damage (including aging, hyperpigmentation, and DNA damage) [15]. However, while evidence supporting a boosting of endogenous antioxidant and xenobiotic stress systems in cells is highly relevant for the therapeutic potential of Fernblock® [16–18], our understanding of the molecular mechanisms by which this occurs is limited.

Here, we contribute evidence suggesting that Fernblock® is capable of upregulating the NRF2 pathway as assessed by different direct and indirect readouts in cultured human cells and that this dose-dependent activation correlates with its protective effect not only against UVB radiation but also against exposure to $PM_{2.5}$. These observations suggest a potential for Fernblock® not only as a natural activity against the detrimental effects of a broad range of environmental sources of xenobiotic stress and aging but also as a potential tool for activating the NRF2 pathway.

2. Materials and Methods

2.1. Cell Culture and Treatments. The nontumorigenic human keratinocyte cell line HaCaT was used for *in vitro* studies (Cell Line Service, Eppelheim, Germany). Cells were subcultured in different plate formats according to assay (see below), in Dulbecco's modified Eagle's medium (DMEM) supplemented with 10% (*v*/*v*) fetal bovine serum (FBS), 50 units/ml penicillin, and 50 μg/ml streptomycin, in an incubator at 5% CO_2, 37°C, and 95% humidity. Rat adrenal pheochromocytoma PC12 cells were maintained in Dulbecco's modified Eagle's medium supplemented with 5% fetal calf serum and 10% horse serum. All cell culture reagents were purchased from Gibco Inc. (Paisley, UK). Human Epidermal Keratinocytes (NHEK; KURABO Co., Japan; Cat. No. KM4109, Lot No. 04644) were grown in HuMedia KG2 (KURABO Cat. No. KK-2150S) and assayed in HuMedia KB2 (KURABO Cat. No. KK-2350S). Human vaginal malignant melanoma cells (HMVII; European Collection of Authenticated Cell Cultures (ECACC), UK; Cat. No. 92042701, Lot No. 14B033) were grown and assayed in RPMI1640, supplemented with 10% FBS and penicillin-streptomycin. All cell culture reagents were purchased from Gibco Inc. (Paisley, UK).

Treatments as described in different experiments were applied on cultures at 50-60% confluence from 10 mg/ml stocks in all cases, and FBS supplementation was reduced to 1%. Fernblock® was provided by Cantabria Labs (Spain). A Standard Reference Material (SRM) for experimental modelling of air pollutants at $PM_{2.5}$ was purchased from Sigma-Aldrich (UK; Diesel Particulate Matter 1650b) and was routinely sonicated to avoid aggregation for 30 min′ for immediate use during the next hour. Sulforaphane was purchased from Sigma-Aldrich (Japan; Sulforaphane S4441-5MG).

2.2. Reagents and Antibodies. Cell viability was measured using an assay based on MTT (3-(4,5-dimethylthiazol-2-yl)-2,5-diphenyltetrazolium bromide) (Sigma-Aldrich, St Louis, USA). The following primary antibodies were used in the performed immunofluorescence and western blot assays: mouse anti α-tubulin (Sigma-Aldrich, St Louis, USA), anti-beclin1 (Cell Signaling, #3738), anti-HO-1 (Cell Signaling, #70081), anti-LC3 (Abcam, Ab58610), anti-NQO1 (Cell Signaling, #3187), and anti-NRF2 (Abcam, ab89443), The secondary antibodies employed were mouse IgG-Alexa 488 and rabbit IgG-Alexa 546 (Invitrogen, Oregon, USA) and mouse IgG peroxidase and rabbit IgG peroxidase (Thermo Scientific, Rockford, USA). The markers used for the *in vivo* staining were monodansylcadaverine (MDC) for phagolysosomes and LysoTracker Green (LTG) for lysosomes. Hoechst 33258 (Sigma-Aldrich) was used for cellular staining.

2.3. Luciferase Assays for NRF2 Activity in PC12 Cells. Complementary oligonucleotides spanning a functional antioxidant response element (ARE) from the human NQO1 gene reference promoter sequence (-473 to -440) were annealed and ligated into the pGL4.27 vector (Promega, Madison, WI, USA). The resulting reporter vector was stably transfected onto PC12 using Lipofectamine 2000 (Invitrogen, Carlsbad, CA, USA) according to the manufacturer's instructions. Firefly activity in cell lysates from each assayed condition was measured in a luminometer using a Picagene LT2.0 Luminescence Reagent (Toyo Ink, Tokyo, Japan) according to the manufacturer's instructions. Results shown are derived

as mean values and standard deviations from three independent experiments.

2.4. Assays for Studying UVB-Induced Damage in Human Keratinocytes. NHEKs were seeded onto 6-well culture plates at 300,000 cells/well. After 24 h spreading, cells were switched to KB2 medium supplemented with either vehicle (DMSO) or 31.3 μg/ml Fernblock® for 24 additional hours. Cultures were then rinsed in PBS, irradiated with UVB (90 mJ/cm^2) using a F1215 unit (Muranaka Medical Instruments Co. Ltd., Japan), and further cultured in KB2 for 6 h (cytokine expression assays), 24 h (cell counting and NRF2 activity assays), or 72 h (melanization assays).

Cell counting was automated from Hoechst 33342-stained samples using the ImageXpress Micro platform (Molecular Devices LLC, San José, CA, USA). For gene expression assays, total cell RNA was isolated using the RNeasy mini kits (QIAGEN) and reverse-transcribed using ReverTra Ace technology (Toyobo Co., Osaka, Japan). cDNAs were then quantitated by real-time PCR ($^{(-\Delta\Delta Ct}$ method) using the ABI TaqMan™ Fast Advanced Master Mix (Thermo Scientific, USA) and the following ABI TaqMan™ probes for human sequences: catalase (CAT) (Hs00156308_m1), glutathione peroxidase (GPX) (ABI TaqMan Probe: Hs00829989_gH), GPX 4 (ABI TaqMan Probe: Hs00157812_m1), HO-1 (ABI TaqMan Probe: Hs00157 965_m1), NQO1 (ABI TaqMan Probe: Hs00168547_m1), interleukin (IL)6 (ABI TaqMan Probe: Hs00174131_m1), and IL8 (ABI TaqMan Probe: Hs00174103_m1).

Melanin production was assayed as follows: KB2 72 h-conditioned medium from NHEKs supplemented and irradiated as indicated (see above) was diluted 1 : 1 with HMVII medium and added to a monolayer of HMVII cells 24 h post-seeding. After 48 h culture for uptake, HMVII cells were trypsinized, pelleted, and treated with 2 N NaOH for 40 min at 80°C. Melanin content was measured by absorbance within a 405 nm–620 nm range using a plate spectrophotometer, corrected for cell viability (as assessed by trypan blue exclusion staining), and normalized to values observed in cells exposed to supernatants from nonirradiated cells ("control").

2.5. Cellular Toxicity in $PM_{2.5}$-Exposed HaCaT Keratinocytes. Toxicity of different concentrations of Fernblock® and $PM_{2.5}$was inferred by the MTT colorimetric assay in HaCaT cells 24 and 48 h posttreatment. Briefly, cells were exposed after indicated treatment times to 50 μg/ml MTT (3-(4,5-dimethylthiazol-2-yl)-2,5-diphenyltetrazolium bromide) at 37°C for 3 hours in the dark. Precipitated formazan was solubilized in DMSO (PanReac, Barcelona, Spain), and absorption was measured at 542 nm in a spectrophotometer (Spectra Fluor, Tecan). Cellular toxicity was expressed as the percentage of formazan absorption from the different treatment conditions compared to nontreated cells. Results shown are derived as mean values and standard deviations from three independent experiments.

2.6. Immunofluorescence Microscopy and Image Analysis. Active formation of phagolysosomal vacuoles was monitored by incubation of cells grown on coverslips with MDC for 10 min. Lysosomal compartment was decorated with LysoTracker Green™ (Molecular Probes), following the manufacturer's instructions. After briefly washing cells with PBS, slides were immediately mounted for image acquisition under UV or green excitation light.

For immunostaining, cells grown on the coverslips were fixed in a 3.7% formaldehyde solution in PBS for 10 min, washed with PBS 1X three times, and permeabilized with Triton X-100 0.1% in PBS during 30 min in agitation. Samples were incubated with primary antibodies for 1 h at 37°C, inside a humid chamber. After washing with PBS, cells were incubated with secondary antibodies for 45 min at 37°C. Nuclei were counterstained with Hoechst 33258. Coverslips were then washed with PBS and mounted with ProLong® antifade mounting medium (Molecular Probes). Images were acquired on an Olympus BX61 epifluorescence microscope equipped with filter sets for fluorescence microscopy: ultraviolet (exciting filter BP360-390), blue (exciting filter BP460-490), and green (exciting filter BP510-550), coupled to an Olympus CCD DP70 digital camera. LC3 immunofluorescence was quantified using ImageJ from at least fifty cells from each condition. NRF2 activation was assessed by separately computing nuclear and cytoplasmic intensities, from fifty cells from each condition. Figures were prepared using the Adobe Photoshop CS5 extended version 12.0 software (Adobe Systems Inc., USA).

2.7. Western Blotting. Cells were lysed in RIPA buffer (150 mM NaCl, 1% Triton X-100, 1% deoxycholate, 0.1% SDS, 10 mM Tris-HCl pH 7.2, and 5 mM EDTA), supplemented with phosphatase inhibitors and protease inhibitor cocktail tablets (Sigma-Aldrich, St. Louis, MO). Protein concentration was measured by BCA assay (Thermo Scientific-Pierce, Rockford, USA). Protein samples were subjected to SDS-PAGE and blotted to Immobilon-P PVDF membranes (Millipore Co., Massachusetts, USA). Membranes were blocked in PBS-tween 0.1% with 5% nonfat dried milk for 1 h at 25°C and then incubated with primary antibodies overnight at 4°C. After extensive washing with PBS-tween 0.1%, membranes were incubated with peroxidase-conjugated secondary antibodies. Signal was developed by chemiluminescence (ECL, Amersham Pharmacia Biotech, Little Chalfont, UK) and acquired on a ChemiDocTR XRS+ high definition system (Bio-Rad). Bands corresponding to the different proteins were digitalized employing the Image Lab version 3.0.1 (Bio-Rad Laboratories). This assay was performed at least three times for each target.

2.8. Statistical Analysis. Data are expressed as the mean value of at least three experiments ± standard deviations (SD). The statistical analysis was made using the statistical package of the program GraphPad Prism 6. Statistical significance was determined using a t-test and analysis of variance (ANOVA), and $p < 0.05$ was considered statistically significant.

3. Results

3.1. Fernblock® Induces a NRF2-Dependent Transcriptional Pathway which Correlates with Its Protection against UVB Radiation. Previous studies demonstrated that Fernblock®

is capable of exerting a protective effect on cells against UVB irradiation [15–19]. Thus, we first corroborated that Fernblock® treatment had no toxic effect against cell viability (Figure 1(a)), as well as its protective effect attenuating UVB-induced decrease in cell proliferation/viability, as assessed by normalized cell count (Figure 1(b)). However, the molecular mechanisms by which this occurs are not completely characterized. We decided to test the ability of Fernblock® to induce a major endogenous pathway deployed by cells to counteract oxidative and electrophilic stress: the NRF2 pathway.

First, we employed an established cell line of ectodermal lineage (PC12 pheochromocytoma cell line, widely used as a model for studying NRF2 activity [20]), stably expressing a luciferase reporter under the control of a promoter fragment derived from the canonical NRF2 target NAD(P)H Quinone Dehydrogenase 1 (NQO1). Several studies report that the exposure to the organosulfur compound sulforaphane leads to increased transcription of nuclear NRF2 and downstream cytoprotective genes [20–22]. Of note, Fernblock® induced the reporter in a concentration-dependent manner, suggesting that it is capable of upregulating this protective pathway in cells (Figure 1(c)).

We then investigated whether this effect also occurs in keratinocytes and whether it is associated with specific protection from exposure to UVB radiation. qRT-PCR assessment of mRNA levels for several bona fide targets of NRF2 (CAT, GPX 1 and 4, HO-1, and NQO1) revealed that Fernblock® induces the transcription of all these genes in human keratinocytes in a concentration-dependent manner (Figures 1(d)–1(h)). Similar antioxidant effects have been previously observed in a different *in vitro* model with a sulforaphane combination.

Importantly, in line with previous results, these treatment routines with Fernblock® protected keratinocytes from UVB radiation, decreased UVB-dependent induction of inflammatory cytokines IL6 and IL8 (Figure 1(i)), and significantly reduced the induction of melanin production (Figure 1(j)). Because NRF2 is a well-established prosurvival and anti-inflammatory pathway [10, 11], we consider the association of NRF2 induction with protection from UVB-induced damage in cells exposed to Fernblock® to be functionally relevant.

3.2. Fernblock® Protects Human Keratinocytes from Damage Induced by Fine Particle Pollutants ($PM_{2.5}$) in an In Vitro Model. The protective effect of Fernblock® against a broad spectrum of solar radiation is well established [16–18]. We considered whether this protective mechanism might also operate in a different condition leading to severe cell stress: high exposure to fine particle pollutants ($PM_{2.5}$). Exposure of keratinocytes to a SRM of $PM_{2.5}$ decreased cell viability in a concentration-dependent manner (Figure 2). On the other hand, simultaneous addition of Fernblock® in concentrations previously shown to induce NRF2 and protect from UVB-induced cell damage partially reverted toxicity associated with low to moderate concentrations of $PM_{2.5}$ (25-50 μg/ml; Figure 2), although higher $PM_{2.5}$ doses were not counteracted in this *in vitro* model (Figure 2). The selected $PM_{2.5}$ dose was 50 μg/ml for all experiments. Fernblock® doses did not have any intrinsic effect on cell viability in the absence of $PM_{2.5}$ (Figures 1(a) and 2).

3.3. Fernblock® Increases Basal and $PM_{2.5}$-Induced Autophagy in Keratinocytes. We assessed the formation of autophagolysosomal vacuoles to infer canonical autophagy activation, indicative of cell adaption to generic stress. We first visualised the formation of autophagolysosomal vacuoles by MDC staining, as well as expansion of the lysosomal compartment as decorated by LysoTracker Green™. Consistent with a robust induction of xenotoxic stress, visual inspection revealed that exposure to $PM_{2.5}$ increased the formation of autophagolysosomes (MDC+-positive mask) and was associated with an enlargement of the lysosomal compartment (LysoTracker Green+ mask) (Figure 3(a) second column of panels from left), both established features of prosurvival cell adaptive responses. Addition of Fernblock® further enhanced this expansion of the phagolysosomal compartment, and Fernblock® addition alone was also associated with a mild increase in the MDC/LysoTracker+ area (Figure 3(a), right panel columns). These observations are in agreement with experiments assessing relative density of LC3 puncta (indicative of *de novo* phagosome formation and maturation and activation of autophagy flux): Fernblock® increases basal autophagy flux in healthy cells and further enhances the activation provoked by $PM_{2.5}$ exposure, consistent with its protective effect (Figures 3(b) and 3(c)).

These observations suggest that Fernblock® promotes the activation of survival pathways naturally employed by cells in the face of homeostasis challenges, and this induction correlates with its prosurvival and protective effects.

3.4. Fernblock® Upregulates NRF2 Basal Activity and Increases NRF2 Induction upon Exposure to $PM_{2.5}$. Because NRF2 activity is reported to be sensitive to xenotoxic stress from air pollutants [12, 13, 23], and our preliminary data demonstrated that the NRF2-dependent transcriptional pathway is triggered by treatment with Fernblock® (Figure 1), we moved to determine the relationship between Fernblock®-induced protection against $PM_{2.5}$ toxicity and NRF2 regulation. Immunostaining revealed that unchallenged HaCaT keratinocytes in culture have low total and nuclear levels of NRF2 protein (Figures 4(a) and 4(b)). In accordance with the activation of an adaptive cytoprotective response, $PM_{2.5}$ exposure alone leads to a robust increase in total NRF2 levels. Of note, Fernblock® exposure led *per se* to a mild increase specifically of NRF2 nuclear pools and further boosted NRF2 levels in cells exposed to $PM_{2.5}$ (Figures 4(a) and 4(b)). Of note, Fernblock® did not entail the acute increase in cytoplasmic pools of NRF2 observed in cells exposed to $PM_{2.5}$ (fig. S1, see Figure 4(a)).

We further assessed activation of the pathway downstream NRF2 by assessing the levels of two bona fide transcriptional targets of NRF2: NQO1 and HO-1. In line with our previous observations for NRF2 protein levels, $PM_{2.5}$ exposure markedly upregulated NQO1 protein levels as assessed by immunofluorescent staining and western blot in HaCaT cells (Figures 4(c) and 4(d)). Fernblock® promoted

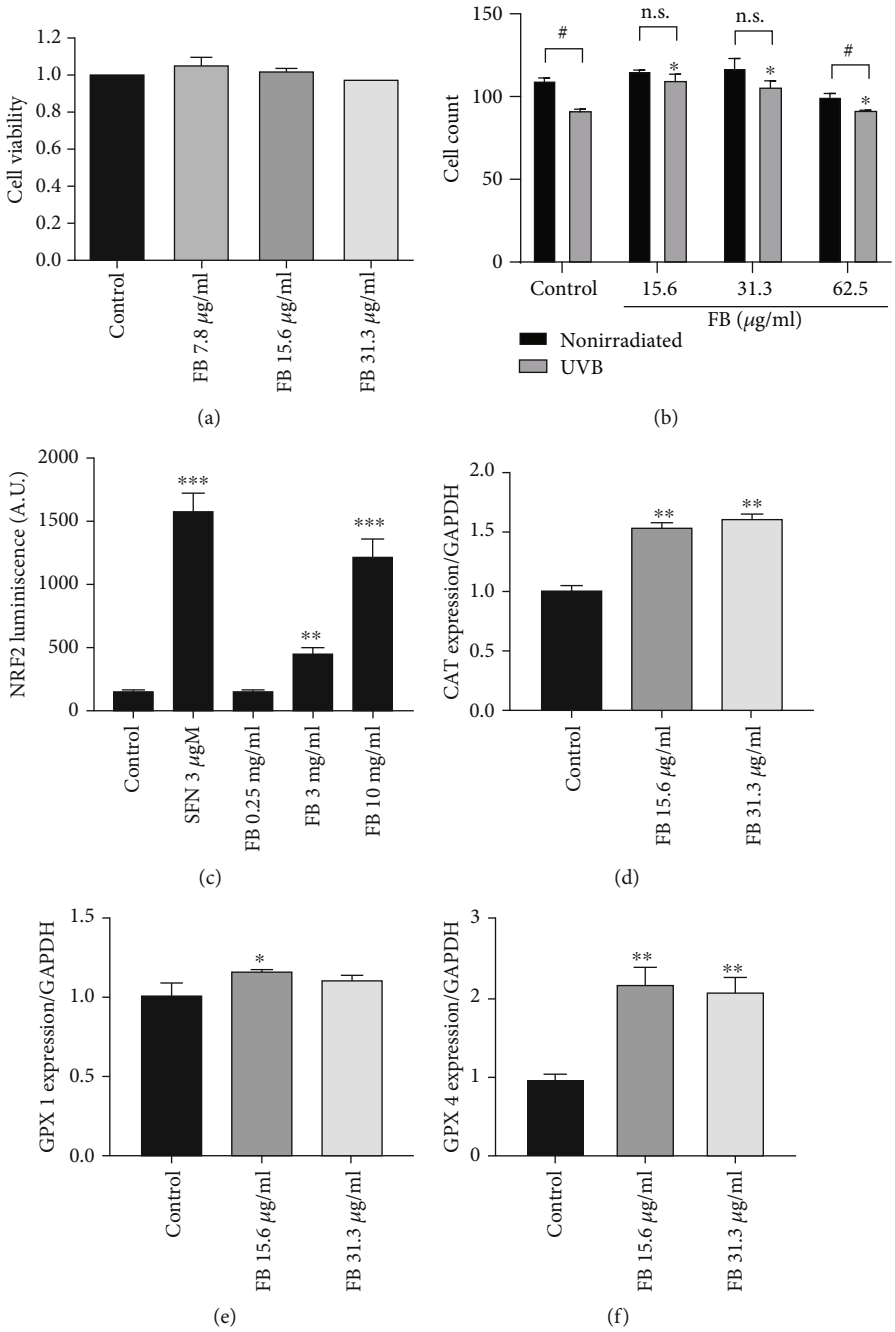

Figure 1: Continued.

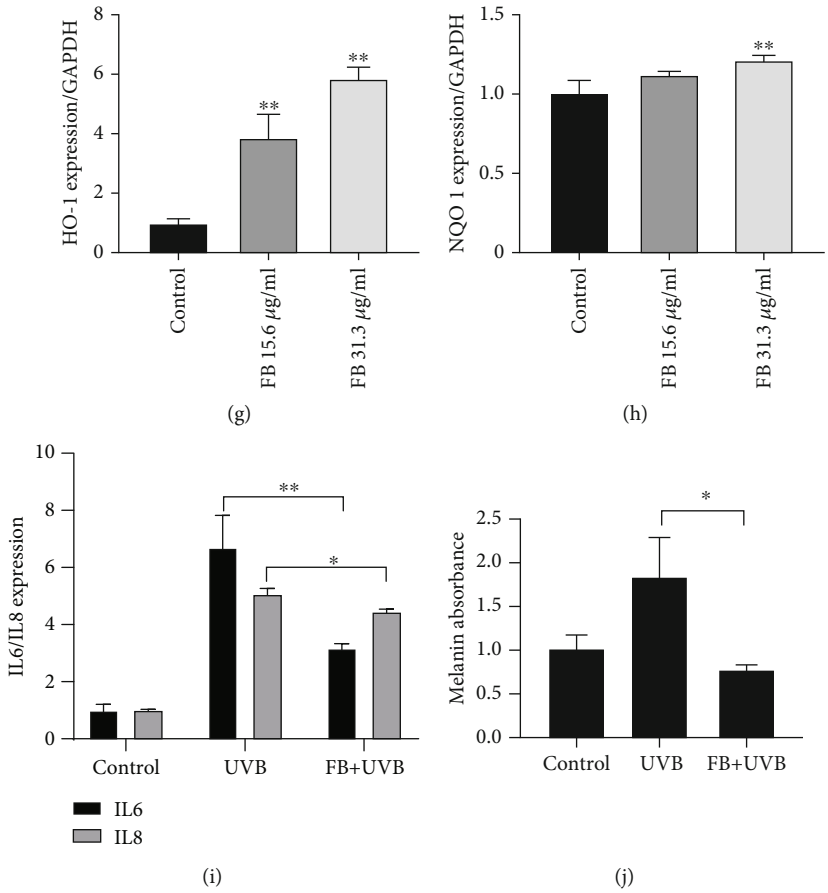

Figure 1: Fernblock® (FB) induces NRF2-dependent transcription activity and attenuates UVB-induced inflammation and melanization. (a) Fernblock® supplementation does not have a significant impact on cell viability as assessed by MTT assay. Data derived from 3 independent replicates and normalized to vehicle-treated samples (black bar, value: 1). (b) Fernblock® supplementation reverts the decrease in viability associated with UVB exposure in keratinocytes, as assessed by cell counts. The effect of UVB exposure (grey bars) is normalized to the corresponding nonirradiated samples (black bars, expressed as 100% viability) for each Fernblock® treatment group. Data are derived from 3 independent biological replicates. n.s.: nonstatistically significant; * and $^{\#}p \leq 0.05$. (c) Fernblock® induces the activity of a synthetic NRF2-dependent luciferase minigene reporter. Stable PC12 cells bearing a NQO1-driven minimal promoter were treated as indicated (vehicle: DMSO; time: 24 h). Data are normalized to control, which is expressed as 100% signal. $n = 3$. (d–h) mRNA expression levels ($^{-\Delta\Delta Ct}$ quantitation method) for indicated genes in human keratinocytes across indicated treatments were assessed by qRT-PCR using TaqMan technology. Data are normalized to the control (vehicle). $n = 3$. (i) mRNA expression levels for either IL6 (black bars) or IL8 (grey bars) across indicated treatment conditions in keratinocytes were assessed by qRT-PCR using TaqMan technology. $n = 3$. (j) Induction of keratinocyte melanization by the indicated treatments was assessed as detailed in Materials and Methods. Data are derived from absorbance across the visible spectrum and normalized to values from control samples. $n = 3$. $^{*}p \leq 0.05$, $^{**}p \leq 0.01$, $^{***}p \leq 0.005$, and $^{****}p \leq 0.0001$.

a moderate increase in NQO1 levels in the absence of $PM_{2.5}$ and significantly boosted their upregulation associated with $PM_{2.5}$ exposure, in accordance with the measurements recorded for NRF2 protein (Figures 4(c) and 4(d)). HO-1 protein levels exhibited an analogous response and Fernblock® significantly enhanced the upregulation associated with $PM_{2.5}$ exposure, as compared to the protective response observed in cells exposed to this particle pollution alone (Figures 5(a) and 5(b)).

4. Discussion

Air pollution is a major challenge to public health and well-being in modern societies, negatively impacting conditions such as cardiovascular disease, respiratory ailments and infections, and cancer. Thus, identifying compounds with protective properties against tissue damage due to this environmental source of xenotoxins is a priority for public health. An organ particularly exposed to damage from pollutants is the skin, and several cutaneous disorders are significantly influenced by environmental xenotoxins. Cellular mechanisms contrasting environmental pollutants include the AhR pathway, which positively regulates cyp450 detoxification systems and artemin [24]; the metal regulatory transcription factor-1 (MTF-1), which promotes the expression of antioxidant genes and metallothioneins in response to accumulation of heavy metals such as silver, cadmium, copper, or zinc [25]; and the conserved NRF2 pathway, which determines broad antioxidant and detoxifying transcriptional processes in response to different

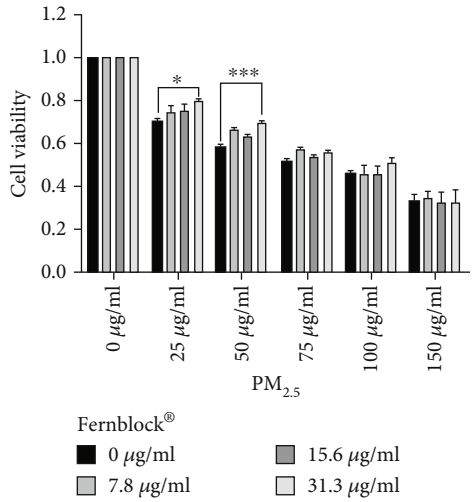

FIGURE 2: Fernblock® protects keratinocytes from $PM_{2.5}$-induced toxicity. MTT assay was performed on HaCaT samples across indicated treatments on $PM_{2.5}$, Fernblock®, or combinations of both compounds (see Materials and Methods). All data are expressed as normalized to untreated samples (leftmost bar group of graph). $n = 3$. $^{*}p \leq 0.05$ and $^{***}p \leq 0.005$.

forms of stress leading to accumulation of ROS and electrophilic stress [9–13]. As such, NRF2 activity has emerged as a particularly attractive target for therapeutic and antiaging skin treatment [11, 26].

Natural compounds able to modulate these protective endogenous pathways are a promising option to reduce the impact of environmental pollution on skin. Several such compounds have in fact been identified which promote the NFR2 cytoprotective activities, including sulforaphane (from cruciferous vegetables) [21], curcumin (from *Curcuma longa*) [27], cinnamaldehyde (from cinnamon) [28], or tanshinones (from *Salvia miltiorrhiza*) [29]. Here, we provide evidence that Fernblock®, a standardized aqueous extract from *Polypodium leucotomos* leaves with proven photoprotective properties *in vivo* and *in vitro* against radiation damage in skin [16–19, 30], also induces protective mechanisms in an experimental model of fine particle $PM_{2.5}$ air pollutants. Moreover, our studies provide novel evidence that the NRF2 transcriptional network is a relevant target upregulated by treatment with Fernblock® and demonstrate a close correlation between the upregulation of these antioxidant signalling pathways and the protective effect against damage from both UVB irradiation and fine particle pollutants. Due to their xenotoxic effect, $PM_{2.5}$ exposure markedly increased total NRF2 protein levels as a defense mechanism, suggesting acute robust activation to counteract oxidative damage (Figures 4(a) and 4(b)). Fernblock® supplementation preferentially increased nuclear pools of NRF2. These observations support a hypothesis whereby Fernblock® is able to increase basal NRF2 activity levels in the absence of xenotoxic agent and further enhance its activation induced against $PM_{2.5}$-induced oxidative stress, thus boosting the cell protection from damage. Several canonical routes downstream NRF2 (including autophagy and the direct NRF2 targets HO-1 and NQO1 which were demonstrated to be significantly impacted by Fernblock®) might play a role in the observed protection against $PM_{2.5}$ damage. Of note, our observations of net protein level upregulation across conditions for the NRF2 targets HO-1 and NQO1 (Figures 4 and 5), together with our data showing a lack of impact on cell proliferation/viability (Figure 1), support a scenario whereby Fernblock® does not provoke cell toxicity and potentially positively regulates NRF2 through other mechanisms (*see below*). The crosstalk between NRF2 with other pathways such as AhR or NF-κB-dependent inflammation networks involved in skin cell adaption to xenotoxins should also be taken into consideration [31, 32]. In addition to the cytoprotective routes driven by NRF2 in most cell types, an important factor to consider is the substantial impact NRF2 has on keratinocyte homeostasis through direct transcriptional control of different specialized structures, such as late cornified envelope 1 (LCE1) family members, keratins, and desmosomal components [33, 34].

Priming of autophagy, an important prosurvival and repairing mechanism [35], has also been demonstrated to be induced by treatment with Fernblock®. These studies thus also raise the important question as to how Fernblock® specifically interacts with cell metabolism, particularly interesting for its systemic (nutraceutical) applications. Modulation of key nodes of energy metabolism regulatory networks that also intersect with autophagy and ROS management, such as AMPK, is amenable though the use of well-established compounds such as metformin [36].

An important consideration that arises from these observations is the potential these mechanisms may have to slow skin aging. Loss of proteostasis and dysregulation of ROS levels and inflammation, decreased autophagy flux, and reduced NRF2 activity are all hallmarks of aging [37]. As stated above, NRF2 has also emerged as a relevant direct transcriptional regulator ensuring the expression of specialized keratinocyte components that decline with age, such as desmosomal proteins. Treatment with Fernblock® is effective for reducing radiation-induced cell senescence and age-associated damage in keratinocytes [17]. The present body of work further highlights the value of Fernblock® as an antiaging agent, whose beneficial effect might be the result of improved NRF2 signalling and autophagy. The potential of these mechanisms to attenuate accumulated oxidative stress and tissue damage is further exemplified by the reduction of UVB-induced melanogenesis, which is closely related to inflammation and oxidative stress in an evolutionarily conserved manner [38]. Adaptive pathways downstream NRF2, including Pi3/Akt signalling [39], autophagy itself [40, 41], and antioxidant effectors (potentially even by inhibiting the oxidative process of melanin biogenesis [42]), have been shown to contrast melanogenesis. Our observations support a model whereby Fernblock® reduces melanogenesis at least in part through upregulation of NRF2-dependent responses.

How does Fernblock® stimulate these prosurvival pathways? While other compounds currently being explored as "boosters" of NRF2 signalling, such as sulforaphane, exert their positive regulation of cytoprotection through canonical

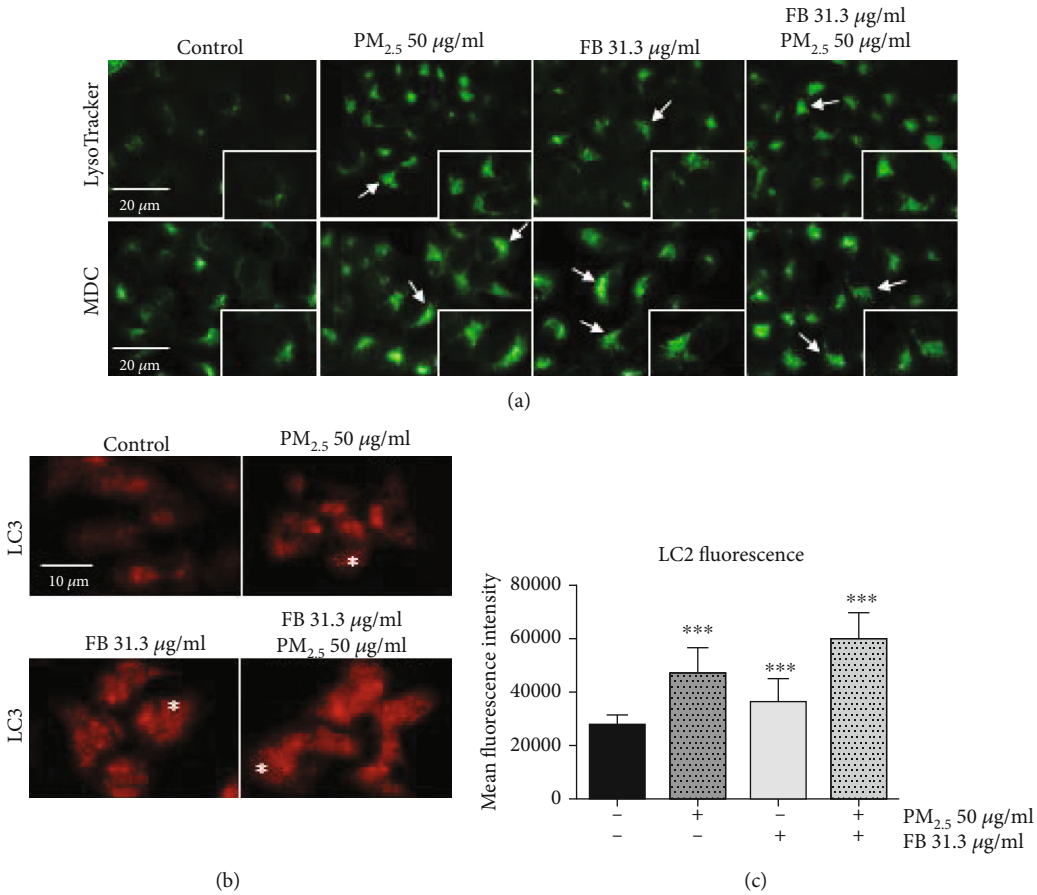

Figure 3: Fernblock® (FB) induces autophagolysosomal activity in keratinocytes *per se* and boosts autophagy flux in $PM_{2.5}$-treated cells. (a) Expansion of the lysosomal compartment (LysoTracker Green™, top panel row) and density of autophagolysosomal vacuoles (MDC, lower panel row) were acquired by immunofluorescence microscopy across indicated treatments in HaCaT cells. Scale bar for whole-field images (20 microns) and 3x enlarged insets are indicated. Cells with significant enlargement of their MDC-positive compartment are indicated with arrows (b, c) Density of LC3 punctate staining, as a proxy for autophagy flux activation, was assessed from immunofluorescence microscopy images on HaCaT cells treated as indicated (see Materials and Methods). Exemplary cells with increased punctate pattern staining are highlighted with asterisks in panels at (b). Data plotted in (c) were derived from 50 cells from 3 independent biological replicates. $^{***}p \leq 0.005$.

mechanisms [22], exact information regarding the molecular mechanisms by which Fernblock® modulates NRF2 and autophagy is lacking. A possible candidate mechanism could be the upregulation of sestrin family proteins, which have recently emerged as pivotal regulators upstream autophagy and ROS management in the cell [43]. A nonexclusive mechanism might be the modulation of cell metabolism and ROS production itself, currently not completely characterized for Fernblock®. It should be noted that autophagy is a relevant target of NRF2 itself: NRF2 drives the expression of essential autophagy regulators such as p62 and LAMP2A, and NRF2 deficiency reduces autophagy flux and favours the accumulation of proteotoxicity precursors [44, 45]. Our observations would agree with a speculative model whereby Fernblock® increases basal autophagy downstream enhanced NRF2 activity. Conversely, autophagy might also contribute to NRF2 activation through KEAP1 turnover, a mechanism likely underpinning the control of ROS through autophagy [46]. An intriguing additional potential mechanism both for Fernblock® antixenotoxic protection in general and for NRF2 regulation in particular may be embodied by the proteostatic network of the Heat Shock Protein response, which suppresses NF-κB activity [47]. Because the identification of tools for promoting exogenous intervention of NRF2 signalling is an important objective across a broad range of fields in biomedicine, our findings highlight a potential use for Fernblock® as a natural compound able to upregulate this pathway, deserving of future research.

While the exact molecular mechanisms responsible for the loss of cell homeostasis upon exposure to $PM_{2.5}$, and their modulation upon treatment with Fernblock®, remain to be fully characterized, our observations support a general model whereby Fernblock® reduces xenotoxicity by priming prosurvival antistress pathways, such as the NRF2 pathway and autophagy, thus reducing the oxidative stress and cell damage provoked by harmful agents such as $PM_{2.5}$. Full characterization of the mechanisms modulated by Fernblock® may provide a framework for establishing personalized intervention and synergistic combinations that simultaneously boost these mechanisms as required.

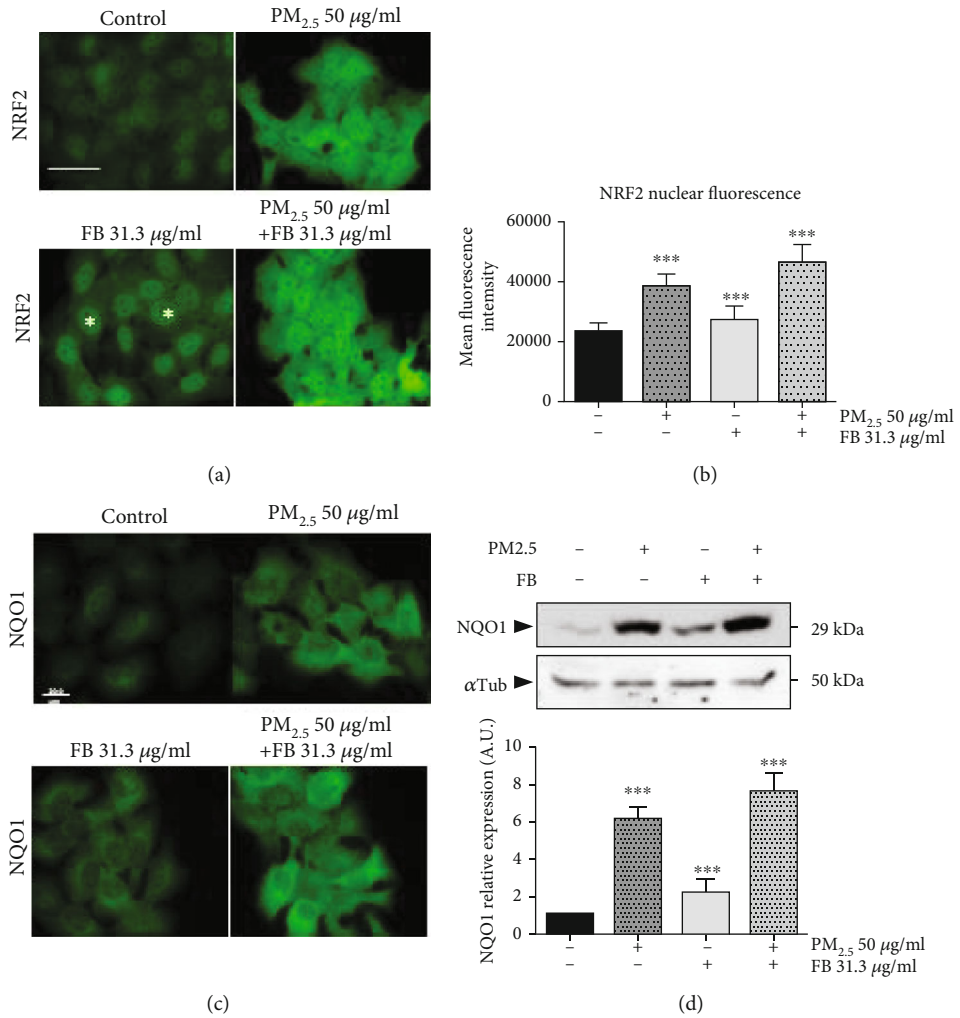

Figure 4: Fernblock® (FB) induces NRF2 activation and downstream transcription in keratinocytes. (a, b) NRF2 induction and activation was monitored in HaCaT cells by immunofluorescence microscopy across indicated treatment conditions. Scale bar (20 microns) is indicated. Exemplary cells with increased NRF2 staining specifically at the nuclear compartment are highlighted with asterisks in panel (a). Data plotted in (b) was derived from 50 cells from 3 independent biological replicates across conditions and expressed as normalized to untreated cells. (c, d) NQO1 induction downstream NRF2 was assessed in HaCaT cells by immunofluorescence microscopy (c) and immunoblotting (d, upper panel) across indicated conditions. (d, lower panel) Densitometric analysis of western blot data from 3 independent biological replicates is plotted as normalized to the signal observed in untreated cells. $^{***}p \leq 0.005$.

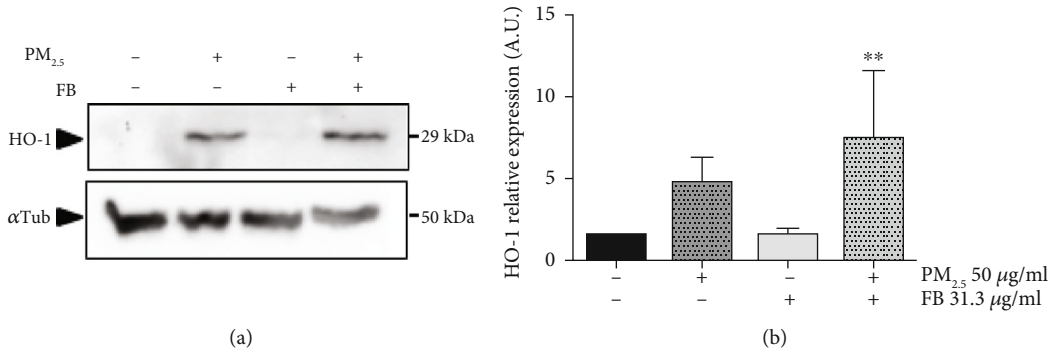

Figure 5: Fernblock® (FB) induces NRF2 activation and downstream transcription in keratinocytes. (a, b) HO-1 induction downstream NRF2 was assessed in HaCaT cells by immunoblotting (a, upper panel) across indicated conditions. (b) Densitometric analysis of western blot data from 3 independent biological replicates is plotted as normalized to the signal observed in untreated cells. $^{**}p \leq 0.01$.

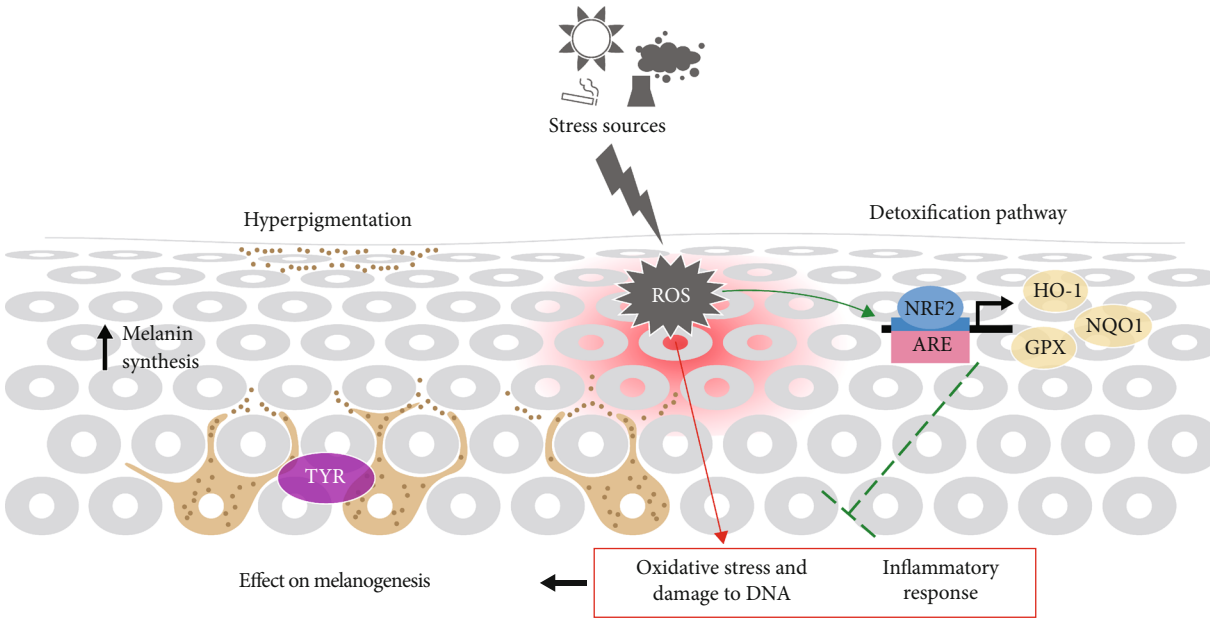

Figure 6: Scheme summarizing mechanisms identified in this study as potential sources of protection induced by Fernblock® against environmental damage of the skin.

5. Conclusions

Our results support NRF2 activation as a potential part of Fernblock®'s protective activity. Moreover, these studies have provided novel evidence that this protective activity is effective against not only oxidative stress derived from UVB radiation but also xenotoxic stress associated with exposure to fine particulate pollutants. Our observations strengthen the notion that Fernblock® can represent a functionally relevant and versatile compound effective against a wide range of environmental sources of tissue damage and aging and support its potential as a valuable tool (fully approved for human use) to elicit NRF2-dependent antistress responses across a wide range of conditions (graphical abstract, Figure 6).

Data Availability

All cell biology, biochemistry and microscopy data supporting the findings of this report are included in this article. Source raw data for all quantitations is fully available upon request.

Conflicts of Interest

S.G. has a consultant role for Cantabria Labs, and A. R.-L. belongs to the Medical Affairs Department at Cantabria Labs, which produced Fernblock®. Y.I. and Y.H. belong to the Rohto Basic Research Development Division, which distributed Fernblock®. The remaining authors declare no conflict of interest.

Authors' Contributions

Pablo Delgado-Wicke and Azahara Rodríguez-Luna contributed equally to this work.

Acknowledgments

We thank employees from Rohto Basic Research Development Division who participated in this study. The assistance of Esther Morel (INIA, Madrid) on the writing and editing of the manuscript is gratefully acknowledged. This research was funded by Cantabria Labs and by the Spanish grant from Instituto de Salud Carlos III and MINECO and FEDER funds (PI18/00708). P.D-W is supported by Comunidad Autónoma de Madrid (CAM).

Supplementary Materials

Figure S1: additional regional intensity analysis for NRF2 staining images from Figure 4(a) are shown. Data plotted are derived from the same image collections as in Figure 4(b). $^{***}p \leq 0.005$. *(Supplementary Materials)*

References

[1] World Health Organization, *Air Pollution And Health: Summary*, 2020, http://www9.who.int/airpollution/ambient/about/en/.

[2] P. Puri, S. K. Nandar, S. Kathuria, and V. Ramesh, "Effects of air pollution on the skin: a review," *Indian Journal of Dermatology, Venereology and Leprology*, vol. 83, no. 4, p. 415, 2017.

[3] M. J. Piao, M. J. Ahn, K. A. Kang et al., "Particulate matter 2.5 damages skin cells by inducing oxidative stress, subcellular organelle dysfunction, and apoptosis," *Archives of Toxicology*, vol. 92, no. 6, article 2197, pp. 2077–2091, 2018.

[4] Q. Li, Y. Yang, R. Chen et al., "Ambient air pollution, meteorological factors and outpatient visits for eczema in Shanghai, China: a time-series analysis," *International Journal of Environmental Research and Public Health*, vol. 13, no. 11, p. 1106, 2016.

[5] M. Kim, L. Y. Li, and J. R. Grace, "Predictability of physicochemical properties of polychlorinated dibenzo-p-dioxins (PCDDs) based on single-molecular descriptor models," *Environmental Pollution*, vol. 213, pp. 99–111, 2016.

[6] C. Juliano and G. Magrini, "Cosmetic ingredients as emerging pollutants of environmental and health concern. A mini-review," *Cosmetics*, vol. 4, no. 2, p. 11, 2017.

[7] A. Zamarrón, E. Morel, S. Lucena et al., "Extract of *Deschampsia antarctica* (EDA) prevents dermal cell damage induced by UV radiation and 2,3,7,8-tetrachlorodibenzo-p-dioxin," *International Journal of Molecular Sciences*, vol. 20, no. 6, article 1356, 2019.

[8] L. Marrot, "Pollution and sun exposure: a deleterious synergy. Mechanisms and opportunities for skin protection," *Current Medicinal Chemistry*, vol. 25, no. 40, pp. 5469–5486, 2018.

[9] P. Moi, K. Chan, I. Asunis, A. Cao, and Y. W. Kan, "Isolation of NF-E2-related factor 2 (Nrf2), a NF-E2-like basic leucine zipper transcriptional activator that binds to the tandem NF-E2/AP1 repeat of the beta-globin locus control region," *Proceedings of the National Academy of Sciences of the United States of America*, vol. 91, no. 21, pp. 9926–9930, 1994.

[10] P. Shaw and A. Chattopadhyay, "Nrf2–ARE signaling in cellular protection: mechanism of action and the regulatory mechanisms," *Journal of Cellular Physiology*, vol. 235, no. 4, pp. 3119–3130, 2019.

[11] M. C. Lu, J. A. Ji, Z. Y. Jiang, and Q. D. You, "The Keap1–Nrf2–ARE pathway as a potential preventive and therapeutic target: an update," *Medicinal Research Reviews*, vol. 36, no. 5, pp. 924–963, 2016.

[12] X. Deng, W. Rui, F. Zhang, and W. Ding, "PM2.5 induces Nrf2-mediated defense mechanisms against oxidative stress by activating PIK3/AKT signaling pathway in human lung alveolar epithelial A549 cells," *Cell Biology and Toxicology*, vol. 29, no. 3, pp. 143–157, 2013.

[13] H. Zhang, H. Liu, K. J. Davies et al., "Nrf2-regulated phase II enzymes are induced by chronic ambient nanoparticle exposure in young mice with age-related impairments," *Free Radical Biology and Medicine*, vol. 52, no. 9, pp. 2038–2046, 2012.

[14] L. Gombau, F. García, A. Lahoz et al., "Polypodium leucotomos extract: antioxidant activity and disposition," *Toxicology in Vitro*, vol. 20, no. 4, pp. 464–471, 2006.

[15] S. Z. Choudhry, N. Bhatia, R. Ceilley et al., "Role of oral *Polypodium leucotomos* extract in dermatologic diseases: a review of the literature," *Journal of Drugs in Dermatology*, vol. 13, no. 2, pp. 148–153, 2014.

[16] S. Gonzalez, Y. Gilaberte, N. Philips, and A. Juarranz, "Fernblock, a nutriceutical with photoprotective properties and potential preventive agent for skin photoaging and photoinduced skin cancers," *International Journal of Molecular Sciences*, vol. 12, no. 12, pp. 8466–8475, 2011.

[17] A. Zamarrón, S. Lorrio, S. González, and Á. Juarranz, "Fernblock prevents dermal cell damage induced by visible and infrared a radiation," *International Journal of Molecular Sciences*, vol. 19, no. 8, article 2250, 2018.

[18] C. Parrado, M. Mascaraque, Y. Gilaberte, A. Juarranz, and S. Gonzalez, "Fernblock (Polypodium leucotomos extract): molecular mechanisms and pleiotropic effects in light-related skin conditions, photoaging and skin cancers, a review," *International Journal of Molecular Sciences*, vol. 17, no. 7, article 1026, 2016.

[19] B. Berman, C. Ellis, and C. Elmets, "*Polypodium leucotomos* - an overview of basic investigative findings," *Journal of Drugs in Dermatology*, vol. 15, no. 2, pp. 224–228, 2016.

[20] B. Bao, M. Q. Zhang, Z. Y. Chen et al., "Sulforaphane prevents PC12 cells from oxidative damage via the Nrf2 pathway," *Molecular Medicine Reports*, vol. 19, no. 6, pp. 4890–4896, 2019.

[21] Y. Morimitsu, Y. Nakagawa, K. Hayashi et al., "A sulforaphane analogue that potently activates the Nrf2-dependent detoxification pathway," *Journal of Biological Chemistry*, vol. 277, no. 5, pp. 3456–3463, 2002.

[22] X. Su, X. Jiang, L. Meng, X. Dong, Y. Shen, and Y. Xin, "Anticancer activity of sulforaphane: the epigenetic mechanisms and the Nrf2 signaling pathway," *Oxidative Medicine and Cellular Longevity*, vol. 2018, Article ID 5438179, 10 pages, 2018.

[23] N. D. Magnani, X. M. Muresan, G. Belmonte et al., "Skin damage mechanisms related to airborne particulate matter exposure," *Toxicological Sciences*, vol. 149, no. 1, pp. 227–236, 2016.

[24] T. Hidaka, E. Ogawa, E. H. Kobayashi et al., "The aryl hydrocarbon receptor AhR links atopic dermatitis and air pollution via induction of the neurotrophic factor artemin," *Nature Immunology*, vol. 18, no. 1, pp. 64–73, 2017.

[25] W. Wu, P. A. Bromberg, and J. M. Samet, "Zinc ions as effectors of environmental oxidative lung injury," *Free Radical Biology and Medicine*, vol. 65, pp. 57–69, 2013.

[26] M. R. de la Vega, A. Krajisnik, D. Zhang, and G. Wondrak, "Targeting NRF2 for improved skin barrier function and photoprotection: focus on the achiote-derived apocarotenoid bixin," *Nutrients*, vol. 9, no. 12, article 1371, 2017.

[27] X. Lin, D. Bai, Z. Wei et al., "Curcumin attenuates oxidative stress in RAW264.7 cells by increasing the activity of antioxidant enzymes and activating the Nrf2-Keap1 pathway," *PLoS One*, vol. 14, no. 5, article e0216711, 2019.

[28] T.-C. Huang, Y.-L. Chung, M.-L. Wu, and S.-M. Chuang, "Cinnamaldehyde enhances Nrf2 nuclear translocation to upregulate phase II detoxifying enzyme expression in HepG2 cells," *Journal of Agricultural and Food Chemistry*, vol. 59, no. 9, pp. 5164–5171, 2011.

[29] S. Tao, Y. Zheng, A. Lau et al., "Tanshinone I activates the Nrf2-dependent antioxidant response and protects against As(III)-induced lung inflammation *in vitro* and *in vivo*," *Antioxidants & Redox Signaling*, vol. 19, no. 14, pp. 1647–1661, 2013.

[30] P. Torricelli, M. Fini, P. A. Fanti, E. Dika, and M. Milani, "Protective effects of Polypodium leucotomosextract against UVB-induced damage in a model of reconstructed human epidermis," *Photodermatology, Photoimmunology & Photomedicine*, vol. 33, no. 3, pp. 156–163, 2017.

[31] S. Shin, N. Wakabayashi, V. Misra et al., "NRF2 modulates aryl hydrocarbon receptor signaling: influence on adipogenesis," *Molecular and Cellular Biology*, vol. 27, no. 20, pp. 7188–7197, 2007.

[32] J. D. Wardyn, A. H. Ponsford, and C. M. Sanderson, "Dissecting molecular cross-talk between Nrf2 and NF-κB response pathways," *Biochemical Society Transactions*, vol. 43, no. 4, pp. 621–626, 2015.

[33] M. Schäfer, H. Farwanah, A. H. Willrodt et al., "Nrf2 links epidermal barrier function with antioxidant defense," *EMBO Molecular Medicine*, vol. 4, no. 5, pp. 364–379, 2012.

[34] A. J. Huebner, D. Dai, M. Morasso et al., "Amniotic fluid activates the nrf2/keap1 pathway to repair an epidermal barrier defect in utero," *Developmental Cell*, vol. 23, no. 6, pp. 1238–1246, 2012.

[35] V. M. Hubbard, R. Valdor, F. Macian, and A. M. Cuervo, "Selective autophagy in the maintenance of cellular homeostasis in aging organisms," *Biogerontology*, vol. 13, no. 1, pp. 21–35, 2012.

[36] M. Foretz and B. Viollet, "Therapy: metformin takes a new route to clinical efficacy," *Nature Reviews Endocrinology*, vol. 11, no. 7, pp. 390–392, 2015.

[37] C. López-Otín, M. A. Blasco, L. Partridge, M. Serrano, and G. Kroemer, "The hallmarks of aging," *Cell*, vol. 153, no. 6, pp. 1194–1217, 2013.

[38] H. Bilandžija, M. Laslo, M. L. Porter, and D. W. Fong, "Melanization in response to wounding is ancestral in arthropods and conserved in albino cave species," *Scientific Reports*, vol. 7, no. 1, article 17148, 2017.

[39] J.-M. Shin, M. Y. Kim, K. C. Sohn et al., "Nrf2 negatively regulates melanogenesis by modulating PI3K/Akt signaling," *PLoS One*, vol. 9, no. 4, article e96035, 2014.

[40] E. S. Kim, H. Chang, H. Choi et al., "Autophagy induced by resveratrol suppresses α-MSH-induced melanogenesis," *Experimental Dermatology*, vol. 23, no. 3, pp. 204–206, 2014.

[41] Y. Yang, G. B. Jang, X. Yang et al., "Central role of autophagic UVRAG in melanogenesis and the suntan response," *Proceedings of the National Academy of Sciences*, vol. 115, no. 33, pp. E7728–E7737, 2018.

[42] A. Chaiprasongsuk, T. Onkoksoong, T. Pluemsamran, S. Limsaengurai, and U. Panich, "Photoprotection by dietary phenolics against melanogenesis induced by UVA through Nrf2-dependent antioxidant responses," *Redox Biology*, vol. 8, pp. 79–90, 2016.

[43] M. Cordani, M. Sánchez-Álvarez, R. Strippoli, A. V. Bazhin, and M. Donadelli, "Sestrins at the interface of ROS control and autophagy regulation in health and disease," *Oxidative Medicine and Cellular Longevity*, vol. 2019, Article ID 1283075, 11 pages, 2019.

[44] M. Pajares, N. Jiménez-Moreno, Á. J. García-Yagüe et al., "Transcription factor NFE2L2/NRF2 is a regulator of macroautophagy genes," *Autophagy*, vol. 12, no. 10, pp. 1902–1916, 2016.

[45] M. Pajares, A. I. Rojo, E. Arias, A. Díaz-Carretero, A. M. Cuervo, and A. Cuadrado, "Transcription factor NFE2L2/NRF2 modulates chaperone-mediated autophagy through the regulation of LAMP2A," *Autophagy*, vol. 14, no. 8, pp. 1310–1322, 2018.

[46] S. Pankiv, T. H. Clausen, T. Lamark et al., "p62/SQSTM1 binds directly to Atg8/LC3 to facilitate degradation of ubiquitinated protein aggregates by autophagy," *Journal of Biological Chemistry*, vol. 282, no. 33, pp. 24131–24145, 2007.

[47] J. P. Stice and A. A. Knowlton, "Estrogen, NFκB, and the heat shock response," *Molecular Medicine*, vol. 14, no. 7-8, pp. 517–527, 2008.

Hindawi
Oxidative Medicine and Cellular Longevity
Volume 2020, Article ID 4063562, 11 pages
https://doi.org/10.1155/2020/4063562

Review Article

NLRP3 Inflammasome and Inflammatory Diseases

Zheng Wang,[1] **Simei Zhang**,[1] **Ying Xiao**,[1] **Wunai Zhang**,[1] **Shuai Wu**,[1] **Tao Qin**,[1] **Yangyang Yue**,[1] **Weikun Qian**,[1] **and Li Li**[2]

[1]*Department of Hepatobiliary Surgery, First Affiliated Hospital, Xi'an Jiaotong University, Xi'an 710061, China*
[2]*Department of Ophthalmology, First Affiliated Hospital, Xi'an Jiaotong University, Xi'an 710061, China*

Correspondence should be addressed to Li Li; eyelili2010@xjtu.edu.cn

Received 6 December 2019; Revised 14 January 2020; Accepted 17 January 2020; Published 18 February 2020

Guest Editor: Marco Cordani

Almost all human diseases are strongly associated with inflammation, and a deep understanding of the exact mechanism is helpful for treatment. The NLRP3 inflammasome composed of the NLRP3 protein, procaspase-1, and ASC plays a vital role in regulating inflammation. In this review, NLRP3 regulation and activation, its proinflammatory role in inflammatory diseases, interactions with autophagy, and targeted therapeutic approaches in inflammatory diseases will be summarized.

1. Introduction

Inflammasomes, first identified by Martinon and coworkers in 2002 [1–3], are a class of cytosolic complexes of proteins that mediate the activation of potent inflammatory mediators. They are integral parts of the innate immune response against invading pathogens and are activated upon cellular infections or stressors that promote the expression, maturation, and release of a multitude of proinflammatory cytokines, triggering a cascade of inflammatory responses [4, 5]. The nucleotide-binding oligomerization- (NOD-) like receptors (NLRs), a newly identified type of pattern recognition receptors (PRRs), which include Toll-like receptors (TLRs), C-type lectins (CTLs), and galectins, mediate the innate immune response to detect pathogenic microbes and other endogenous or exogenous pathogens [6, 7] and are important components of inflammasomes; they are located within the cytoplasm and recognize pathogen/damage-associated molecular patterns (PAMPs/DAMPs) [8–10]. The NLRs comprise 22 human genes and more mouse genes, and their family members are characterized by the presence of a tripartite structure: a central NOD, which is commonly flanked by C-terminal leucine-rich repeats (LRRs) and a N-terminal caspase recruitment domain (CARD) or pyrin domains (PYDs) [4, 11].

There are 4 known inflammasomes (NLRP1, NLRP3, NLRP4, and Aim2 inflammasomes), and they all contain a PRR that belongs to the NLR family [12, 13]. Among these inflammasomes, the NLRP3 inflammasome plays a pivotal role both in shaping immune responses and regulating the integrity of intestinal homeostasis in many common inflammatory diseases [14, 15]. NLRP3, a multiprotein complex consisting of an NLRP3 scaffold, an adaptor apoptosis speck-like protein (ASC) and the effector procaspase-1, initiates the formation of the inflammasome by interacting with ASC, which recruits and activates procaspase-1 to generate active caspase-1 and then converts the cytokine precursors pro-IL-1β and pro-IL-18 into mature and biologically active IL-1β and IL-18, respectively. Once activated, the active IL-1β and IL-18 will trigger a series of inflammatory responses and pyroptotic cell death [10, 16–18].

The NLRP3 inflammasome is produced by bone marrow-derived macrophages (after stimulation by microbial and nonmicrobial factors such as bacterial toxins, particulate matter, and lipopolysaccharide (LPS)) [8, 19]. The mechanism of NLRP3 activation remains elusive. Several molecular and cellular events have been proposed to describe to be involved in inflammasome activation, including K^+ efflux, Ca^{2+} signaling, mitochondrial dysfunction, and reactive oxygen species (ROS) production [9]. For example, particulate matter activates the NLRP3 inflammasome by inducing endocytosis and damage to the lysosome membrane, resulting in the release of cathepsin B into the cytosol [20]. Interestingly, the role of ROS and mitochondrial

perturbation in NLRP3 inflammasome activation remains controversial and requires further investigation [21–24].

NLRP3 has also been implicated in the pathogenesis of a number of complex diseases, notably including metabolic disorders such as type 2 diabetes [25], atherosclerosis [11, 26–29], obesity, and gout [30]. A role for NLRP3 in diseases of the central nervous system is emerging, including Alzheimer's disease and Parkinson's disease [31, 32]. Abnormal activation of the NLRP3 inflammasome might contribute to intestinal cancer, inflammatory diseases, and autoinflammatory diseases such as keratitis/conjunctivitis [16, 33–36]. In this review, NLRP3 regulation and activation, its proinflammatory role in inflammatory diseases, interactions with autophagy, and targeted therapeutic approaches in inflammatory diseases will be summarized.

2. The Role of NLRP3 in Inflammation

Inflammasomes are multiprotein complexes located in macrophages, dendritic cells, and some other immune cells and control the activation of the proteolytic enzyme caspase-1. Caspase-1 then regulates the maturation of IL-1β and IL-18 and the subsequent pyroptosis [37]. The NLRP3 inflammasome is composed of the NLRP3 protein, procaspase-1, and ASC [38]. Procaspase-1 is the effector in the NLRP3 inflammasome with a CARD domain. ASC is a bipartite complex containing a PYD and a CARD, which makes it a bridge connecting the sensor NLRP3 and the effector procaspase-1. NLRP3 inflammasome activation is a self-defending mechanism against invading factors and stress. Upon infection and/or injury, inflammasome components assemble and oligomerize, leading to the autocleavage of procaspase-1 to its active form. Activated caspase-1 transforms proinflammatory cytokines into their mature forms, which then participate in the following inflammatory response [39].

The NLRP3 response to stimuli occurs in the trans-Golgi network [40]. The activation of NLRP3 begins with the recognition of the danger or stressor by the sensor PRRs [41]. PAMPs (including microbial nucleic acids, bacterial secretion systems, and components of microbial cell walls) can be sensed by PPRs [42]. In addition, DAMPs (such as ATP and uric acid crystals) can also trigger PPRs [43]. The activation of the NLRP3 inflammasome is a two-stage process. The first stage is the sensing and producing stage, which begins with the recognition of PAMPs and DAMPs by TLRs. In this stage, TLRs recognize various stress factors and activate NF-κB signaling, resulting in elevated production of precursor proteins, including the NLRP3 protein, pro-IL-1β, and pro-IL-18 [44]. The second stage is the assembly and effector stage, which begins with the assembly of the NLRP3 inflammasome. The NLRP3 protein, ASC, and procaspase-1 assemble into the mature complex, which then transforms the immature forms of IL-1β and IL-18 into their mature forms [45]. IL-1β and IL-18 participate in the subsequent inflammatory effect.

NLRP3 is commonly involved in the immune response to bacteria, viruses, fungi, and parasites [42]. In most cases, the recognition of pathogens in the immune response is indirect. TLRs recognize the particular components of the invader and then induce the NLRP3 inflammasome components to be transcribed and assembled. Microbial stimuli, including Bacterial Muramyl Dipeptide (MDP) [46], bacterial RNA [47], and LPS [47], can activate the NLRP3 inflammasome in a TLR-dependent manner, while living microbes, rather than dead microbes, can induce a particular immune response via the Toll/interleukin-1 receptor domain-containing adaptor-inducing interferon-β- (TRIF-) dependent recognition by the NLRP3 inflammasome [48].

In addition, various danger signals unrelated to infection can trigger the NLRP3 inflammasome, including ROS, Ca^{2+}, nitric oxide (NO), and mitochondrial dysfunction (MtD). The production of ROS in cell has two origins: mitochondria-derived ROS (mtROS) and the cytosolic ROS. The mtROS can act as the second messenger to trigger the activation of inflammasomes after the recognition of PAMPs from microbes or DAMPs [49]. In a research about the muscle wasting, the researchers found that angiotensin II can promote the mtROS production as well as MtD, which further activated NLRP3 inflammasome [50].

The proper function of mitochondria is also crucial for NLRP3 inflammasome activation. Several factors including NO [51] and Ca^{2+} [52] can lead to MtD, which may also trigger the NLRP3 inflammasome activation via the release of oxidized mitochondrial DNA (mtDNA) following the engagement of TLRs [21]. MtD induced by the NLRP3 secondary signal activators can lead to the release of oxidized mtDNA into the cytosol, and then NLRP3 inflammasome is activated by the bondage of mtDNA [53]. Mitophagy, a crucial procedure involved in mitochondrial dynamics, has been reported to has an influence on excessive inflammasome activation. Mitophagy clears damaged mitochondria through a variety of mechanisms, including the activation of the PINK/PARKIN pathway [54], p62 aggregation [55], and SESN2 activation [56].

The endocytosis of silica and asbestos by pulmonary macrophages may activate the NLRP3 inflammasome and ROS signaling, which further leads to silicosis and asbestosis [20]. Similarly, the accumulation of monosodium urate during gout can activate the NLRP3 inflammasome in macrophages [46]. In osteoarthritis, hydroxyapatite crystals are able to activate IL-1β and elevate its production through the NLRP3 inflammasome, thus mediating inflammation and joint diseases [57]. In atherosclerosis, the NLRP3 inflammasome drives IL-1β release, thus contributing to the progression of atherosclerosis [58]. Similarly, the inhibition of caspase-1 and IL-1β activation induced by bone marrow-derived mesenchymal stem cells can suppress the generation of mitochondrial ROS and then inhibit the NLRP3 inflammasome activation [59]. Systemic inflammation has been reported to be related to an overproduction of IL-1β and IL-18 [60]. In a mouse model focusing on systemic inflammatory response syndrome, the researchers found that NLRP3 activates the adaptive immune response in mice during acute pancreatitis. This response depends on IL-1β and IL-18, but not IL-12 [60]. Similar results have also been observed to support the NLRP3 active effect of IL-18 in an engineered mouse model [61]. However, the exact mechanism by which NLRP3 recognizes DAMPs remains

unclear. Studies have reported that K^+ efflux and Ca^{2+} signaling participate in the activation of the NLRP3 inflammasome [62–66]. Among the reported upstream mechanisms involved in the NLRP3 inflammasome, the generation of mitochondrial ROS is an important one [67]. During ischemia and reperfusion, ethanol, obesity (saturated fatty acids), and ROS can induce NLRP3 inflammasome activation [68–70].

In a research about the HBV infection, researchers found that HBeAg could inhibit the NF-κB pathway and ROS production. This effect prevents LPS from inducing NLRP3 inflammasome activation, without interrupting the intracellular calcium concentration and lysosomal rupture [71]. In addition, in a study of RNA viruses, the production of ROS induced by the RIP1-RIP3 complex activated the NLRP3 inflammasome [72]. NADPH oxidase can produce cytosolic ROS, which is responsible for the activation of the NLRP3 inflammasome [73]; nevertheless, proof to the contrary showed that macrophages lacking NADPH oxidase can exhibit normal activation of the NLRP3 inflammasome [74]. Hence, the importance of ROS in NLRP3 inflammasome function has been widely acknowledged, but the exact mechanism remains to be explored.

3. The Crosstalk between NLRP3 and Autophagy

Autophagy is a physiological process that maintains the normal metabolic function and survival of cells. The formation of autophagosome is a feature of autophagy. The first step in autophagosome formation is initiation. The ULK1-Atg13-FIP200 complex is activated and localizes in the endoplasmic reticulum and some other areas. This is followed by a nucleation step driven by class III phosphoinositide 3-kinase complex (consisting of VPS34, VPS15, Beclin 1, ATG14L, and NRBF2) which is activated by ULK1. After the phagophore has almost wrapped the shipment to be degraded, the phagophore stretch and seal the shipment. The elongation step was performed with an Atg5-Atg 12-Atg16L and LC3II-PE conjugate. Then, autophagosome fuses to lysosomes to form autophagolysosomes [75].

Autophagy recycles cellular proteins and damaged organelles to obtain metabolic energy during starvation or stress to modulate cell survival in many diseases. In normoxia, autophagy is essential for maintaining corneal epithelium physiology and cell survival [76]. Additionally, autophagy serves as an essential process in resisting infection by degrading pathogens. In keratitis, the innate immune response, including autophagy, is activated when pathogens adhere to the ocular surface [77]. Interestingly, some viruses (such as HSV1) inhibit autophagy (by binding of the virus protein ICP34.5 to the host protein Beclin 113) and reduce damage [78]. In addition, excessive or abnormal autophagy can lead to cell death. The autophagy of dendritic cells enhanced the activation of CD^{4+} T cells and pathological keratitis, which significantly promoted the occurrence of herpes simplex keratitis [79]. Interfering with autophagy may be able to intervene in this incurable infectious blindness.

Normally, activation of the inflammasome, including NLRP3, triggers an antiviral inflammatory response that clears the virus and cures the inflamed tissue. NLRP3-knockout mice with keratitis induced by HSV1 developed more severe disease than infected wild-type animals, with stromal keratitis lesions occurring earlier and having more angiogenesis; this result may be related to the nuclear translocation of the NLRP3-IRF4 complex in Th2 cells, which promotes the expression of the IL-4, IL-5, and IL-13 genes to fight the HSV1 infection [80, 81]. In addition, the NLRP3/caspase-1/IL-1β pathway plays an important role in leukocyte aggregation and fighting infection during Aspergillus fumigatus infection [36]. However, the abnormal activation of the inflammasome will lead to harmful overwhelming inflammation, which may damage the infected tissue. Persistent and abnormal NLRP3 signaling is the basis of many chronic and degenerative diseases, including Stargardt disease type 1 [82], Alzheimer's disease [83], atherosclerosis [84], atrial fibrillation [85], osteoarthritis [86], and cancer [87] (Table 1).

The relationship between autophagy and NLRP3 is complex. Some studies have shown that autophagy could inhibit priming and assembly stages of the NLRP3 inflammasome [88]. In autophagy-deficient cells, including autophagic protein depletion [89], activation of the inflammatory NLRP3 complex is enhanced due to mitochondrial dysfunction such as excessive mitochondrial ROS production and changes in mitochondrial membrane permeability [90], contributed to IL-1β and IL-18 secretion. Loss of autophagy/mitophagy can lead to a buildup of cytosolic reactive oxygen species and mitochondrial DNA, which can, in turn, activate immune signaling pathways that ultimately lead to the releases of inflammatory cytokines, including IL-1α, IL-1β, and IL-18 [91]. In addition, mitophagy can clear damage mitochondria through a variety of mechanisms, including activation of the PINK/PARKIN pathway [91], p62 aggregation [92], and SESN2 activation [91], thereby preventing excessive inflammation activation. Research has shown that resveratrol inhibits NLRP3 activation in macrophages by inhibiting mitochondrial damage and enhancing autophagy [93]. Studies have also shown that autophagosomes can directly encapsulate and degrade inflammasome components, including the linker molecules ASC, NLRP3, and pro-IL-1β [94]. However, some studies have also shown that autophagy promotes NLRP3 activation. Zearalenone increases autophagy and triggers NLRP3 resonance activation by promoting NF-κB activation and nuclear translocation, ultimately resulting in cell pyroptosis [95]. In turn, NLRP3 has an effect on autophagy activation. The induction of NLRP3 inflammasomes in macrophages triggers the activation of the G-protein RalB and then the activation of autophagy, which tempers inflammation by eliminating active inflammasomes to prevent a cascade of amplified inflammatory responses [93]. Nevertheless, the inflammation induced by the NLRP3 inflammasome can also inhibit autophagy. In neuritis, the neuroinflammation promoted by NLRP3 inflammatory complexes may be amplified and regulated by a glia maturation factor, thus inhibiting the clearance of the protein aggregates that formed as a result of the

Table 1: Role of NLRP3 inflammasome in disease.

Disease	Responsible factor	Effect	Ref
Aspergillus fumigatus keratitis	NLRP3, caspase-1, and IL-1β	Pannexin 1 channels play important roles in the regulation of progression and leucocyte aggregation during corneal *A. fumigatus* infection via the NLRP3/caspase-1/IL-1β pathway.	[36]
Stargardt disease type 1	NLRP3, ROS, IL-1β, and IL-18	Aberrant buildup of atRAL promotes the death of RPE cells via NLRP3 inflammasome activation.	[82]
Alzheimer's disease	NLRP3, caspase-1, and IL-1β	Strongly enhanced the active NLRP3/caspase-1 axis in human mild cognitive impairment and brains with Alzheimer's disease.	[83]
Atherosclerosis	NLRP3	NLRP3 was overexpressed in aorta of patients with coronary atherosclerosis.	[84]
Atrial fibrillation	NLRP3	The inhibition of NLRP3 as a potential novel AF therapy approach.	[85]
Osteoarthritis	NLRP3, caspase-1, and IL-1β	Inhibition to the release of inflammasome NLRP3 exerts protection on osteoarthritis leading to the downregulation of inflammatory cytokines.	[85]
Cancer	NLRP3, caspase-1, IL-1β, and IL-18	Dysregulation of NLRP3 inflammasome activation is involved in tumor pathogenesis.	[87]

autophagic pathway [96]. In nonalcoholic steatohepatitis, NLRP3 and caspase-1 can inhibit autophagy by regulating the PINK/PARKIN pathway [91]. Additionally, the NLRP3 inflammasome inhibitor MCC950 can activate autophagy and PPARα through mTOR inhibition [97]. In conclusion, the complex relationship between NLRP3 and autophagy needs more research to provide new ideas for clinical treatment.

4. The Therapeutic Prospect of NLRP3 on Related Diseases

In clinical settings, the NLRP3 inflammasome is upregulated in myocardial fibroblasts mainly during acute myocardial infarction (AMI) [98]. van Hout et al. [99] also proved that the inflammasome can be inhibited by MCC950 in large animal AMI models. In addition, the immune complexes in systemic lupus erythematosus (SLE) patients can trigger the NLRP3 inflammasome, activate macrophages, and cause cell and tissue damage [100]. A recent study [101] has shown that citral can inhibit the expression of pro-IL-1β mediated by endotoxin and the activation of the NLRP3 inflammasome mediated by ATP, which is intriguing for the treatment of SLE. Moreover, activation of the NLRP3 inflammasome also plays an important role in the nonspecific inflammation of inflammatory bowel disease (IBD). It is noteworthy that Villani et al. [102] found that the SNP rs10733113 in the NLRP3 gene region is a Crohn's disease susceptibility gene. Subsequently, Lewis et al. [103] also reported that men carrying the c10x motif in card8, Q705k in NLRP3, and wild-type NOD2 showed susceptibility to Crohn's disease. In addition, a recent study [104] has shown that dysfunctional CARD8 mutations can also activate the NLRP3 inflammasome and contribute to the occurrence of Crohn's disease. Clarification of the exact physiological mechanism of the NLRP3 inflammasome will undoubtedly guide the development of effective treatments for IBD in the future.

NLRP3 inflammasomes are of great importance to therapies targeting inflammation due to their critical role in regulating inflammation. In many bacterial infections, pathogens activate NLRP3-based inflammation through the secretion of pore-forming toxins by Staphylococcus aureus [105]. Vibrio cholerae secretes toxins to activate NLRP3 similar to Staphylococcus aureus. In vivo, mice lacking inflammatory components showed that caspase-1 and ASC had protective effects against Vibrio cholerae infection [106]. NLRP3 was beneficial for mice during pneumonia caused by Streptococcus pneumoniae, and NLRP3$^{-/-}$ mice had higher bacterial load and higher mortality than wild-type mice [107]. The NLRP3 inflammasome can also be activated by viruses, such as influenza A, through the recognition of viral RNA [108]. Recent studies [109, 110] have shown that the NLRP3 inflammasome can be activated by superficial fungi such as T. schoenleinii and M. canis or their components through direct or indirect pathways to produce active inflammatory factors, which play an important role in host immunity. Currently, it has been found that the mechanisms against infection of nonsuperficial fungi may be related to the NLRP3 inflammasome [111–113]. NLRP3 can recognize Candida albicans, activate the NLRP3 inflammation complex, and induce pro-IL-1β processing, maturation, and secretion [114, 115]. The mortality rate of NLRP3 or ASC gene-deficient mice after infection with Cryptococcus neoformans was higher than that of wild-type mice, and the bacterial load in the lung tissues of NLRP3-deficient mice was significantly higher than that of wild-type mice [116]. These results showed that the NLRP3 inflammasome plays an important role in the host response to cryptococcal infection.

In eye diseases, the NLRP3 inflammasome has been shown to contribute to diabetic retinopathy [117], acute

Table 2: Inhibitors of NLRP3 pathways as well as their effects in cell cultures, animal models, or patients of inflammatory diseases.

Inhibitors	Molecular mechanism	Cell/animal model/patients	Ref
MCC950	Block the ATPase domain of NLRP3 and inhibit the activation of typical and atypical NLRP3 inflammasome	Autoimmune encephalomyelitis Cryopyrin-associated periodic syndrome Muckle-Wells syndrome	[124]
MNS	Bind to the LRR and NACHT domains and suppress ATPase activity of NLRP3	Bone marrow-derived macrophages	[91]
CY-09	Inhibit NLRP3 ATPase activity	Cryopyrin-associated autoinflammatory syndrome Type 2 diabetes Synovial fluid cells from gout patients	[137]
OLT1177	Inhibit NLRP3 ATPase activity and block canonical and noncanonical activation of NLRP3 inflammasome	Human blood-derived macrophages Human blood neutrophils Monocytes isolated from patients with cryopyrin-associated periodic syndrome Spleen cells from mice	[128]
Glyburide	Inhibit ATP-sensitive K^+ channels, act as downstream of the P2X7 receptor, and inhibit ASC aggregation	Bone marrow-derived macrophages Familial cold-associated autoinflammatory syndrome patients	[129]
16673-34-0	Interfere the downstream of NLRP3 conformational changes and bind to ASC	Acute myocardial infarction	[138]
JC124	Block ASC aggregation, caspase-1 activation, and IL-1β secretion	Acute myocardial infarction Alzheimer's disease	[139] [140]
BHB	Inhibit K^+ efflux and block ASC aggregation	Muckle-Wells syndrome Familial cold autoinflammatory syndrome Urate crystal-induced peritonitis	[70]
Parthenolide	Inhibit caspase-1 activation and NLRP3 ATPase activity	Bone marrow-derived macrophages Cystic fibrosis	[131] [141]
Bay 11-7082	Alkylation of cysteine residues of the NLRP3 ATPase region	Psoriasis-like dermatitis Diabetic nephropathy	[142] [143]

glaucoma [118], age-related macular degeneration [119], Behcet's syndrome, and dry eye disease [120]. In addition, in a mouse model of Pseudomonas aeruginosa keratitis, the inhibition of caspase-1 and the killing of bacteria by ciprofloxacin reduced the severity of corneal inflammation [121]. Another study showed that in a mouse model of keratitis, the level of IL-1 increased starting at 4 h after infection [122]. Treatment with the IL-1 receptor antagonist anakinra has also proven successful in the treatment of scleritis and episcleritis in the context of different rheumatic conditions [123].

To treat NLRP3-related diseases, researchers have found several inhibitors of NLRP3 or IL-1β, including direct inhibitors of NLRP3 proteins such as MCC950 [124, 125], 3,4-methylenedioxy-β-nitrostyrene (MNS) [126], CY-09 [127], and OLT1177 [128], indirect inhibitors such as glyburide [129], 16673-34-0, and JC124 [130], and inhibitors of components of the complex such as β-hydroxybutyrate (BHB) [70], parthenolide, and bay 11-7082 [131] (Table 2). The NLRP3 inflammasome can also produce IL-18, which leads to physical disorders [132]. Compared to blocking IL-1β, specific targeting with NLRP3 inhibitors may be a good choice for related diseases [133]. However, the Food and Drug Administration (FDA) does not currently approve these drugs. Future research should focus on the development of structure-oriented direct inhibitors to improve the specificity and effectiveness.

5. Discussion

NLRP3 plays a vital role in various inflammatory diseases by altering immune responses or regulating the integrity of intestinal homeostasis. ROS, K^+ efflux, and Ca^{2+} signaling have been suggested to activate NLRP3 [9], but the specific mechanism remains unclear. Particularly, the role of ROS in NLRP3 inflammasome activation remains controversial, and it has been revealed that the cytosolic ROS induced by NADPH is responsible for the activation of the NLRP3 inflammasome [73]. However, other studies have shown that macrophages lacking NADPH oxidase exhibit normal activation of the NLRP3 inflammasome [74]. Therefore, we can conclude that the function of ROS is undetermined in the NLRP3 inflammasome, and more precise research about the mechanism is necessary.

The NLRP3 inflammasome is composed of the NLRP3 protein, procaspase-1, and ASC [134] and can generate active caspase-1 and then convert the cytokine precursors

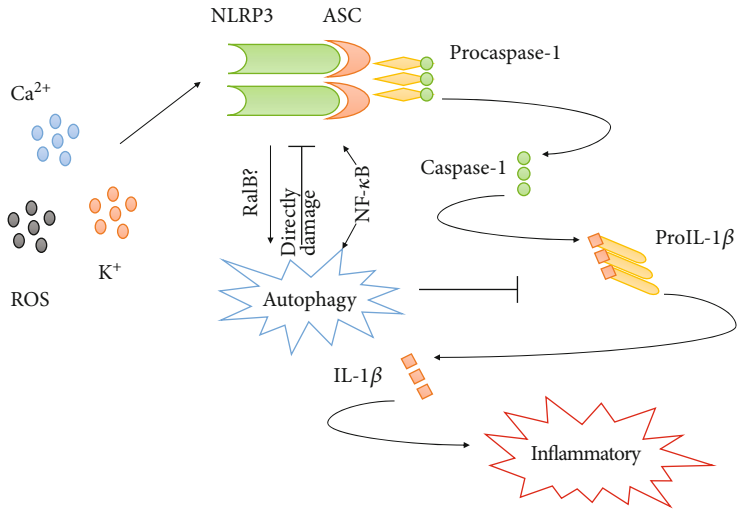

Figure 1: NLRP3 inflammasome-mediated inflammation and autophagy have complex and bidirectional regulatory effects. After being stimulated by Ca^{2+}, K^+, or ROS, the NLRP3 inflammasome is activated and recruits and activates procaspase-1 to generate active caspase-1, which then converts the cytokine precursor pro-IL-1β or other proinflammatory cytokines into mature and biologically active forms and triggers a series of inflammatory responses and pyroptotic cell death. However, this process can be regulated and interrupted by autophagy via damage of NLRP3 inflammasome; however, NLRP3 can promote cell autophagy via activation of the G-protein RalB. Interestingly, the relationship between NLRP3 and autophagy is not definitively understood, and there have also been reports that contradict the above statement such as NF-κB activation can modulate the NLRP3 and autophagy in same direction.

pro-IL-1β and pro-IL-18 into mature and biologically active IL-1β and IL-18, respectively. Ultimately, active IL-1β and IL-18 trigger a series of inflammatory responses and pyroptotic cell death [17, 18, 135]. As an important physiological process, autophagy is also strongly associated with the NLRP3 inflammasome. Many studies have shown that autophagosomes can directly encapsulate and degrade inflammasome components, including the linker molecules ASC, NLRP3, and pro-IL-1β [90, 93, 94]. Nevertheless, other researchers have demonstrated that autophagy can promote the activation of the NLRP3 inflammasome and that NLRP3 also triggers autophagy by activating the G-protein RalB in turn [95–97]. NLRP3 and autophagy have a complex relationship, and an exploration of this relationship will be helpful for understanding the mechanism of inflammation (Figure 1).

The NLRP3 inflammasome is considered a promising target for the treatment of many diseases associated with inflammation. In AMI, SLE, IBD, Crohn's disease, bacterial infections, eye diseases, etc., the NLRP3 inflammasome plays a critical role in regulating pathological processes [98, 100, 102–105, 119, 136]. Although several inhibitors of the NLRP3 inflammasome have been developed, they have not been approved by the FDA and more basic and clinical research to confirm the curative effects is necessary. With in-depth research on the mechanism of the NLRP3 inflammasome, we believe that a more exact mechanism of the NLRP3 inflammasome itself and its relationship with autophagy will be uncovered and that more specific and effective inhibitors will be exploited.

Conflicts of Interest

The authors declare no conflicts of interest.

Acknowledgments

The authors thank all laboratory members for ongoing discussions. This work was funded by the National Natural Science Foundation of China (NSFC 81872008) and the Science and Technology Innovation as a Whole Plan Project of Shaanxi Province, China. The authors acknowledge all financial supports for this work.

References

[1] S. R. Ali, M. Karin, and V. Nizet, "Signaling cascades and inflammasome activation in microbial infections," *Inflammasome*, vol. 2, no. 1, 2016.

[2] L. F. Gentile, A. L. Cuenca, A. G. Cuenca et al., "Improved emergency myelopoiesis and survival in neonatal sepsis by caspase-1/11 ablation," *Immunology*, vol. 145, no. 2, pp. 300–311, 2015.

[3] I. Jorgensen and E. A. Miao, "Pyroptotic cell death defends against intracellular pathogens," *Immunological Reviews*, vol. 265, no. 1, pp. 130–142, 2015.

[4] K. Schroder and J. Tschopp, "The inflammasomes," *Cell*, vol. 140, no. 6, pp. 821–832, 2010.

[5] H. Yaribeygi, N. Katsiki, A. E. Butler, and A. Sahebkar, "Effects of antidiabetic drugs on NLRP3 inflammasome activity, with a focus on diabetic kidneys," *Drug Discovery Today*, vol. 24, no. 1, pp. 256–262, 2019.

[6] C. Bourgeois and K. Kuchler, "Fungal pathogens—a sweet and sour treat for *toll*-like receptors," *Frontiers in Cellular and Infection Microbiology*, vol. 2, p. 142, 2012.

[7] B. Z. Shao, Z. Q. Xu, B. Z. Han, D. F. Su, and C. Liu, "NLRP3 inflammasome and its inhibitors: a review," *Frontiers in Pharmacology*, vol. 6, p. 262, 2015.

[8] G. Y. Chen and G. Nunez, "Inflammasomes in intestinal inflammation and cancer," *Gastroenterology*, vol. 141, no. 6, pp. 1986–1999, 2011.

[9] Y. He, H. Hara, and G. Nunez, "Mechanism and regulation of NLRP3 inflammasome activation," *Trends in Biochemical Sciences*, vol. 41, no. 12, pp. 1012–1021, 2016.

[10] T. Prochnicki and E. Latz, "Inflammasomes on the crossroads of innate immune recognition and metabolic control," *Cell Metabolism*, vol. 26, no. 1, pp. 71–93, 2017.

[11] A. Grebe, F. Hoss, and E. Latz, "NLRP3 inflammasome and the IL-1 pathway in atherosclerosis," *Circulation Research*, vol. 122, no. 12, pp. 1722–1740, 2018.

[12] M. Lamkanfi and V. M. Dixit, "Mechanisms and functions of inflammasomes," *Cell*, vol. 157, no. 5, pp. 1013–1022, 2014.

[13] F. Lu, Z. Lan, Z. Xin et al., "Emerging insights into molecular mechanisms underlying pyroptosis and functions of inflammasomes in diseases," *Journal of Cellular Physiology*, vol. 235, no. 4, pp. 3207–3221, 2019.

[14] C. Pellegrini, L. Antonioli, G. Lopez-Castejon, C. Blandizzi, and M. Fornai, "Canonical and non-canonical activation of NLRP3 inflammasome at the crossroad between immune tolerance and intestinal inflammation," *Frontiers in Immunology*, vol. 8, p. 36, 2017.

[15] E. Elinav, J. Henao-Mejia, and R. A. Flavell, "Integrative inflammasome activity in the regulation of intestinal mucosal immune responses," *Mucosal Immunol*, vol. 6, no. 1, pp. 4–13, 2013.

[16] M. S. J. Mangan, E. J. Olhava, W. R. Roush, H. M. Seidel, G. D. Glick, and E. Latz, "Erratum: Targeting the NLRP3 inflammasome in inflammatory diseases," *Nature Reviews Drug Discovery*, vol. 17, no. 9, p. 688, 2018.

[17] A. Liston and S. L. Masters, "Homeostasis-altering molecular processes as mechanisms of inflammasome activation," *Nature Reviews Immunology*, vol. 17, no. 3, pp. 208–214, 2017.

[18] A. Lu, V. G. Magupalli, J. Ruan et al., "Unified polymerization mechanism for the assembly of ASC-dependent inflammasomes," *Cell*, vol. 156, no. 6, pp. 1193–1206, 2014.

[19] F. Martinon, V. Petrilli, A. Mayor, A. Tardivel, and J. Tschopp, "Gout-associated uric acid crystals activate the NALP3 inflammasome," *Nature*, vol. 440, no. 7081, pp. 237–241, 2006.

[20] V. Hornung, F. Bauernfeind, A. Halle et al., "Silica crystals and aluminum salts activate the NALP3 inflammasome through phagosomal destabilization," *Nature Immunology*, vol. 9, no. 8, pp. 847–856, 2008.

[21] Z. Zhong, S. Liang, E. Sanchez-Lopez et al., "New mitochondrial DNA synthesis enables NLRP3 inflammasome activation," *Nature*, vol. 560, no. 7717, pp. 198–203, 2018.

[22] N. Subramanian, K. Natarajan, M. R. Clatworthy, Z. Wang, and R. N. Germain, "The adaptor MAVS promotes NLRP3 mitochondrial localization and inflammasome activation," *Cell*, vol. 153, no. 2, pp. 348–361, 2013.

[23] R. Allam, K. E. Lawlor, E. C. W. Yu et al., "Mitochondrial apoptosis is dispensable for NLRP3 inflammasome activation but non-apoptotic caspase-8 is required for inflammasome priming," *EMBO Reports*, vol. 15, no. 9, pp. 982–990, 2014.

[24] E. I. Elliott and F. S. Sutterwala, "Initiation and perpetuation of NLRP3 inflammasome activation and assembly," *Immunological Reviews*, vol. 265, no. 1, pp. 35–52, 2015.

[25] H. Yaribeygi, M. T. Mohammadi, R. Rezaee, and A. Sahebkar, "Fenofibrate improves renal function by amelioration of NOX-4, IL-18, and p53 expression in an experimental model of diabetic nephropathy," *Journal of Cellular Biochemistry*, vol. 119, no. 9, pp. 7458–7469, 2018.

[26] H. Wen, J. P. Y. Ting, and L. A. J. O'Neill, "A role for the NLRP3 inflammasome in metabolic diseases—did Warburg miss inflammation?," *Nature Immunology*, vol. 13, no. 4, pp. 352–357, 2012.

[27] H. Zhang, X. Gong, S. Ni, Y. Wang, L. Zhu, and N. Ji, "C1q/TNF-related protein-9 attenuates atherosclerosis through AMPK-NLRP3 inflammasome singling pathway," *International Immunopharmacology*, vol. 77, 2019.

[28] B. A. Ference, H. N. Ginsberg, I. Graham et al., "Low-density lipoproteins cause atherosclerotic cardiovascular disease. 1. Evidence from genetic, epidemiologic, and clinical studies. A consensus statement from the European Atherosclerosis Society Consensus Panel," *European Heart Journal*, vol. 38, no. 32, pp. 2459–2472, 2017.

[29] Z. Hoseini, F. Sepahvand, B. Rashidi, A. Sahebkar, A. Masoudifar, and H. Mirzaei, "NLRP3 inflammasome: its regulation and involvement in atherosclerosis," *Journal of Cellular Physiology*, vol. 233, no. 3, pp. 2116–2132, 2018.

[30] H. Y. Kim, H. J. Lee, Y. J. Chang et al., "Interleukin-17-producing innate lymphoid cells and the NLRP3 inflammasome facilitate obesity-associated airway hyperreactivity," *Nature Medicine*, vol. 20, no. 1, pp. 54–61, 2014.

[31] C. Ising, C. Venegas, S. Zhang et al., "NLRP3 inflammasome activation drives tau pathology," *Nature*, vol. 575, no. 7784, pp. 669–673, 2019.

[32] S. Wang, Y. H. Yuan, N. H. Chen, and H. B. Wang, "The mechanisms of NLRP3 inflammasome/pyroptosis activation and their role in Parkinson's disease," *International Immunopharmacology*, vol. 67, pp. 458–464, 2019.

[33] E. Tourkochristou, I. Aggeletopoulou, C. Konstantakis, and C. Triantos, "Role of NLRP3 inflammasome in inflammatory bowel diseases," *World Journal of Gastroenterology*, vol. 25, no. 33, pp. 4796–4804, 2019.

[34] L. Liu, Y. Dong, M. Ye et al., "The pathogenic role of NLRP3 inflammasome activation in inflammatory bowel diseases of both mice and humans," *Journal of Crohn's and Colitis*, vol. 11, no. 6, pp. 737–750, 2017.

[35] C. de Torre-Minguela, P. Mesa Del Castillo, and P. Pelegrin, "The NLRP3 and pyrin inflammasomes: implications in the pathophysiology of autoinflammatory diseases," *Frontiers in Immunology*, vol. 8, p. 43, 2017.

[36] X. Yang, G. Zhao, J. Yan et al., "Pannexin 1 channels contribute to IL-1β expression via NLRP3/caspase-1 inflammasome inAspergillus FumigatusKeratitis," *Current Eye Research*, vol. 44, no. 7, pp. 716–725, 2019.

[37] J. Liu and X. Cao, "Cellular and molecular regulation of innate inflammatory responses," *Cellular & Molecular Immunology*, vol. 13, no. 6, pp. 711–721, 2016.

[38] A. Lu and H. Wu, "Structural mechanisms of inflammasome assembly," *FEBS Journal*, vol. 282, no. 3, pp. 435–444, 2015.

[39] R. C. Rai, "Host inflammatory responses to intracellular invaders: review study," *Life Sciences*, vol. 240, p. 117084, 2020.

[40] Y. Zhen and H. Zhang, "NLRP3 inflammasome and inflammatory bowel disease," *Frontiers in Immunology*, vol. 10, p. 276, 2019.

[41] P. Broz and V. M. Dixit, "Inflammasomes: mechanism of assembly, regulation and signalling," *Nature Reviews Immunology*, vol. 16, no. 7, pp. 407–420, 2016.

[42] L. Franchi, R. Munoz-Planillo, and G. Nunez, "Sensing and reacting to microbes through the inflammasomes," *Nature Immunology*, vol. 13, no. 4, pp. 325–332, 2012.

[43] E. Latz and P. Duewell, "NLRP3 inflammasome activation in inflammaging," *Seminars in Immunology*, vol. 40, pp. 61–73, 2018.

[44] B. Z. Shao, S. L. Wang, P. Pan et al., "Targeting NLRP3 inflammasome in inflammatory bowel disease: putting out the fire of inflammation," *Inflammation*, vol. 42, no. 4, pp. 1147–1159, 2019.

[45] K. V. Swanson, M. Deng, and J. P. Y. Ting, "The NLRP3 inflammasome: molecular activation and regulation to therapeutics," *Nature Reviews Immunology*, vol. 19, no. 8, pp. 477–489, 2019.

[46] F. Martinon, L. Agostini, E. Meylan, and J. Tschopp, "Identification of bacterial muramyl dipeptide as activator of the NALP3/cryopyrin inflammasome," *Current Biology*, vol. 14, no. 21, pp. 1929–1934, 2004.

[47] T. D. Kanneganti, N. Ozören, M. Body-Malapel et al., "Bacterial RNA and small antiviral compounds activate caspase-1 through cryopyrin/Nalp3," *Nature*, vol. 440, no. 7081, pp. 233–236, 2006.

[48] L. E. Sander, M. J. Davis, M. V. Boekschoten et al., "Detection of prokaryotic mRNA signifies microbial viability and promotes immunity," *Nature*, vol. 474, no. 7351, pp. 385–389, 2011.

[49] Y. Yang, A. V. Bazhin, J. Werner, and S. Karakhanova, "Reactive oxygen species in the immune system," *International Reviews of Immunology*, vol. 32, no. 3, pp. 249–270, 2013.

[50] Y. Liu, X. Bi, Y. Zhang, Y. Wang, and W. Ding, "Mitochondrial dysfunction/NLRP3 inflammasome axis contributes to angiotensin II-induced skeletal muscle wasting via PPAR-γ," *Laboratory Investigation*, 2019.

[51] E. Caballano-Infantes, J. Terron-Bautista, A. Beltrán-Povea et al., "Regulation of mitochondrial function and endoplasmic reticulum stress by nitric oxide in pluripotent stem cells," *World Journal of Stem Cells*, vol. 9, no. 2, pp. 26–36, 2017.

[52] C. Giorgi, S. Marchi, and P. Pinton, "The machineries, regulation and cellular functions of mitochondrial calcium," *Nature Reviews Molecular Cell Biology*, vol. 19, no. 11, pp. 713–730, 2018.

[53] K. Shimada, T. R. Crother, J. Karlin et al., "Oxidized mitochondrial DNA activates the NLRP3 inflammasome during apoptosis," *Immunity*, vol. 36, no. 3, pp. 401–414, 2012.

[54] A. Nardin, E. Schrepfer, and E. Ziviani, "Counteracting PINK/parkin deficiency in the activation of mitophagy: a potential therapeutic intervention for Parkinson's disease," *Current Neuropharmacology*, vol. 14, no. 3, pp. 250–259, 2016.

[55] A. L. Bujak, J. D. Crane, J. S. Lally et al., "AMPK activation of muscle autophagy prevents fasting-induced hypoglycemia and myopathy during aging," *Cell Metabolism*, vol. 21, no. 6, pp. 883–890, 2015.

[56] M.-J. Kim, S. H. Bae, J.-C. Ryu et al., "SESN2/sestrin2 suppresses sepsis by inducing mitophagy and inhibiting NLRP3 activation in macrophages," *Autophagy*, vol. 12, no. 8, pp. 1272–1291, 2016.

[57] C. Jin, P. Frayssinet, R. Pelker et al., "NLRP3 inflammasome plays a critical role in the pathogenesis of hydroxyapatite-associated arthropathy," *Proceedings of the National Academy of Sciences of the United States of America*, vol. 108, no. 36, pp. 14867–14872, 2011.

[58] T. Karasawa and M. Takahashi, "Role of NLRP3 inflammasomes in atherosclerosis," *Journal of Atherosclerosis and Thrombosis*, vol. 24, no. 5, pp. 443–451, 2017.

[59] S. Li, H. Wu, D. Han et al., "A novel mechanism of mesenchymal stromal cell-mediated protection against sepsis: restricting inflammasome activation in macrophages by increasing mitophagy and decreasing mitochondrial ROS," *Oxidative Medicine and Cellular Longevity*, vol. 2018, Article ID 3537609, 15 pages, 2018.

[60] M. Sendler, C. van den Brandt, J. Glaubitz et al., "NLRP3 Inflammasome Regulates Development of Systemic Inflammatory Response and Compensatory Anti-Inflammatory Response Syndromes in Mice With Acute Pancreatitis," *Gastroenterology*, vol. 158, no. 1, pp. 253–269.e14, 2020.

[61] E. S. Weiss, C. Girard-Guyonvarc'h, D. Holzinger et al., "Interleukin-18 diagnostically distinguishes and pathogenically promotes human and murine macrophage activation syndrome," *Blood*, vol. 131, no. 13, pp. 1442–1455, 2018.

[62] L. Franchi, T. D. Kanneganti, G. R. Dubyak, and G. Nunez, "Differential requirement of P2X7 receptor and intracellular K^+ for caspase-1 activation induced by intracellular and extracellular bacteria," *Journal of Biological Chemistry*, vol. 282, no. 26, pp. 18810–18818, 2007.

[63] V. Petrilli, S. Papin, C. Dostert, A. Mayor, F. Martinon, and J. Tschopp, "Activation of the NALP3 inflammasome is triggered by low intracellular potassium concentration," *Cell Death & Differentiation*, vol. 14, no. 9, pp. 1583–1589, 2007.

[64] G. S. Lee, N. Subramanian, A. I. Kim et al., "The calcium-sensing receptor regulates the NLRP3 inflammasome through Ca^{2+} and cAMP," *Nature*, vol. 492, no. 7427, pp. 123–127, 2012.

[65] M. Rossol, M. Pierer, N. Raulien et al., "Extracellular Ca^{2+} is a danger signal activating the NLRP3 inflammasome through G protein-coupled calcium sensing receptors," *Nature Communications*, vol. 3, no. 1, 2012.

[66] T. Murakami, J. Ockinger, J. Yu et al., "Critical role for calcium mobilization in activation of the NLRP3 inflammasome," *Proceedings of the National Academy of Sciences of the United States of America*, vol. 109, no. 28, pp. 11282–11287, 2012.

[67] L. Minutoli, D. Puzzolo, M. Rinaldi et al., "ROS-mediated NLRP3 inflammasome activation in brain, heart, kidney, and testis ischemia/reperfusion injury," *Oxidative Medicine and Cellular Longevity*, vol. 2016, Article ID 2183026, 10 pages, 2016.

[68] Y. Wang, Y. Wu, J. Chen, S. Zhao, and H. Li, "Pirfenidone attenuates cardiac fibrosis in a mouse model of TAC-induced left ventricular remodeling by suppressing NLRP3 inflammasome formation," *Cardiology*, vol. 126, no. 1, pp. 1–11, 2013.

[69] S. Alfonso-Loeches, J. R. Urena-Peralta, M. J. Morillo-Bargues, J. Oliver-De La Cruz, and C. Guerri, "Role of mitochondria ROS generation in ethanol-induced NLRP3 inflammasome activation and cell death in astroglial cells," *Frontiers in Cellular Neuroscience*, vol. 8, p. 8, 2014.

[70] Y. H. Youm, K. Y. Nguyen, R. W. Grant et al., "The ketone metabolite β-hydroxybutyrate blocks NLRP3

inflammasome-mediated inflammatory disease," *Nature Medicine*, vol. 21, no. 3, pp. 263–269, 2015.

[71] X. Yu, P. Lan, X. Hou et al., "HBV inhibits LPS-induced NLRP3 inflammasome activation and IL-1β production via suppressing the NF-κB pathway and ROS production," *Journal of Hepatology*, vol. 66, no. 4, pp. 693–702, 2017.

[72] X. Wang, W. Jiang, Y. Yan et al., "RNA viruses promote activation of the NLRP3 inflammasome through a RIP1-RIP3-DRP1 signaling pathway," *Nature Immunology*, vol. 15, no. 12, pp. 1126–1133, 2014.

[73] C. Dostert, V. Pétrilli, R. Van Bruggen, C. Steele, B. T. Mossman, and J. Tschopp, "Innate immune activation through Nalp3 inflammasome sensing of asbestos and silica," *Science*, vol. 320, no. 5876, pp. 674–677, 2008.

[74] R. van Bruggen, M. Y. Köker, M. Jansen et al., "Human NLRP3 inflammasome activation is Nox1-4 independent," *Blood*, vol. 115, no. 26, pp. 5398–5400, 2010.

[75] M. Y. Wu and J. H. Lu, "Autophagy and macrophage functions: inflammatory response and phagocytosis," *Cells*, vol. 9, no. 1, p. 70, 2020.

[76] G. Wang, Y. Xue, Y. Wang et al., "The role of autophagy in the pathogenesis of exposure keratitis," *Journal of Cellular and Molecular Medicine*, vol. 23, no. 6, pp. 4217–4228, 2019.

[77] T. P. O'Brien, "Management of bacterial keratitis: beyond exorcism towards consideration of organism and host factors," *Eye*, vol. 17, no. 8, pp. 957–974, 2003.

[78] A. M. Yakoub and D. Shukla, "Autophagy stimulation abrogates herpes simplex virus-1 infection," *Scientific Reports*, vol. 5, no. 1, 2015.

[79] Y. Jiang, X. Yin, P. M. Stuart, and D. A. Leib, "Dendritic cell autophagy contributes to herpes simplex virus-driven stromal keratitis and immunopathology," *mBio*, vol. 6, no. 6, 2015.

[80] F. Gimenez, S. Bhela, P. Dogra et al., "The inflammasome NLRP3 plays a protective role against a viral immunopathological lesion," *Journal of Leukocyte Biology*, vol. 99, no. 5, pp. 647–657, 2016.

[81] M. Bruchard, C. Rebe, V. Derangere et al., "The receptor NLRP3 is a transcriptional regulator of T_H2 differentiation," *Nature Immunology*, vol. 16, no. 8, pp. 859–870, 2015.

[82] Y. Liao, H. Zhang, D. He et al., "Retinal pigment epithelium cell death is associated with NLRP3 inflammasome activation by All-transRetinal," *Investigative Opthalmology & Visual Science*, vol. 60, no. 8, pp. 3034–3045, 2019.

[83] M. T. Heneka, M. P. Kummer, A. Stutz et al., "NLRP3 is activated in Alzheimer's disease and contributes to pathology in APP/PS1 mice," *Nature*, vol. 493, no. 7434, pp. 674–678, 2013.

[84] F. Zheng, S. Xing, Z. Gong, and Q. Xing, "NLRP3 inflammasomes show high expression in aorta of patients with atherosclerosis," *Heart, Lung and Circulation*, vol. 22, no. 9, pp. 746–750, 2013.

[85] C. Yao, T. Veleva, L. Scott Jr. et al., "Enhanced cardiomyocyte NLRP3 inflammasome signaling promotes atrial fibrillation," *Circulation*, vol. 138, no. 20, pp. 2227–2242, 2018.

[86] Y. Sun, W. Liu, H. Zhang et al., "Curcumin prevents osteoarthritis by inhibiting the activation of inflammasome NLRP3," *Journal of Interferon & Cytokine Research*, vol. 37, no. 10, pp. 449–455, 2017.

[87] M. Moossavi, N. Parsamanesh, A. Bahrami, S. L. Atkin, and A. Sahebkar, "Role of the NLRP3 inflammasome in cancer," *Molecular Cancer*, vol. 17, no. 1, p. 158, 2018.

[88] X. Qu, H. Gao, L. Tao et al., "Autophagy inhibition-enhanced assembly of the NLRP3 inflammasome is associated with cisplatin-induced acute injury to the liver and kidneys in rats," *Journal of Biochemical and Molecular Toxicology*, vol. 33, no. 1, p. e22208, 2019.

[89] K. Nakahira, J. A. Haspel, V. A. K. Rathinam et al., "Autophagy proteins regulate innate immune responses by inhibiting the release of mitochondrial DNA mediated by the NALP3 inflammasome," *Nature Immunology*, vol. 12, no. 3, pp. 222–230, 2011.

[90] A. Salminen, K. Kaarniranta, and A. Kauppinen, "Inflammaging: disturbed interplay between autophagy and inflammasomes," *Aging*, vol. 4, no. 3, pp. 166–175, 2012.

[91] J. Harris, N. Deen, S. Zamani, and M. A. Hasnat, "Mitophagy and the release of inflammatory cytokines," *Mitochondrion*, vol. 41, pp. 2–8, 2018.

[92] Z. Zhong, A. Umemura, E. Sanchez-Lopez et al., "NF-κB Restricts Inflammasome Activation via Elimination of Damaged Mitochondria," *Cell*, vol. 164, no. 5, pp. 896–910, 2016.

[93] Y. P. Chang, S. M. Ka, W. H. Hsu et al., "Resveratrol inhibits NLRP3 inflammasome activation by preserving mitochondrial integrity and augmenting autophagy," *Journal of Cellular Physiology*, vol. 230, no. 7, pp. 1567–1579, 2015.

[94] C. S. Shi, K. Shenderov, N. N. Huang et al., "Activation of autophagy by inflammatory signals limits IL-1β production by targeting ubiquitinated inflammasomes for destruction," *Nature Immunology*, vol. 13, no. 3, pp. 255–263, 2012.

[95] X. Wang, L. Jiang, L. Shi et al., "Zearalenone induces NLRP3-dependent pyroptosis via activation of NF-κB modulated by autophagy in INS-1 cells," *Toxicology*, vol. 428, p. 152304, 2019.

[96] M. E. Ahmed, S. Iyer, R. Thangavel et al., "Co-localization of glia maturation factor with NLRP3 inflammasome and autophagosome markers in human Alzheimer's disease brain," *Journal of Alzheimer's Disease*, vol. 60, no. 3, pp. 1143–1160, 2017.

[97] F. Marin-Aguilar, B. Castejon-Vega, E. Alcocer-Gomez et al., "NLRP3 inflammasome inhibition by MCC950 in aged mice improves health via enhanced autophagy and PPARα activity," *The Journals of Gerontology: Series A*, 2019.

[98] O. Sandanger, T. Ranheim, L. E. Vinge et al., "The NLRP3 inflammasome is up-regulated in cardiac fibroblasts and mediates myocardial ischaemia-reperfusion injury," *Cardiovascular Research*, vol. 99, no. 1, pp. 164–174, 2013.

[99] G. P. J. van Hout, L. Bosch, G. H. J. M. Ellenbroek et al., "The selective NLRP3-inflammasome inhibitor MCC950 reduces infarct size and preserves cardiac function in a pig model of myocardial infarction," *European Heart Journal*, vol. 38, no. 11, pp. ehw247–ehw836, 2017.

[100] J. Zhao, H. Wang, Y. Huang et al., "Lupus nephritis: glycogen synthase kinase 3β promotion of renal damage through activation of the NLRP3 inflammasome in lupus-prone mice," *Arthritis & Rheumatology*, vol. 67, no. 4, pp. 1036–1044, 2015.

[101] S. M. Ka, J. C. Lin, T. J. Lin et al., "Citral alleviates an accelerated and severe lupus nephritis model by inhibiting the activation signal of NLRP3 inflammasome and enhancing Nrf2 activation," *Arthritis Research & Therapy*, vol. 17, no. 1, 2015.

[102] A. C. Villani, M. Lemire, G. Fortin et al., "Common variants in the *NLRP3* region contribute to Crohn's disease susceptibility," *Nature Genetics*, vol. 41, no. 1, pp. 71–76, 2009.

[103] G. J. Lewis, D. C. O. Massey, H. Zhang et al., "Genetic association between NLRP3 variants and Crohn's disease does not replicate in a large UK panel," *Inflammatory Bowel Diseases*, vol. 17, no. 6, pp. 1387–1391, 2011.

[104] L. Mao, A. Kitani, M. Similuk et al., "Loss-of-function CARD8 mutation causes NLRP3 inflammasome activation and Crohn's disease," *Journal of Clinical Investigation*, vol. 128, no. 5, pp. 1793–1806, 2018.

[105] R. Munoz-Planillo, L. Franchi, L. S. Miller, and G. Nunez, "A critical role for hemolysins and bacterial lipoproteins in Staphylococcus aureus-induced activation of the Nlrp3 inflammasome," *The Journal of Immunology*, vol. 183, no. 6, pp. 3942–3948, 2009.

[106] C. Toma, N. Higa, Y. Koizumi et al., "Pathogenic Vibrio activate NLRP3 inflammasome via cytotoxins and TLR/-nucleotide-binding oligomerization domain-mediated NF-κB signaling," *Journal of Immunology*, vol. 184, no. 9, pp. 5287–5297, 2010.

[107] M. Witzenrath, F. Pache, D. Lorenz et al., "The NLRP3 inflammasome is differentially activated by pneumolysin variants and contributes to host defense in pneumococcal pneumonia," *Journal of Immunology*, vol. 187, no. 1, pp. 434–440, 2011.

[108] I. C. Allen, M. A. Scull, C. B. Moore et al., "The NLRP3 inflammasome mediates in vivo innate immunity to influenza A virus through recognition of viral RNA," *Immunity*, vol. 30, no. 4, pp. 556–565, 2009.

[109] S. L. Cassel, S. Joly, and F. S. Sutterwala, "The NLRP3 inflammasome: a sensor of immune danger signals," *Seminars in Immunology*, vol. 21, no. 4, pp. 194–198, 2009.

[110] H. Li, S. Wu, L. Mao et al., "Human pathogenic fungus Trichophyton schoenleinii activates the NLRP3 inflammasome," *Protein & Cell*, vol. 4, no. 7, pp. 529–538, 2013.

[111] S. Joly and F. S. Sutterwala, "Fungal pathogen recognition by the NLRP3 inflammasome," *Virulence*, vol. 1, no. 4, pp. 276–280, 2010.

[112] P. Lee, D. J. Lee, C. Chan, S. W. Chen, I. Ch'en, and C. Jamora, "Dynamic expression of epidermal caspase 8 simulates a wound healing response," *Nature*, vol. 458, no. 7237, pp. 519–523, 2009.

[113] E. J. Robertson, J. M. Wolf, and A. Casadevall, "EDTA inhibits biofilm formation, extracellular vesicular secretion, and shedding of the capsular polysaccharide glucuronoxylomannan by Cryptococcus neoformans," *Applied and Environmental Microbiology*, vol. 78, no. 22, pp. 7977–7984, 2012.

[114] N. C. Silva, J. M. Nery, and A. L. T. Dias, "Aspartic proteinases ofCandidaspp.: role in pathogenicity and antifungal resistance," *Mycoses*, vol. 57, no. 1, pp. 1–11, 2014.

[115] L. A. Braga-Silva and A. L. S. Santos, "Aspartic protease inhibitors as potential anti-Candida albicans drugs: impacts on fungal biology, virulence and pathogenesis," *Current Medicinal Chemistry*, vol. 18, no. 16, pp. 2401–2419, 2011.

[116] K. Nakamura, A. Miyazato, G. Xiao et al., "Deoxynucleic acids from Cryptococcus neoformans activate myeloid dendritic cells via a TLR9-dependent pathway," *Journal of Immunology*, vol. 180, no. 6, pp. 4067–4074, 2008.

[117] L. Perrone, T. S. Devi, K. I. Hosoya, T. Terasaki, and L. P. Singh, "Thioredoxin interacting protein (TXNIP) induces inflammation through chromatin modification in retinal capillary endothelial cells under diabetic conditions," *Journal of Cellular Physiology*, vol. 221, no. 1, pp. 262–272, 2009.

[118] W. Chi, F. Li, H. Chen et al., "Caspase-8 promotes NLRP1/NLRP3 inflammasome activation and IL-1β production in acute glaucoma," *Proceedings of the National Academy of Sciences*, vol. 111, no. 30, pp. 11181–11186, 2014.

[119] W. A. Tseng, T. Thein, K. Kinnunen et al., "NLRP3 inflammasome activation in retinal pigment epithelial cells by lysosomal destabilization: implications for age-related macular degeneration," *Investigative Opthalmology & Visual Science*, vol. 54, no. 1, pp. 110–120, 2013.

[120] Q. Zheng, Y. Ren, P. S. Reinach et al., "Reactive oxygen species activated NLRP3 inflammasomes initiate inflammation in hyperosmolarity stressed human corneal epithelial cells and environment- induced dry eye patients," *Experimental Eye Research*, vol. 134, pp. 133–140, 2015.

[121] A. Thakur, R. P. Barrett, J. A. Hobden, and L. D. Hazlett, "Caspase-1 inhibitor reduces severity ofPseudomonas aeruginosaKeratitis in mice," *Investigative Opthalmology & Visual Science*, vol. 45, no. 9, pp. 3177–3184, 2004.

[122] N. Cole, E. B. H. Hume, S. Khan, L. Garthwaite, T. C. R. Conibear, and M. D. P. Willcox, "The role of CXC chemokine receptor 2 in *Staphylococcus aureus* keratitis," *Experimental Eye Research*, vol. 127, pp. 184–189, 2014.

[123] C. Fabiani, J. Sota, G. M. Tosi et al., "The emerging role of interleukin (IL)-1 in the pathogenesis and treatment of inflammatory and degenerative eye diseases," *Clinical Rheumatology*, vol. 36, no. 10, pp. 2307–2318, 2017.

[124] R. C. Coll, A. A. B. Robertson, J. J. Chae et al., "A small-molecule inhibitor of the NLRP3 inflammasome for the treatment of inflammatory diseases," *Nature Medicine*, vol. 21, no. 3, pp. 248–255, 2015.

[125] R. C. Coll, J. R. Hill, C. J. Day et al., "MCC950 directly targets the NLRP3 ATP-hydrolysis motif for inflammasome inhibition," *Nature Chemical Biology*, vol. 15, no. 6, pp. 556–559, 2019.

[126] Y. He, S. Varadarajan, R. Munoz-Planillo, A. Burberry, Y. Nakamura, and G. Nunez, "3,4-Methylenedioxy-β-nitrostyrene inhibits NLRP3 inflammasome activation by blocking assembly of the inflammasome," *Journal of Biological Chemistry*, vol. 289, no. 2, pp. 1142–1150, 2014.

[127] Y. Huang, H. Jiang, Y. Chen et al., "Tranilast directly targets NLRP3 to treat inflammasome-driven diseases," *EMBO Molecular Medicine*, vol. 10, no. 4, 2018.

[128] C. Marchetti, B. Swartzwelter, F. Gamboni et al., "OLT1177, a β-sulfonyl nitrile compound, safe in humans, inhibits the NLRP3 inflammasome and reverses the metabolic cost of inflammation," *Proceedings of the National Academy of Sciences*, vol. 115, no. 7, pp. E1530–E1539, 2018.

[129] M. Lamkanfi, J. L. Mueller, A. C. Vitari et al., "Glyburide inhibits the Cryopyrin/Nalp3 inflammasome," *The Journal of Cell Biology*, vol. 187, no. 1, pp. 61–70, 2009.

[130] R. Kuwar, A. Rolfe, L. Di et al., "A novel small molecular NLRP3 inflammasome inhibitor alleviates neuroinflammatory response following traumatic brain injury," *Journal of Neuroinflammation*, vol. 16, no. 1, p. 81, 2019.

[131] C. Juliana, T. Fernandes-Alnemri, J. Wu et al., "Anti-inflammatory compounds parthenolide and Bay 11-7082 are direct inhibitors of the inflammasome," *Journal of Biological Chemistry*, vol. 285, no. 13, pp. 9792–9802, 2010.

[132] R. Nowarski, R. Jackson, N. Gagliani et al., "Epithelial IL-18 equilibrium controls barrier function in colitis," *Cell*, vol. 163, no. 6, pp. 1444–1456, 2015.

[133] A. Zahid, B. Li, A. J. K. Kombe, T. Jin, and J. Tao, "Pharmacological inhibitors of the NLRP3 inflammasome," *Frontiers in Immunology*, vol. 10, p. 2538, 2019.

[134] Z. Hu and J. Chai, "Structural mechanisms in NLR inflammasome assembly and signaling," *Current Topics in Microbiology and Immunology*, vol. 397, pp. 23–42, 2016.

[135] M. S. J. Mangan, E. J. Olhava, W. R. Roush, H. M. Seidel, G. D. Glick, and E. Latz, "Targeting the NLRP3 inflammasome in inflammatory diseases," *Nature Reviews Drug Discovery*, vol. 17, no. 8, pp. 588–606, 2018.

[136] W. Chi, F. Li, H. Chen et al., "Caspase-8 promotes NLRP1/NLRP3 inflammasome activation and IL-1 production in acute glaucoma," *Proceedings of the National Academy of Sciences*, vol. 111, no. 30, pp. 11181–11186, 2014.

[137] H. Jiang, H. He, Y. Chen et al., "Identification of a selective and direct NLRP3 inhibitor to treat inflammatory disorders," *The Journal of Experimental Medicine*, vol. 214, no. 11, pp. 3219–3238, 2017.

[138] C. Marchetti, S. Toldo, J. Chojnacki et al., "Pharmacologic inhibition of the NLRP3 inflammasome preserves cardiac function after ischemic and nonischemic injury in the mouse," *Journal of Cardiovascular Pharmacology*, vol. 66, no. 1, pp. 1–8, 2015.

[139] J. Fulp, L. He, S. Toldo et al., "Structural insights of benzenesulfonamide analogues as NLRP3 inflammasome inhibitors: design, synthesis, and biological characterization," *Journal of Medicinal Chemistry*, vol. 61, no. 12, pp. 5412–5423, 2017.

[140] J. Yin, F. Zhao, J. E. Chojnacki et al., "NLRP3 inflammasome inhibitor ameliorates amyloid pathology in a mouse model of Alzheimer's disease," *Molecular Neurobiology*, vol. 55, no. 3, pp. 1977–1987, 2018.

[141] A. Saadane, S. Masters, J. DiDonato, J. Li, and M. Berger, "Parthenolide inhibits IκB Kinase, NF-κB activation, and inflammatory response in cystic fibrosis cells and mice," *American Journal of Respiratory Cell and Molecular Biology*, vol. 36, no. 6, pp. 728–736, 2007.

[142] N. Irrera, M. Vaccaro, A. Bitto et al., "BAY 11-7082 inhibits the NF-κB and NLRP3 inflammasome pathways and protects against IMQ-induced psoriasis," *Clinical Science*, vol. 131, no. 6, pp. 487–498, 2017.

[143] S. R. Kolati, E. R. Kasala, L. N. Bodduluru et al., "BAY 11-7082 ameliorates diabetic nephropathy by attenuating hyperglycemia- mediated oxidative stress and renal inflammation via NF-κB pathway," *Environmental Toxicology and Pharmacology*, vol. 39, no. 2, pp. 690–699, 2015.

Hindawi
Oxidative Medicine and Cellular Longevity
Volume 2019, Article ID 8135985, 14 pages
https://doi.org/10.1155/2019/8135985

Review Article

Autophagy: Multiple Mechanisms to Protect Skin from Ultraviolet Radiation-Driven Photoaging

Mei Wang,[1,2] Pourzand Charareh,[3] Xia Lei,[2] and Julia Li Zhong[1]

[1]*National Innovation and Attracting Talents "111" Base, Key Laboratory of Biorheological Science and Technology, Ministry of Education, Chongqing University, Chongqing 400044, China*
[2]*Department of Dermatology, Daping Hospital, Army Medical University, Chongqing 400042, China*
[3]*Department of Pharmacy and Pharmacology, University of Bath, Bath BA2 7AY, UK*

Correspondence should be addressed to Xia Lei; leixia1979@sina.com and Julia Li Zhong; jlzhong@cqu.edu.cn

Received 9 September 2019; Accepted 26 November 2019; Published 13 December 2019

Guest Editor: Manuela Antoniol

Autophagy is an essential cellular process that maintains balanced cell life. Restriction in autophagy may induce degenerative changes in humans. Natural or pathological aging of susceptible tissues has been linked with reduced autophagic activity. Skin photoaging is an example of such pathological condition caused by ambient solar UV radiation exposure. The UV-induced production of reaction oxygen species (ROS) has been linked to the promotion and progression of the photoaging process in exposed tissues. Accordingly, it has been suggested that autophagy is capable of delaying the skin photoaging process caused by solar ultraviolet (UV), although the underlying mechanism is still under debate. This review highlights several plausible mechanisms by which UV-induced ROS activates the cellular signaling pathways and modulates the autophagy. More specifically, the UV-mediated regulation of autophagy and age-related transcription factors is discussed to pinpoint the contribution of autophagy to antiphotoaging effects in the skin. The outcome of this review will provide insights into design intervention strategies for delaying the phenomenon of sunlight-induced photodamage, photoaging, and other aging-related chronic diseases based on factors that activate the autophagy process in the skin.

1. Introduction

Autophagy is a vital homeostatic cellular process of either clearing surplus or damaged cell components notably lipids and proteins or recycling the content of the cells' cytoplasm to promote cell survival and adaptive responses during starvation and other oxidative and/or genotoxic stress conditions. Autophagy may also become a means of supplying nutrients to maintain a high cellular proliferation rate when needed [1]. Genotoxic stress usually occurs by a series of environmental and pharmacological agents, notably by solar ultraviolet (UV) radiation. It has been suggested that the induction of autophagy under these conditions is to try to alleviate the effects of oxidative DNA damage [2]. All UV components of sunlight, i.e., UVA (320-400 nm), UVB (280-320 nm), and UVC (100-280 nm), are capable of both causing DNA damage and inducing autophagy. Moreover, UV radiation of sunlight is capable of regulating a number of autophagy-linked genes [3–6]. Nevertheless, the mechanisms underlying these processes have not yet been fully elucidated. It is known that loss of autophagy leads to both photodamage and the initiation of photoaging in UV-exposed skin. Autophagy restriction may also induce several skin-related chronic disorders as well as skin cancer. This review will focus on critically appraising the cellular mechanisms suggested for the antiphotoaging action of the autophagy machinery in the skin cells induced by solar UV radiation.

1.1. Photoaging Mediated by UV Radiation. Skin aging is a highly complex and coordinated biological event comprising natural aging and solar radiation-mediated photoaging. The former process occurs naturally and results from slow tissue degeneration [7], while the latter occurs due to the

accumulation of unavoidable chronic sun exposures in daily life. Once photoaging is initiated, collagen fibers are degraded, the skin becomes subsequently loose with wrinkles, and the pigmentation occurs on the skin due to abnormal proliferation of melanocytes. In addition, increasing matrix metalloproteinase (MMP) content leads to intracellular matrix degradation, inflammatory infiltrates, and vessel ectasia [8]. Prolonged UV exposure is considered to be a major cause of photoaging, leading to the abovementioned phenomena in the skin [9, 10].

The solar UV radiation that reaches the surface of the earth is composed of the longer UVA (320-400 nm) and the shorter UVB (280-320 nm) wavebands, respectively. Both radiations penetrate through the thick ozone layer and reach the biosphere. Long-wave UVA that comprises about 95% of solar terrestrial UV penetrates deeply into the dermal layer and even reaches the subcutaneous layer of the skin. Because of its oxidative nature, UVA is capable of damaging DNA and other biomolecules by ROS generation [11]. UVA-induced ROS formation has been implicated in the oxidation of DNA bases leading to signature DNA lesions such as 8-oxo-deoxyguanine (8-oxodG) which is a known potent mutagenic lesion [12]. The UVA component of sunlight has been considered the main cause of prominent changes in the dermal extracellular matrix (ECM) of the photoaged skin. UVB, which represents about 5% of terrestrial UV, can reach at least the epidermis as well as the upper dermis and can induce dermal changes through epidermis-to-dermis signaling [13]. The different biological effects of UVA and UVB are related to the type of biomolecules that they interact with.

UVB radiation is primarily a DNA-damaging agent because it is directly absorbed by DNA and is known to cause cyclobutane pyrimidine dimers (CPDs) and 6-4 pyrimidine pyrimidone dimers (6-4PP) [14]. The unrepaired DNA lesions cause DNA mutation during cell division which may lead to the initiation of carcinogenesis [15]. Both nonenzymatic (i.e., glutathione and ascorbic acid) and enzymatic antioxidants such as superoxide dismutase (SOD), catalase (CAT), glutathione peroxidase (GPX), glutathione reductase, and thioredoxin reductase (TRX) are essential components of the skin defense against ROS-mediated damage. Nevertheless, the excess ROS production by UV radiation can overwhelm the endogenous antioxidant capacity of the skin. The latter justifies the use of exogenous antioxidants as photoprotectants to neutralize UV-mediated ROS production [16]. It has been suggested that both UVA and UVB initiate photoaging [17] by producing reactive oxygen species (ROS) that destroy cellular macromolecules such as proteins, lipids, and, more importantly, the genomic DNA [18]. UVA is known to be the oxidizing component of sunlight, and its damaging effect on biomolecules occurs indirectly, *via* the generation of ROS through its interaction with a variety of chromophores (e.g., porphyrins, bilirubin, and melanin) [19, 20]. Although ROS production by UVA can lead to DNA damage (Figure 1) [21], it has been recently shown that the proteome is one of the major targets of damage by UVA-induced ROS [22]. UVB, while it does have an oxidative component, induces specific lesions into DNA and damages proteins mostly by direct absorption [23]. UVC can cause damage to human health but is absorbed by the stratospheric ozone layer. It is a strong DNA-damaging agent, and this property has been exploited in building artificial UVC (207-222 nm) lamps that assess potent antimicrobial properties, and unlike the germicidal 254 nm UVC source, it is not harmful to the human skin due to its limited penetration distance of 207 nm light in biological samples (e.g., stratum corneum) compared with that of 254 nm light. This lamp source is an important agent against drug-resistant bacteria and airborne aerosolized viruses. Nevertheless, very low level of UVC can inactivate more than 95% of aerosolized H1N1 influenza virus [24, 25].

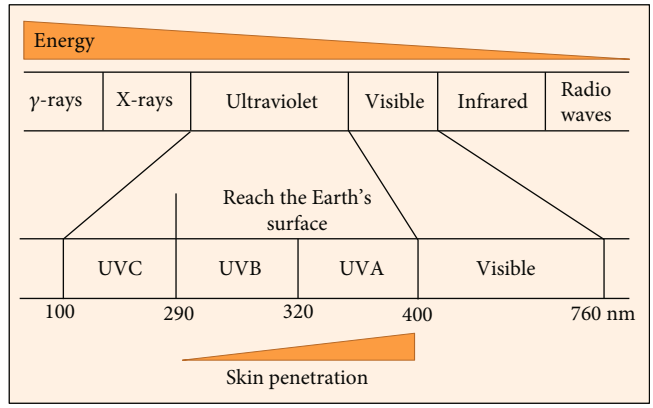

Figure 1: Ultraviolet (UV) as a component of the electromagnetic spectrum.

UVA and UVB have different effects on skin aging. Continuous UVB exposure can induce keratinocytes to produce more interleukin 1α (IL-1α), which initiates granulocyte-macrophage colony stimulatory factor (GM-CSF) secretion in an autocrine manner. Both IL-1α and GM-CSF molecules enter dermal tissues and activate fibroblasts to produce neprilysin. Neprilysin cleaves and disrupts the elastic fibrous network that wraps the fibroblasts. The combination of elastic and collagen fiber deficiency reduces skin elasticity, hence assisting in the formation of skin wrinkles. However, continuous exposure to UVA radiation leads the keratinocytes to produce GM-CSF in lower amounts than UVB exposure but activates dermal fibroblasts to the same extent as UVB radiation. Furthermore, UVA penetrates the dermal layers of the skin and immediately stimulates the expression of MMP-1 and secretion of IL-6, which mainly lead to sagging of the skin [26].

UV exposure is a major factor that induces photoaging. In particular, UVA irradiation induces ROS and subsequently promotes the oxidation of membrane lipids to form oxidized phospholipid-protein adducts. These oxidized adducts are cleared and degraded by autophagy to prevent cellular damage. Autophagy caused by environmental insults including UV radiation and the consequent generation of ROS appears necessary for survival and cell function as well as homeostasis and immune tolerance [27]. In keratinocytes, the basal level of autophagy augments considerably upon solar UV exposure, leading to epidermal thickening (hyperkeratosis) and then epidermal hyperplasia which acts as a

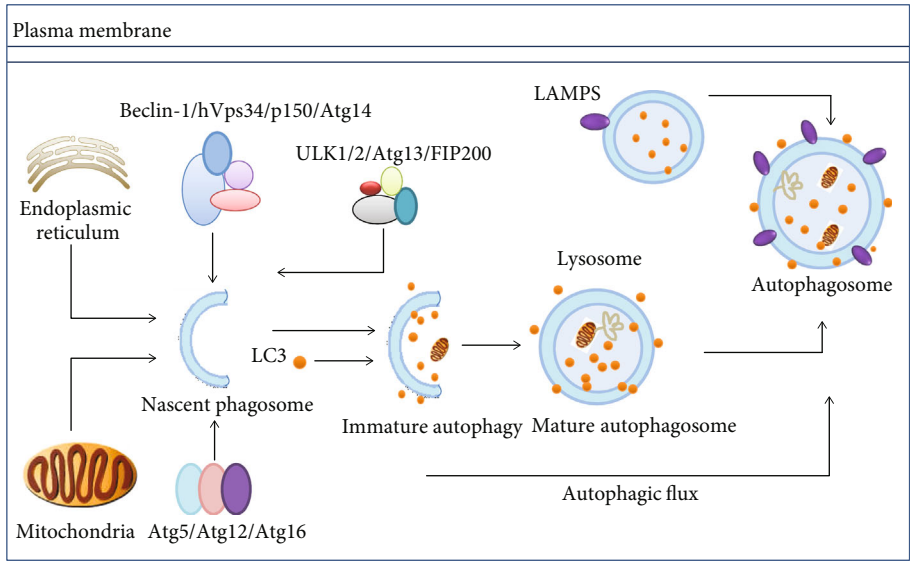

Figure 2: Overview of macroautophagy. Despite the occurrence of two membranes, bulk proteins and damaged organelles (ER and mitochondria) along with selective cargo within the cytoplasm are being engulfed, by small autophagosomes that fuse later to give full-sized autophagosomes. A number of autophagy-linked proteins and protein complexes are taking part in a highly coordinated procedure. Following fusion of autophagosomes with lysosomes, autolysosomes that decompose autophagic cargo to release recyclable biomolecules and macromolecules within the cytoplasm are formed (proteins involved: autophagy-linked enzymes Atg5, Atg12, Atg13, Atg14, and Atg16; autophagy-related proteins; Beclin-1 (Atg6); p150; (Vps15) serine/threonine-protein kinase. Vps34: class III phosphoinositide 3-kinase; Atg7: ubiquitin-E1-like enzyme; ULK1/2: unc-51-like autophagy-activating kinase 1/2; FIP200: family-interacting protein of 200 kD; LAMP2A: lysosomal-linked membrane protein 2A; LC3: microtubule-associated proteins 1A/1B light chain 3).

protection against the penetration of UV rays to the skin [28]. The skin pigmentation has also been linked to autophagy, as it depends on the melanin from phagocytosed melanocytes engulfed by the keratinocytes [29]. Additionally, the promotion of lysosomal-dependent decomposition and reutilization of cytoplasmic inclusions in autophagy has recently been linked with aging [30, 31]. It has also been shown that decreased autophagy is linked with increased aging, while stimulating autophagy enhances antiaging effects [32–34]. Defects in autophagy have also been shown to cause severe inflammatory reaction in the skin, because of the activation of inflammasome activation, as well as the induction of ROS production by UVR and aberrant liberation of proinflammatory cytokine release [35]. In an attempt to gain an insight into these phenomena, it is necessary to review the recent findings in the mechanism underlying the autophagy process and machinery.

Within the electromagnetic spectrum, UV wavelengths are in the range of 100–400 nm. The UV components are further divided into several wavebands notably UVC, UVB, and UVA. UVC is absorbed by the stratospheric ozone layer, so only UVA and UVB can reach the surface of the Earth. With waveband increasing, tissue transmission is increased, while the energy is decreased. Thus, UVA can penetrate much deeper into the skin than UVB.

2. Autophagy Machinery

Autophagy is an essential, evolutionarily conserved lysosomal degradation pathway that eliminates protein aggregates and damaged organelles to control the quality of the cytoplasm [36]. It concludes in macroautophagy, chaperone-mediated autophagy, and microautophagy [36, 37].

Macroautophagy which is the main emphasis of the current review is a phenomenon that is predominantly involved in the degradation and clearance of nonliving proteins as well as the degradation of various subcellular organelles. It is highly conserved from unicellular organisms to human [38].

While autophagy in mammalian cells naturally occurs under normal circumstances, it can also be initiated under stress conditions. These include conditions such as starvation, infection by multiple types of pathogens, or exposure to pharmacological mediators, especially rapamycin. Moreover, despite its major role in restoring cellular homeostasis via the release of macromolecular nutrients, autophagy can promote the clearing of misfolded proteins as well as broken cellular inclusions and organelles (Figure 2). In macroautophagy, a double-membrane structure which is called the isolation membrane (or the phagophore) outgrows from the endoplasmic membrane (ER). It has been shown that the Golgi, the plasma membrane, and mitochondria also contribute to the growth of the budding autophagosome [39]. Macroautophagy occurs in three phases. These include the initiation of phagophores, then elongation phase, and the final degradation phase.

2.1. Initiation of Autophagy. Normally, the formation of autophagosomes initiates at the assembly points on phagophore assembly sites. Phagophore formation mainly demands the class III phosphoinositide 3-kinase (PI3K) Vps34, which functions in macromolecular complexes containing autophagy-linked proteins Atg6 (Beclin-1) and

Atg14 as well as the Vps15 (p150) protein. Numerous proteins are involved in the early phases of autophagy notably autophagy-linked proteins Atg5, Atg12, and Atg16 as well as the focal adhesion kinase enzyme (FAK) and the 200 kDa family-interacting protein (FIP200), which constitutes the mammalian ortholog after conjugation with autophagy-linked proteins Atg1 (or ULK1) and Atg13 [40].

2.2. Elongation. Two ubiquitination-like reactions are associated with the elongation of phagophore membranes. Initially, ubiquitin-like Atg12 forms a complex with Atg5 by enzymatic conjugation to Atg7 (i.e., an E1 ubiquitin-activating-like enzyme) and Atg10 (i.e., an E2 ubiquitin-complexing mimicking enzyme). The autophagy-linked Atg5-Atg12 protein complex formation with Atg16L1 occurs through noncovalent binding. The complex then attaches to phagophores [41] and detaches from mature autophagosomes. During the second system of autophagosome formation, LC3 (MAP-LC3/Atg8/LC3) links to lipid phosphatidylethanolamine (PE) and gets stimulated by Atg7 (E1-like) and Atg3 (E2-like) to produce LC3-II [40]. Numerous LC3-positive autophagosomes that are randomly formed within the cytoplasm translocate along with the microtubules towards lysosomes in a dynein-dependent way and accumulate in the vicinity of the microtubule-organizing center (MTOC) adjacent to the nuclear membrane. Both lysosomes and autophagosomes are fused together by the action of two SNARE proteins, viz., Vti1B and VAMP8 [42].

2.3. Degradation of Autophagosomes. LC3-II promotes targeted degradation of long-lived and extensively utilized proteins, their aggregates, and injured or dead cellular organelles by interacting with adaptor proteins. P62 as a selective adaptor attaches to cargo proteins for the final degradation. In addition, p62 attachment may also occur through the LC3-interacting region (LIR) to link with LC3-II located on the outer side of the autophagosome membrane [43]. In addition, p62 is a target of specific substrates to the autophagosome and LC3-II and is used as a measure of autophagic flux [43]. The adaptor and cargo are degraded upon autophagosome-lysosome fusion. Autophagy products are recycled within the cytosol and help to restore important cellular processes following exposure to stressors and starvation.

3. Autophagy- and UV-Mediated Photoaging

The skin faces environmental UV exposure insult that causes oxidative damage to macromolecules [44]. Nuclear factor erythroid-derived 2-like 2 (Nrf2) activation/response is a centerpiece in resistance to oxidative stress, by upregulating antioxidant molecules and detoxifying enzymes to remove the ROS-mediated oxidative damage of cellular inclusions [3]. Autophagy is defined as an intracellular degradation phenomenon that is initiated to degrade oxidized lipids and metabolic wastes following UV exposure. It is therefore thought to decrease the progression of photoaging [45, 46].

In response to UVA irradiation or oxidized lipids, the Nrf2-driven antioxidant response activates the expression of cellular antioxidants and detoxifying enzymes such as heme oxygenase 1 (HO-1) [47–49]. In parallel to this process, proteins that were modified by ROS are cleared via proteasomal, autophagosomal, and lysosomal pathways in the cells [50]. Moreover, autophagosome LC3-II is formed through Atg7-dependent conjugation to a link between a PE (phosphatidylethanolamine) anchor and LC3 (the microtubule-linked protein 1 light chain 3). Cargo targeted for degradation is appropriated and destined for LC3-II via certain adaptor proteins, especially p62 (adaptor protein sequestosome 1 or SQSTM1). The complete structure is a spherical autophagosome with lysosomes that decompose various cargo proteins [51]. The involvement of both UVA- and UVA-oxidized PAPC- (1-palmitoyl-2-arachidonoyl-sn-glycero-3-phosphocholine-) mediated autophagy in epidermis-residing keratinocytes was reported. Various ROS induce rapid growth of high molecular weight protein masses comprising many different autophagy-related adaptor proteins, notably p62 (SQSTM1) in autophagy-deficient (Atg7-negative) keratinocytes [3]. Furthermore, autophagy is important in degrading proteins and modifying lipids following various environmental stresses, including UV exposure.

UVA-mediated ROS production mainly oxidizes phospholipids, which later forms oxidized phospholipid-protein adducts [3]. Autophagy then promotes the degradation of these metabolic adducts following UVA irradiation. Aging and aging-related diseases can be ravaged by minimizing these protein-based adducts and aggregates, crosslinking, and finally removing potentially toxic protein fragments from the cells. However, autophagy-mediated clearance of such waste declines over time [52], leading to an increase in oxidized phospholipid-protein adducts [53] and oxidized combination groups [54], which together accumulate and contribute to skin photoaging.

The mechanism of UV-induced autophagy still needs to be revealed because UVA irradiation induces autophagy that is impaired by treatment with the singlet oxygen quencher NaN3 [3, 55]. Similarly, UVB-induced autophagy is blocked by various antioxidants [56]. UV exposure promotes the formation of oxidized phospholipids, oxysterols, and cholesterol in keratinocytes [3, 57]. Moreover, 25-hydroxycholesterol (25-OH) is one of the oxidized lipids formed by UV exposure that is sufficient to activate autophagy in the skin keratinocytes and to perform a crucial function in inducing morphological changes and differentiation [57].

The inactivation of the essential autophagy-related genes significantly decreases the functions of sweat glands in aging mice [34]. It is suggested that ROS are critical cellular signal transducers and that solar UV light potentially generates ROS in the human skin [58]. Solar UV radiation modulates the activity of some autophagy/aging-linked genes [6]. It is imperative to highlight the types of stress regulation and the mechanism for both UVA and UVB irradiation. These factors are shown to regulate aging and autophagy as well as the relationship between aging and autophagy. In addition, UV radiation functions as the major environmental risk factor which causes skin cancer as about 50% of skin cancers are related to UV exposure [59]. In skin cancer, autophagy can be either oncogenic or tumor-suppressive, which mainly depends on the tumor cell type, stage of

progression, carcinogenic context, etc. Autophagy acts as a tumor-suppressive mechanism by promoting ROS clearance, DNA repair, and oncogenic protein substrates [60, 61]. Alternatively, autophagy also facilitates tumor development by autophagy-mediated intracellular recycling that provides macromolecules with sustained cell proliferation. Additionally, autophagy has also been shown to be associated with UV-induced skin diseases, such as hyperpigmentation [62].

4. UV Radiation-Mediated Cell Signaling Pathway

Solar UV exposure is a crucial part of environmental stress that affects skin tissue damage. Exposure to solar UV radiation induces ROS to activate some cell surface receptors, e.g., epidermal growth factor receptor (EGFR) and tumor necrosis factor receptor (TNFR), and to initiate cell survival or apoptosis-associated signaling cascades [63, 64]. Solar UV radiation activates one of the serine/threonine protein kinase family proteins and is associated with cellular signaling, i.e., the mitogen-activated protein kinase (MAPK) pathway. In general, the MAPK pathways comprise three diverse pathways, viz., c-Jun NH2-terminal kinase (JNK), p38 MAPK (p38 kinase), and extracellular signal-regulated kinase (ERK) pathways [65]. The ERK cascade induces cell proliferation and promotes cell survival, while the other two pathways (JNK and p38 kinase) provide protection and proapoptotic effects, respectively [66, 67]. Each of the serine/-threonine protein kinase family activates a different stimulus or cellular stress by targeting specific intracellular proteins. Normally, ERK activation is induced by UVA-mediated ROS, but JNK is mainly activated by UVC, while p38 kinases could be activated by all UV wavelengths (including UVA, UVB, and UVC) to modify DNA damage response [68, 69]. In addition, solar UV radiation can trigger the p53 pathway activity via induction of p53 upregulated modulator of apoptosis (PUMA) and phorbol-12-myristate-13-acetate-induced protein 1 (PMAIP1 or NOXA), resulting in Bcl-2 inhibition and thereby suppressing apoptosis progression [63, 70]. Thus, solar UV as an oxidative agent modulates signal transduction pathways in the cellular response (Figure 3).

5. UV-Induced Signaling Pathways and Modulation of Autophagy

Diverse signaling networks are involved in regulating autophagy, and two major kinases mTOR (mechanistic target of rapamycin) and AMPK (AMP-activated protein kinase) are linked to aging and lifespan regulation (Figure 3). mTOR, as a negative regulator of autophagy, integrates signals from nutrients and stress to control cellular growth and metabolism. When stimulated by environmental stress, such as solar UV, mTOR phosphorylates the unc-51-like autophagy-inhibiting kinase (ULK) 1 and activates it to form a complex with Atg13 and FIP200, thereby inhibiting autophagy. Inversely, inhibition of mTOR promotes autophagy [71]. In contrast to mTOR, AMPK activation induces the autophagy process and AMPK itself is activated by energy stress, which is sensed through an increase in the AMP/ATP ratio. Upon activation, AMPK stimulates autophagy through multiple mechanisms. First, it phosphorylates and activates ULK1 and Beclin-1-VPS34 to promote the early steps of autophagosome induction. Second, AMPK inhibits mTOR by phosphorylating and inhibiting RAPTOR (regulatory-associated protein of mTOR), an important adaptor for mTOR kinase activity. Finally, AMPK stimulates tuberous sclerosis complex (TSC) 1-TSC2 complex activity, which inhibits mTOR. Oxidative stress, such as UV exposure, notably UVB-induced the phosphorylation of AMPK and increased levels of the AMPK downstream target genes acetyl-CoA-carboxylase (ACC) and ULK1 in wild-type MEF cells. AMPK activation by UVB increases LC3-II levels and autophagic flux, whereas an AMPK knockdown significantly reduces LC3-II levels [5]. Serine/threonine-specific protein kinase B (PKB or Akt) inhibits autophagy through mTOR activation, and PI3K/Akt activation is induced by UVB radiation [72, 73]. The UV resistance-associated gene (UVRAG) generally acts as an autophagy promoter, and inhibition of UVRAG levels causes autophagy to activate suppression [74]. Upon stabilization by UVB, autophagy initiation activates the transcription of AMPK, Sesn2, TSC2, and UVRAG [6]. In addition, p53 accumulation is increased in mammalian cells following UV radiation [75]. UV-mediated signaling pathways involved in autophagy are depicted in (Figure 3). Together, autophagy was modulated by various UV-mediated signaling pathways.

6. UV Directs the Regulation of Autophagy and Aging-Related Transcriptional Factors

6.1. Mammalian Target of Rapamycin (mTOR). The mTOR exists in two different enzymatic isoforms, i.e., mTORC1 and mTORC2. They are primary negative regulators of autophagy in almost all eukaryotic organisms. These enzymatic isoforms regulate various types of substrates, such as the Akt/mTOR pathway, which is an important mediator of natural aging [76]. Young et al. and Young and Narita identified that mTORC1 activity is suppressed in Ras senescence following the mitotic phase and that its inactivation coincides with the initiation of autophagy during the transition phase [77, 78]. Recently, it was reported that solar UV exposure, mainly in the 290-320 nm region (UVB), activates the mTORC2/Akt/IKKα signaling cascade in human HaCaT keratinocytes, while suppression of mTORC2 inhibits UVB-mediated activation of NF-κB via downregulation of Akt/IKK signaling. In addition, the UV-mediated induction of mTORC2 signaling in skin aging is directly linked to stimulation of NF-κB [79]. Various stressors, particularly starvation, inhibit the activation of mTOR while promoting the expression of ULK1, ULK2, and Atg13 leads to starvation-mediated initiation of autophagy (Table 1) [40].

6.2. Silent Mating Type Information Regulation 2 Homologs (Sirtuins or SIRTs). The NAD(+)-dependent sirtuin enzymes are well-known modulators of aging, enhancing the lifespan of organisms [80] due to their extensive biological roles in metabolic control, cell death and survival, gene repression, repair of damaged DNA, morphogenesis, natural aging, and inflammation [81]. During cellular senescence, the expression

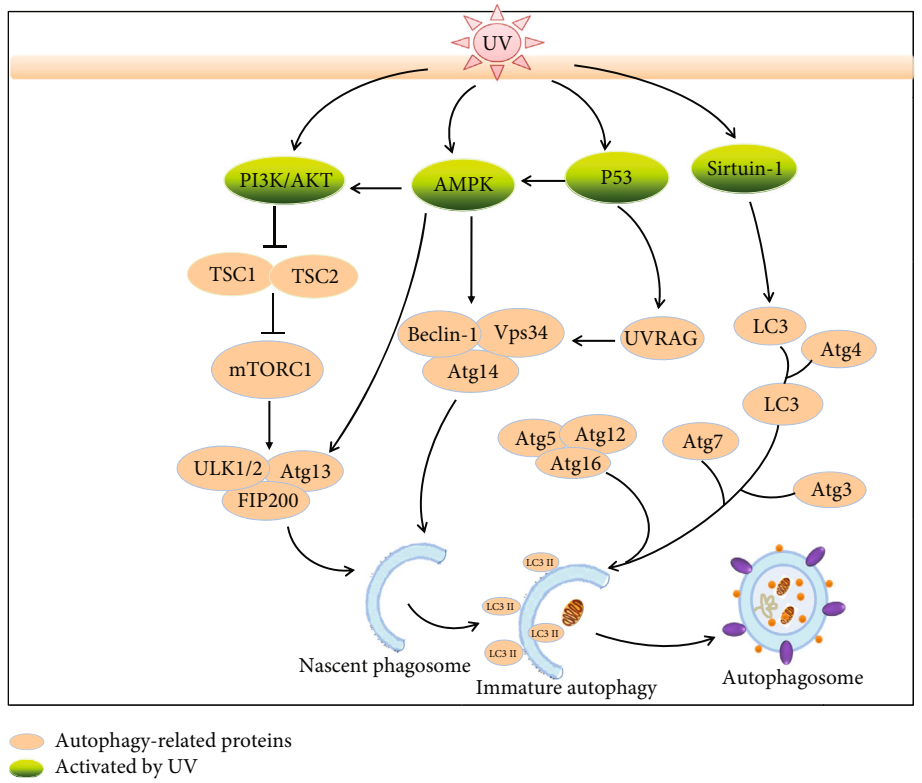

Figure 3: UV radiation modulates the autophagy process via multiple signaling pathways (AMPK, PI3K/Akt, p53, and sirtuin-1). Solar UV irradiation promotes PI3K/Akt activation to inhibit TSC1/2. These signals converge on mTORC1 (mTOR, RAPTOR, and mLST8), which coordinately modifies the ULK complex to affect early steps of the autophagosome process. UV exposure also affects the signaling pathways through the mTOR-AMPK axis by activating ULK1/2 and promoting preautophagosomal structure formation. The nascent phagosome is subsequently modified by a complex of Beclin-1, ATG14, and Vps34, to form the isolation membrane structures. The expansion of the latter complex is associated with two ubiquitin-like reactions involving Atg7, Atg5, Atg12, Atg16, and Atg3 and ultimately conjugates phosphatidylethanolamine (PE) to LC3. UV activates signaling through the AMPK-Beclin-1/Vps34 complex or the p53-UVRAG-Beclin-1/Vps34 complex, which are involved in the formation of nascent phagosomes. The deacetylase sirtuin-1, a posttranscriptionally acetylating core autophagy protein, is modulated by UV to regulate LC3-I to conjugate LC3 to activate autophagy, and Atgs are involved in the conjugation machinery. LC3-PE conjugation targets LC3 to autophagosomal membranes where it is required for membrane expansion and cargo sequestration. Finally, the autophagosome is sealed and the sequestered cargo is delivered to the lysosome through autophagosome-lysosome fusion. PI3K/Akt: phosphatidylinositol 3-kinase/protein kinase B; MAPK: mitogen-activated protein kinase; mTOR: mammalian target of rapamycin; p53: tumor protein p53: sirtuin-1: silent mating type information regulation 2 homolog; PE: phosphatidylethanolamine; ULK: Unc-51-like autophagy-inhibiting kinase; UVRAG: UV resistance-associated gene; TSC: tuberous sclerosis complex; LC3: microtubule-associated protein 1A/1B light chain 3; FIP200: 200 kDa family-interacting protein.

of SIRT-1 decreases, while transgenic overexpression of SIRT-1 induces cell proliferation to inhibit senescence [37, 82]. Recently, seven different sirtuins (i.e., SIRT-1 to SIRT-7) have been reported in humans, and the levels of their expressions have also been well documented in human epidermal and dermal cells [83]. SIRT-1 expression has been reported to decline following UV exposure in skin keratinocytes [84]. It is specifically localized in the cell nucleus and sometimes in the cytoplasm. It has been reported that SIRT-1's cytoplasmic location is highly effective as the initiator of autophagy. Resveratrol mediates autophagy in enucleated cells through SIRT-1, suggesting that SIRT-1 initiates autophagy *via* a non-nuclear process [85]. Accordingly, SIRT-1 deacetylates the autophagy-related genes Atg5, Atg7, and Atg8/LC3 and the transcription factor forkhead box 3, which stimulates the expression of proautophagic genes [86]. Consequently, SIRTs induce cellular senescence in keratinocytes and particularly SIRT-1, which deacetylates autophagy-linked genes (Table 1).

6.3. Forkhead Box Class O (FoxOs). In mammals, four different FoxO proteins have been isolated, viz., FoxO1 (FoxO1a), FoxO3 (FoxO3a), FoxO4, and FoxO6 [87]. FoxOs are involved in counteracting oxidative stress and cell fate regarding cell apoptosis or senescence. FoxOs are situated downstream of insulin and insulin-like growth factor-1 (IGF-1), which accelerates aging by suppressing FoxOs [88]. Some studies reported that both UVA and UVB irradiation significantly decrease the expression of FoxO1a and type I collagen (COL1A) mRNA in fibroblasts, while MMP-1 and MMP-2 expression levels are increased [89]. FoxO is homologous to the *Caenorhabditis elegans* (*C. elegans*) transcription factor abnormal dauer formation-16 (DAF-16), which is a downstream gene of the insulin receptor DAF-2 and is actively involved in the regulation of organism lifespan [90]. In various other nematodes, DAF-2 mutants (DAF-2 encodes a hormone receptor similar to the insulin and IGF-1 receptor) have been inactivated by either DAF-16 or

Table 1: Activation of UVR-responsive genes and their association with autophagy.

Gene	Relation to aging	Type of UV radiation	Relation to autophagy	References
mTOR (mTORC1 and mTORC2)	mTORC1 suppresses RAS-induced senescence, and mTORC2 induces skin aging through activation of NF-κB cascade	UVB activates the mTORC2/Akt/IKKα pathway	mTOR negatively regulates autophagy via Atg13, ULK1, and ULK2	[73–77]
Sirtuins	Sirtuins modulate lifespan, while SIRT-1 inhibits senescence	UV exposure deceases SIRT-1 in skin keratinocytes	SIRT-1 induces autophagy through deacetylation and activation of autophagy-related genes ATG5, ATG7, and ATG8/LC3.	[40, 78–83]
FoxOs	FoxOs are regulated by IGF-1, while IGF-1 induces aging	FoxO3 induces autophagy by glutamine metabolism; FoxO1 overexpression induces autophagic flux formation	UVA and UVB radiation decreases FoxO1 expression in fibroblasts	[84–89]
PPARδ	PPARδ prevents photoaging by the inhibition of MMP-1	UVB attenuates PPARδ through the induction of MMP-1 secretion	PPARδ activation induces autophagy marker Beclin-1 and LC3 expression	[90, 91]
Hsp70	eHsp70 treatment prolongs lifespan of mice	UVB chronic exposure induces ROS-mediated apoptosis and decreases macrophagy	HSPA8/HSC70 plays an important role in chaperone-mediated autophagy. Hsp70 links to the proteasome shuttle factor UBQLN2 to degrade misfolded proteins	[92–96]
Nrf2	Nrf2 deficiency in mice following UVB irradiation promotes mouse photoaging; repression of the Nrf2-mediated antioxidative response contributes to premature aging	UVA exposure increases Nrf2 expression in fibroblasts. UVB induces mouse photoaging by Nrf2 depletion	Nrf2 knockout reduces expression of autophagic genes in embryo fibroblasts	[97, 98]
HO-1	Disturbances in HO-1 level are associated with age-dependent disorder pathogenesis	Both UVA and UVB induce detoxifying enzyme HO-1 expression	HO-1 and autophagy are upregulated by LPS in primary mouse hepatocytes; pharmacological knockdown or inhibition of HO-1 prevents autophagy	[99–108]
NF-κB	NF-κB pathway is involved in progression of aging, and NF-κB inhibition attenuates oxidative stress, DNA damage, and delayed cellular senescence	UV activates NF-κB to form two phases Curcumin combined with UVA induces apoptosis by inhibition of NF-κB activity, and UVA exposure activates NF-κB	Inhibition of NF-κB promotes autophagy, while autophagy suppression restores NF-κB activity	[109–125]

autophagy inhibition using genetic or molecular approaches. However, genetic modifications for overexpressing DAF-16/FoxO proteins might enhance autophagy in *C. elegans*. The latter provides evidence for the important role of FoxOs in autophagy. Furthermore, FoxO3 can enhance autophagy via regulating the glutamine metabolism. The targeting or selective activation of FoxOs (FoxO3, FoxO4) leads to an increase in glutamine production. The activation of FoxOs possibly directs mTOR inhibition by inhibiting translocation of FoxOs into the lysosomal membranes in a glutamine synthetase-dependent manner, which consequently enhances autophagy progression [91]. In neonatal rat cardiac myocytes, upregulation of either SIRT-1 or FoxO1 is sufficient for autophagic flux induction, whereas both are required for glucose deprivation-induced autophagy (Table 1) [92]. Taken together, autophagy-related factors appear to be involved in UV-mediated photoaging.

7. UV Modulated Oxidative Stress-Related Factors

7.1. Peroxisome Proliferation-Activated Receptor δ (PPARδ). The ligand-inducible transcription factor PPARδ has been reported to regulate diverse biological phenomena to maintain homeostasis within skin tissues. PPARδ and its specific ligand, GW501516, are activated in human dermal fibroblasts (HDFs) that markedly decrease UVB-induced expression of MMP-1 and ROS generation. PPARδ-driven inhibition of MMP-1 expression is linked with the recovery of original COL-I and COL-III levels, which is mainly due to the prevention of photoaging and restoration of skin integrity [93]. GW501516 treatment also upregulates two well-known autophagy-related markers (Beclin-1 and LC3-II), and PPARβ/δ-knockout mice show a sharp drop in autophagic marker levels (Table 1) [94].

7.2. Heat Shock Protein 70 (HSP70). HSP70 is a well-known heat shock protein and is normally expressed under certain stresses, such as heat stressors or exposure to heavy metals. HSPs play a crucial role in controlling 3-dimensional protein folding and removing damaged proteins and cellular inclusions [95]. HSP70 plays a critical role in numerous neurodegenerative diseases that are often linked to aging, and treatment with exogenous recombinant human Hsp70 (eHsp70) extends the lifespan of aged mice [96]. During continuous but intermittent UVB exposure, HSP70 transgenic animal models show a slight drop in skin elasticity and epidermal hyperplasia, which is thought to be due to low doses of UVB and the related low production of ROS. This leads to induction of apoptosis in fibroblasts while reducing the infiltration of neutrophils and macrophages within the skin tissue [97]. In chaperone-induced autophagy, cytoplasmic proteins with a clearly exposed pentapeptide motif (KFERQ) are the main targets of HSPA8/HSC70 (heat shock 70 kDa protein 8). Following recognition of their exact motif by HSPA8 and subsequent binding with lysosomal-linked membrane protein 2A (LAMP2A), target proteins undergo unfolding and finally translocate within the lysosomal lumen for their final degradation [98]. It is suggested that the proteasome shuttle factor UBQLN2 identifies client-bound Hsp70 and links it to the proteasome for degradation of accumulated and misfolded proteins in the mouse brain [99] (Table 1).

7.3. NF-E2-Related Factor 2 (Nrf2). Nrf2 is a member of the NF-E2 family of basic leucine zipper transcription factors, and its cytoplasmic inhibitor Kelch-like ECH-associated protein 1 (Keap1) is a major protein that coordinates at the transcriptional level to induce or regulate the expression of different antioxidant enzymes. Under homoeostatic conditions, Keap1 usually keeps Nrf2 tightly bound within the cytoplasm. Upon stimulation (UV or H_2O_2), mainly via potent ROS, the Nrf2-Keap1 protein complex is disrupted, and Nrf2 rapidly translocates into the nucleus to target specific genes via heterodimeric combinations with a small Maf protein [100]. UVA irradiation is mainly involved in Nrf2 nuclear translocation and accumulation; hence, it can modulate the downstream effectors [49]. Our previous studies have also suggested that UVA irradiation increases the expression of Nrf2 and its target gene product, HO-1, in human skin fibroblasts [101]. It was reported that UVB irradiation of $Nrf2^{-/-}$ mice accelerates skin photoaging [102]. Furthermore, Kubben and colleagues revealed that repression of the Nrf2-mediated antioxidant response is a critical contributor to premature aging [103]. An Nrf2 knockout in embryonic fibroblasts exhibits reduced expression of autophagic genes, which were rescued by an Nrf2-expressing lentivirus and impaired autophagy flux following exposure to H_2O_2. On the other hand, Nrf2 regulates autophagy-associated gene (p62, ULK1, and Atg5) expression in a mouse model of Alzheimer's disease [104]. Meanwhile, p62 interacts with Keap1 at the Nrf2-binding site, and any overexpression or deficiency of p62 in autophagy competes with the interaction between Nrf2 and Keap1, resulting in stabilization of Nrf2 and activation of its downstream targets. This finding indicates that various pathological conditions are linked with excessive accumulation of p62, which potentiates Nrf2 and delineates unexpected functions of selective autophagy by regulating the expression of cellular defense enzymes at the transcriptional level (Table 1) [105]. Taken together, Nrf2 activation by UV appears to be associated with autophagy.

7.4. Heme Oxygenase (HO) System. HO-1 is one of the main stress response proteins induced following UVA radiation. To date, two isoforms of the HO system, HO-1 and HO-2, have been defined. The HO system is reported to degrade heme molecules into carbon monoxide (CO), free cellular ferrous iron (Fe), and biliverdin [106]. Both of these HO isoforms share approximately 45% amino acid sequence similarity, with HO-2 mainly present in a constitutive form and HO-1 present in inducible forms within the skin cell [107]. HO is evolutionarily conserved in the human genome, and HO-1 (approximately 32 kDa) and HO-2 (approximately 36 kDa) are encoded by the HMOX1 and HMOX2 genes, respectively. It was found that HO-1 has high anti-inflammatory and antiapoptotic properties that are vital in preventing inflammation-related cell signaling [108]. On

the other hand, disturbances in the HO-1 level are associated with some age-dependent disorder pathogenesis, including neurodegeneration, macular degeneration, and cancer [109]. The expression of HO-1 varies according to tissue type. The highest expression in fibroblasts occurs following exposure to ROS-mediated oxidative stress, while epidermal keratinocytes have low levels of HO-1. In contrast, their constitutive expression of HO-2 is high [110] in keratinocytes. The increased expression of HO under oxidative stress conditions is likely to relate to its cytoprotective role [111, 112]. Additionally, UVB effects on skin are well documented, and UVB barely induces HO-1, possibly due to its low production of ROS [113]. It was also found that lipopolysaccharide (LPS) mediates autophagy signals in macrophages via Toll-like receptor 4 (TLR4). This process is dependent on the HO-1 signaling pathway in macrophages [114]. A large amount of data reveals that HO-1 and autophagy are both upregulated in liver cells after cervical ligation and puncture in C57BL/6 mice or in primary mouse hepatocytes upon exposure to LPS. The pharmacological prevention of HO-1 expression through either tin protoporphyrin or knockdown procedures also reduces the production of autophagic signaling in such models and causes additional hepatocellular injury and apoptotic death (Table 1) [115].

7.5. Nuclear Factor-Kappa B (NF-κB). NF-κB is a well-known transcription factor activated by UV light exposure [116]. It is an acute inducer that produces cell responses to inflammation-producing cytokines, signal creation, various types of pathogens, and cell stresses. In resting cells, NF-κB remains silent in the cytoplasm through stoichiometric linkage with its inhibitory proteins, i.e., IκBs. The NF-κB pathway is involved in accelerating the progression of aging [117], and NF-κB attenuates oxidative stress and DNA damage and delays cellular senescence [118]. A low dose of UVB irradiation activates AP-1 and NF-κB, resulting in elevated MMP expression that degrades collagen and elastin and thus disrupts the integrity of skin tissue, leading to solar scars that accumulate over a lifetime due to repeated and continuous low doses of solar light exposure in photoaging [119]. This dormant NF-κB pool is activated by certain inflammatory triggers that activate the IκB kinase (IKK) complexes and allow targeted phosphorylation of the canonical IκB proteins (IκBα, IκB-β, and IκB-ε), targeting them for ubiquitination and proteasomal degradation. As a result, NF-κB sequentially gathers within the nucleus and activates associated genes [120]. UV radiation activates NF-κB primarily in two segments, i.e., a DNA damage-independent stage [116, 121] and a DNA damage-dependent stage (>24 hours) [122]. The late stage of NF-κB activation has been well studied and involves activating IKK by linking with the DNA double-stranded break-activated kinase ataxia telangiectasia mutated (ATM) [123]. Furthermore, a combination of a low concentration (0.2-1 μg/ml) of curcumin and UVA irradiation might induce apoptosis in human skin keratinocytes through enhanced fragmentation of the nucleus, discharge of cytochrome c from mitochondria, initiation of the caspase cascade (Casp-8 and Casp-9), and disruption of NF-κB cascades [124]. Previously, Reelfs and coworkers reported that UVA irradiation-activated proinflammatory NF-κB factors are iron-dependent in human skin fibroblasts [125]. Moreover, after exposure to UVA radiation, NF-κB is activated following degradation of its regulatory inhibitory protein (IκBα) and via its extended iron-dependent, IκBα-independent activation [126]. In various studies, NF-κB has been reported to exert an anti-inflammatory effect by delaying accumulation of the autophagy receptor p62/SQSTM1 and the "NF-κB-p62 mitophagy" pathway is a macrophage-intrinsic regulatory loop that restrains specific proinflammatory processes and arranges a self-limiting host reaction to help restore homeostasis and ultimately repair tissues [127]. In addition, NF-κB RELA cytosolic ubiquitination is stimulated by TLR2 signaling and leads to its degradation through SQSTM1/p62-mediated autophagy, while inhibition of autophagy rescues NF-κB activity and shapes hepatoma-polarized M2 macrophages [128]. Furthermore, inhibition of NF-κB leads to cells becoming sensitive to perturbations in mitochondrial metabolism and autophagy in B cell lymphoma [129] (Table 1). NF-κB therefore modulates photodamage and photoaging mediated by UV and is also involved in mitophagy and macrophagy.

8. Conclusion

UV exposure is a major factor that induces photoaging by elevating the level of oxidized lipid and metabolite aggregate levels. Loss of autophagy leads to diverse cellular dysfunctions that exacerbate the aging process, while elevated autophagy generally promotes cellular homeostasis, prolongs lifespan, and improves health life quality. Autophagy induction increases metabolite adduct degradation by UV irradiation-induced ROS which in turn lead to inhibition of photoaging. In contrast, a decrease in autophagy is likely to promote skin photoaging and the promotion of UV-induced damage. The current approach to prevent photoaging mainly relies on the avoidance of sunlight exposure to the skin. Antioxidants and DNA repair-related enzymes can be added as ingredients to sunscreens to enhance their photoprotective potential against sunlight exposure to the skin. While much progress has been made in combatting photoaging triggered by UV, the role of autophagy in resisting photoaging yet remains to be elucidated. Autophagy plays a critical role in UV-induced apoptosis, DNA damage repair, oxidized lipid removal, and so on. Autophagy may therefore be considered a new pathway to prevent photoaging and skin cancer. The understanding of the mechanisms underlying the switch between autophagy and photoaging provides valuable insights into UV-associated diseases and therapeutic methods. This in turn should offer a molecular platform for autophagy-targeted treatment to slow down aging-related chronic diseases including photoaging and other UV-induced oxidative disorders such as skin cancer.

Abbreviations

ACC: Acetyl-CoA carboxylase
Atg7: Ubiquitin-E1-like enzyme
COL1A: Type I collagen

ECM: Extracellular matrix
ERK: Extracellular signal-regulated kinase
ER: Endoplasmic membrane
FAK: Focal adhesion kinase
FIP200: Family-interacting protein of 200 kDa
FoxO: Forkhead box class O
GM-CSF: Granulocyte-macrophage colony stimulatory factor
HDFs: Human dermal fibroblasts
HO: Heme oxygenase
HSP70: Heat shock protein 70
IGF-1: Insulin-like growth factor-1
IL: Interleukin
JNK: c-Jun NH2-terminal kinase
Keap1: Kelch-like ECH-associated protein 1
LAMP2A: Lysosomal-linked membrane protein 2A
LC3: Microtubule-associated protein 1A/1B light chain 3
MAPK: Mitogen-activated protein kinase
MMPs: Matrix metalloproteinases
mTOR: Mammalian target of rapamycin
NF-κB: Nuclear factor-kappa B
Nrf2: Nuclear factor erythroid-derived 2-like 2
PMAIP1: Phorbol-12-myristate-13-acetate-induced protein 1
PPARδ: Peroxisome proliferation-activated receptor δ
PUMA: p53 upregulated modulator of apoptosis
ROS: Reactive oxygen species
Sirtuin: Silent mating type information regulation 2 homolog
TLR4: Toll-like receptor 4
UV: Ultraviolet.

Additional Points

Highlights. (1) UV-mediated ROS generation promotes the progression of the photoaging process. (2) Increased autophagy delays the UV-mediated photoaging, and the inhibition of autophagy enhances the UV-mediated photoaging process. (3) UV-mediated ROS generation activates the signaling pathways responsible for the modulation of the autophagy process. (4) UV directs the regulation of autophagy and aging-related transcriptional factors.

Conflicts of Interest

Julia Li Zhong also works voluntarily at the Dermatology Unit of Chongqing University and as an honorary professor at the Traditional Chinese Medical Institute of Chongqing. All the other authors declare that they have no competing interests.

Authors' Contributions

All authors contributed to the writing of this manuscript and approved its final version.

Acknowledgments

We apologize to all colleagues whose work could not be cited owing to space limitations. This work was supported by the National Natural Science Foundation of China (81573073, 81573071, and 81773348), the Natural Science Foundation of Chongqing (cstc2017jcyjbx0044), and the Graduate Student Research Innovation Project (CYB16040).

References

[1] G. Kroemer, G. Marino, and B. Levine, "Autophagy and the integrated stress response," *Molecular Cell*, vol. 40, no. 2, pp. 280–293, 2010.

[2] A. T. Vessoni, E. C. Filippi-Chiela, C. F. M. Menck, and G. Lenz, "Autophagy and genomic integrity," *Cell death and differentiation*, vol. 20, no. 11, pp. 1444–1454, 2013.

[3] Y. Zhao, C.-F. Zhang, H. Rossiter et al., "Autophagy is induced by UVA and promotes removal of oxidized phospholipids and protein aggregates in epidermal keratinocytes," *The Journal of Investigative Dermatology*, vol. 133, no. 6, pp. 1629–1637, 2013.

[4] A. S. Bess, I. T. Ryde, D. E. Hinton, and J. N. Meyer, "UVC-induced mitochondrial degradation via autophagy correlates with mtDNA damage removal in primary human fibroblasts," *Journal of Biochemical and Molecular Toxicology*, vol. 27, no. 1, pp. 28–41, 2013.

[5] L. Qiang, C. Wu, M. Ming, B. Viollet, and Y. Y. He, "Autophagy controls p38 activation to promote cell survival under genotoxic stress," *Journal of Biological Chemistry*, vol. 288, no. 3, pp. 1603–1611, 2013.

[6] A. Sample and Y. Y. He, "Autophagy in UV damage response," *Photochemistry and Photobiology*, vol. 93, no. 4, pp. 943–955, 2017.

[7] J. Uitto, "The role of elastin and collagen in cutaneous aging: intrinsic aging versus photoexposure," *Journal of Drugs in Dermatology*, vol. 7, 2 Suppl, 2008.

[8] M. Yaar and B. A. Gilchrest, "Photoageing: mechanism, prevention and therapy," *The British Journal of Dermatology*, vol. 157, no. 5, pp. 874–887, 2007.

[9] K. Tanaka, K. Asamitsu, H. Uranishi et al., "Protecting skin photoaging by NF-kappaB inhibitor," *Current Drug Metabolism*, vol. 11, no. 5, pp. 431–435, 2010.

[10] A. P. Schuch, N. C. Moreno, N. J. Schuch, C. F. M. Menck, and C. C. M. Garcia, "Sunlight damage to cellular DNA: focus on oxidatively generated lesions," *Free radical Biology & Medicine*, vol. 107, pp. 110–124, 2017.

[11] S. Dunaway, R. Odin, L. Zhou, L. Ji, Y. Zhang, and A. L. Kadekaro, "Natural antioxidants: multiple mechanisms to protect skin from solar radiation," *Frontiers in Pharmacology*, vol. 9, p. 392, 2018.

[12] H. Hayakawa, A. Taketomi, K. Sakumi, M. Kuwano, and M. Sekiguchi, "Generation and elimination of 8-oxo-7,8-dihydro-2′-deoxyguanosine 5′-triphosphate, a mutagenic substrate for DNA synthesis, in human cells," *Biochemistry*, vol. 34, no. 1, pp. 89–95, 1995.

[13] H. Takeuchi and T. M. Runger, "Longwave UV light induces the aging-associated progerin," *The Journal of Investigative Dermatology*, vol. 133, no. 7, pp. 1857–1862, 2013.

[14] J. Cadet, M. Berger, T. Douki et al., "Effects of UV and visible radiation on DNA-final base damage," *Biological Chemistry*, vol. 378, no. 11, pp. 1275–1286, 1997.

[15] E. A. Davidson, "DNA Repair and Mutagenesis 2ND EDITION,," *Shock*, vol. 26, no. 2, p. 221, 2006.

[16] R. M. Tyrrell, "Modulation of gene expression by the oxidative stress generated in human skin cells by UVA radiation and the restoration of redox homeostasis," *Photochemical & Photobiological Sciences : Official journal of the European Photochemistry Association and the European Society for Photobiology*, vol. 11, no. 1, pp. 135–147, 2012.

[17] M. Cavinato and P. Jansen-Durr, "Molecular mechanisms of UVB-induced senescence of dermal fibroblasts and its relevance for photoaging of the human skin," *Experimental Gerontology*, vol. 94, pp. 78–82, 2017.

[18] K. Scharffetter-Kochanek, P. Brenneisen, J. Wenk et al., "Photoaging of the skin from phenotype to mechanisms," *Experimental Gerontology*, vol. 35, no. 3, pp. 307–316, 2000.

[19] G. T. Wondrak, M. K. Jacobson, and E. L. Jacobson, "Endogenous UVA-photosensitizers: mediators of skin photodamage and novel targets for skin photoprotection," *Photochemical & photobiological sciences : Official journal of the European Photochemistry Association and the European Society for Photobiology*, vol. 5, no. 2, pp. 215–237, 2006.

[20] S. Grether-Beck, A. Marini, T. Jaenicke, and J. Krutmann, "Photoprotection of human skin beyond ultraviolet radiation," *Photodermatology, Photoimmunology & Photomedicine*, vol. 30, no. 2-3, pp. 167–174, 2014.

[21] O. Reelfs, I. M Eggleston, and C. Pourzand, "Skin protection against UVA-induced iron damage by multiantioxidants and iron chelating drugs/prodrugs," *Current Drug Metabolism*, vol. 11, no. 3, pp. 242–249, 2010.

[22] P. Karran and R. Brem, "Protein oxidation, UVA and human DNA repair," *DNA Repair*, vol. 44, pp. 178–185, 2016.

[23] A. Aroun, J. L. Zhong, R. M. Tyrrell, and C. Pourzand, "Iron, oxidative stress and the example of solar ultraviolet A radiation," *Photochemical & Photobiological Sciences : Official Journal of the European Photochemistry Association and the European Society for Photobiology*, vol. 11, no. 1, pp. 118–134, 2012.

[24] M. Buonanno, B. Ponnaiya, D. Welch et al., "Germicidal efficacy and mammalian skin safety of 222-nm UV light," *Radiation Research*, vol. 187, no. 4, pp. 483–491, 2017.

[25] D. Welch, M. Buonanno, V. Grilj et al., "Far-UVC light: a new tool to control the spread of airborne-mediated microbial diseases," *Scientific Reports*, vol. 8, no. 1, p. 2752, 2018.

[26] G. Imokawa, H. Nakajima, and K. Ishida, "Biological mechanisms underlying the ultraviolet radiation-induced formation of skin wrinkling and sagging II: over-expression of neprilysin plays an essential role," *International Journal of Molecular Sciences*, vol. 16, no. 4, pp. 7776–7795, 2015.

[27] P. Sil, S. W. Wong, and J. Martinez, "More than skin deep: autophagy is vital for skin barrier function," *Frontiers in Immunology*, vol. 9, p. 1376, 2018.

[28] J. D'Orazio, S. Jarrett, A. Amaro-Ortiz, and T. Scott, "UV radiation and the skin," *International Journal of Molecular Sciences*, vol. 14, no. 6, pp. 12222–12248, 2013.

[29] D. Murase, A. Hachiya, K. Takano et al., "Autophagy has a significant role in determining skin color by regulating melanosome degradation in keratinocytes," *The Journal of Investigative Dermatology*, vol. 133, no. 10, pp. 2416–2424, 2013.

[30] U. T. Brunk, C. B. Jones, and R. S. Sohal, "A novel hypothesis of lipofuscinogenesis and cellular aging based on interactions between oxidative stress and autophagocytosis," *Mutation Research*, vol. 275, no. 3-6, pp. 395–403, 1992.

[31] M. Hansen, D. C. Rubinsztein, and D. W. Walker, "Autophagy as a promoter of longevity: insights from model organisms," *Nature Reviews Molecular Cell Biology*, vol. 19, no. 9, pp. 579–593, 2018.

[32] F. Madeo, N. Tavernarakis, and G. Kroemer, "Can autophagy promote longevity?," *Nature Cell Biology*, vol. 12, no. 9, pp. 842–846, 2010.

[33] L. R. Lapierre, C. Kumsta, M. Sandri, A. Ballabio, and M. Hansen, "Transcriptional and epigenetic regulation of autophagy in aging," *Autophagy*, vol. 11, no. 6, pp. 867–880, 2015.

[34] S. Sukseree, S. Bergmann, K. Pajdzik et al., "Suppression of epithelial autophagy compromises the homeostasis of sweat glands during aging," *Journal of Investigative Dermatology*, vol. 138, no. 9, pp. 2061–2063, 2018.

[35] T. Kimura, Y. Isaka, and T. Yoshimori, "Autophagy and kidney inflammation," *Autophagy*, vol. 13, no. 6, pp. 997–1003, 2017.

[36] D. C. Rubinsztein, P. Codogno, and B. Levine, "Autophagy modulation as a potential therapeutic target for diverse diseases," *Nature reviews Drug discovery*, vol. 11, no. 9, pp. 709–730, 2012.

[37] D. C. Rubinsztein, G. Mariño, and G. Kroemer, "Autophagy and aging," *Cell*, vol. 146, no. 5, pp. 682–695, 2011.

[38] M. Jin, X. Liu, and D. J. Klionsky, "SnapShot: selective autophagy," *Cell*, vol. 152, no. 1-2, pp. 368–368.e2, 2013.

[39] C. A. Lamb, T. Yoshimori, and S. A. Tooze, "The autophagosome: origins unknown, biogenesis complex," *Nature reviews Molecular cell biology*, vol. 14, no. 12, pp. 759–774, 2013.

[40] B. Ravikumar, S. Sarkar, J. E. Davies et al., "Regulation of mammalian autophagy in physiology and pathophysiology," *Physiological Reviews*, vol. 90, no. 4, pp. 1383–1435, 2010.

[41] I. Tanida, T. Ueno, and E. Kominami, "LC3 conjugation system in mammalian autophagy," *The International Journal of Biochemistry & Cell Biology*, vol. 36, no. 12, pp. 2503–2518, 2004.

[42] N. Furuta, N. Fujita, T. Noda, T. Yoshimori, and A. Amano, "Combinational soluble N-ethylmaleimide-sensitive factor attachment protein receptor proteins VAMP8 and Vti1b mediate fusion of antimicrobial and canonical autophagosomes with lysosomes," *Molecular Biology of the Cell*, vol. 21, no. 6, pp. 1001–1010, 2010.

[43] S. Pankiv, T. H. Clausen, T. Lamark et al., "p62/SQSTM1 binds directly to Atg8/LC3 to facilitate degradation of ubiquitinated protein aggregates by autophagy," *Journal of Biological Chemistry*, vol. 282, no. 33, pp. 24131–24145, 2007.

[44] M. S. Rybchyn, W. G. M. De Silva, V. B. Sequeira et al., "Enhanced repair of UV-induced DNA damage by 1,25-dihydroxyvitamin D_3 in skin is linked to pathways that control cellular energy," *Journal of Investigative Dermatology*, vol. 138, no. 5, pp. 1146–1156, 2018.

[45] J. A. Zhang, B. R. Zhou, Y. Xu et al., "MiR-23a-depressed autophagy is a participant in PUVA- and UVB-induced premature senescence," *Oncotarget*, vol. 7, no. 25, pp. 37420–37435, 2016.

[46] D. Qin, R. Ren, C. Jia et al., "Rapamycin protects skin fibroblasts from ultraviolet B-induced photoaging by suppressing

the production of reactive oxygen species," *Cellular Physiology and Biochemistry : International journal of Experimental Cellular Physiology, Biochemistry, and Pharmacology*, vol. 46, no. 5, pp. 1849–1860, 2018.

[47] F. Gruber, H. Mayer, B. Lengauer et al., "NF-E2-related factor 2 regulates the stress response to UVA-1-oxidized phospholipids in skin cells," *FASEB Journal : Official Publication of the Federation of American Societies for Experimental Biology*, vol. 24, no. 1, pp. 39–48, 2010.

[48] X. Gao and P. Talalay, "Induction of phase 2 genes by sulforaphane protects retinal pigment epithelial cells against photooxidative damage," *Proceedings of the National Academy of Sciences of the United States of America*, vol. 101, no. 28, pp. 10446–10451, 2004.

[49] A. Hirota, Y. Kawachi, K. Itoh et al., "Ultraviolet A irradiation induces NF-E2-related factor 2 activation in dermal fibroblasts: protective role in UVA-induced apoptosis," *The Journal of Investigative Dermatology*, vol. 124, no. 4, pp. 825–832, 2005.

[50] R. A. Dunlop, U. T. Brunk, and K. J. Rodgers, "Oxidized proteins: mechanisms of removal and consequences of accumulation," *IUBMB Life*, vol. 61, no. 5, pp. 522–527, 2009.

[51] N. Mizushima, "Autophagy: process and function," *Genes & Development*, vol. 21, no. 22, pp. 2861–2873, 2007.

[52] O. Yamaguchi and K. Otsu, "Role of autophagy in aging," *Journal of Cardiovascular Pharmacology*, vol. 60, no. 3, pp. 242–247, 2012.

[53] R. Widmer, I. Ziaja, and T. Grune, "Protein oxidation and degradation during aging: role in skin aging and neurodegeneration," *Free Radical Research*, vol. 40, no. 12, pp. 1259–1268, 2006.

[54] T. Grune, T. Reinheckel, and K. J. Davies, "Degradation of oxidized proteins in mammalian cells," *Faseb Journal Official Publication of the Federation of American Societies for Experimental Biology*, vol. 11, no. 7, pp. 526–534, 1997.

[55] M. Yan, Z. Liu, H. Yang et al., "Luteolin decreases the UVA-induced autophagy of human skin fibroblasts by scavenging ROS," *Molecular Medicine Reports*, vol. 14, no. 3, pp. 1986–1992, 2016.

[56] M. Cavinato, R. Koziel, N. Romani et al., "UVB-induced senescence of human dermal fibroblasts involves impairment of proteasome and enhanced autophagic activity," *The Journals of Gerontology Series A: Biological Sciences and Medical Sciences*, vol. 72, no. 5, pp. glw150–glw639, 2016.

[57] E. Olivier, M. Dutot, A. Regazzetti et al., "Lipid deregulation in UV irradiated skin cells: role of 25-hydroxycholesterol in keratinocyte differentiation during photoaging," *The Journal of Steroid Biochemistry and Molecular Biology*, vol. 169, pp. 189–197, 2017.

[58] G. G. Rodney, R. Pal, and R. Abo-Zahrah, "Redox regulation of autophagy in skeletal muscle," *Free Radical Biology and Medicine*, vol. 98, pp. 103–112, 2016.

[59] R. Peto, "The fraction of cancer attributable to lifestyle and environmental factors in the UK in 2010," *British Journal of Cancer*, vol. 105, no. S2, p. S1, 2011.

[60] E. White, "Deconvoluting the context-dependent role for autophagy in cancer," *Nature Reviews Cancer*, vol. 12, no. 6, pp. 401–410, 2012.

[61] L. Poillet-Perez, G. Despouy, R. Delage-Mourroux, and M. Boyer-Guittaut, "Interplay between ROS and autophagy in cancer cells, from tumor initiation to cancer therapy," *Redox Biology*, vol. 4, pp. 184–192, 2015.

[62] T. Yu, J. Zuber, and J. Li, "Targeting autophagy in skin diseases," *Journal of Molecular Medicine*, vol. 93, no. 1, pp. 31–38, 2015.

[63] C. Lopez-Camarillo, E. A. Ocampo, M. L. Casamichana, C. Perez-Plasencia, E. Alvarez-Sanchez, and L. A. Marchat, "Protein kinases and transcription factors activation in response to UV-radiation of skin: implications for carcinogenesis," *International Journal of Molecular Sciences*, vol. 13, no. 1, pp. 142–172, 2012.

[64] T. L. D. Marais, T. Kluz, D. Xu et al., "Transcription factors and stress response gene alterations in human keratinocytes following solar simulated ultraviolet radiation," *Scientific Reports*, vol. 7, no. 1, p. 13622, 2017.

[65] G. Pearson, F. Robinson, T. Beers Gibson et al., "Mitogen-activated protein (MAP) kinase pathways: regulation and physiological functions," *Endocrine Reviews*, vol. 22, no. 2, pp. 153–183, 2001.

[66] A. Minden, A. Lin, M. McMahon et al., "Differential activation of ERK and JNK mitogen-activated protein kinases by Raf-1 and MEKK," *Science*, vol. 266, no. 5191, pp. 1719–1723, 1994.

[67] C. R. Weston and R. J. Davis, "The JNK signal transduction pathway," *Current Opinion in Genetics & Development*, vol. 12, no. 1, pp. 14–21, 2002.

[68] A. M. Bode and Z. Dong, "Mitogen-activated protein kinase activation in UV-induced signal transduction," *Science Signaling*, vol. 2003, no. 167, p. re2, 2003.

[69] J. L. Zhong, L. Yang, F. Lü et al., "UVA, UVB and UVC induce differential response signaling pathways converged on the eIF2α phosphorylation," *Photochemistry and Photobiology*, vol. 87, no. 5, pp. 1092–1104, 2011.

[70] Y. Zhang, D. Xing, and L. Liu, "PUMA promotes Bax translocation by both directly interacting with Bax and by competitive binding to Bcl-X L during UV-induced apoptosis," *Molecular Biology of the Cell*, vol. 20, no. 13, pp. 3077–3087, 2009.

[71] Y. C. Kim and K.-L. Guan, "mTOR: a pharmacologic target for autophagy regulation," *The Journal of Clinical Investigation*, vol. 125, no. 1, pp. 25–32, 2015.

[72] L. Wei, S. Zhu, J. Wang, and J. Liu, "Activation of the phosphatidylinositol 3-kinase/Akt signaling pathway during porcine circovirus type 2 infection facilitates cell survival and viral replication," *Journal of Virology*, vol. 86, no. 24, pp. 13589–13597, 2012.

[73] B. Zhang, Z. Zhao, X. Meng, H. Chen, G. Fu, and K. Xie, "Hydrogen ameliorates oxidative stress via PI3K-Akt signaling pathway in UVB-induced HaCaT cells," *International Journal of Molecular Medicine*, vol. 41, no. 6, pp. 3653–3661, 2018.

[74] Y. Yang, C. Quach, and C. Liang, "Autophagy modulator plays a part in UV protection," *Autophagy*, vol. 12, no. 9, pp. 1677-1678, 2016.

[75] X. Lu and D. P. Lane, "Differential induction of transcriptionally active p53 following UV or ionizing radiation: defects in chromosome instability syndromes?," *Cell*, vol. 75, no. 4, pp. 765–778, 1993.

[76] Y. Romero, M. Bueno, R. Ramirez et al., "mTORC1 activation decreases autophagy in aging and idiopathic pulmonary fibrosis and contributes to apoptosis resistance in IPF fibroblasts," *Aging Cell*, vol. 15, no. 6, pp. 1103–1112, 2016.

[77] A. R. Young, M. Narita, M. Ferreira et al., "Autophagy mediates the mitotic senescence transition," *Genes & Development*, vol. 23, no. 7, pp. 798–803, 2009.

[78] A. R. Young and M. Narita, "Connecting autophagy to senescence in pathophysiology," *Current Opinion in Cell Biology*, vol. 22, no. 2, pp. 234–240, 2010.

[79] Y. J. Choi, K. M. Moon, K. W. Chung et al., "The underlying mechanism of proinflammatory NF-κB activation by the mTORC2/Akt/IKKα pathway during skin aging," *Oncotarget*, vol. 7, no. 33, pp. 52685–52694, 2016.

[80] M. Kaeberlein, M. McVey, and L. Guarente, "The SIR2/3/4 complex and SIR2 alone promote longevity in Saccharomyces cerevisiae by two different mechanisms," *Genes & Development*, vol. 13, no. 19, pp. 2570–2580, 1999.

[81] M. B. Scher, A. Vaquero, and D. Reinberg, "SirT3 is a nuclear NAD+-dependent histone deacetylase that translocates to the mitochondria upon cellular stress," *Genes & Development*, vol. 21, no. 8, pp. 920–928, 2007.

[82] M. C. Haigis and D. A. Sinclair, "Mammalian sirtuins: biological insights and disease relevance," *Annual Review of Pathology*, vol. 5, pp. 253–295, 2010.

[83] C. A. Benavente, S. A. Schnell, and E. L. Jacobson, "Effects of niacin restriction on sirtuin and PARP responses to photodamage in human skin," *PLoS One*, vol. 7, no. 7, 2012.

[84] C. Cao, S. Lu, R. Kivlin et al., "SIRT1 confers protection against UVB- and H2O2-induced cell death via modulation of p53 and JNK in cultured skin keratinocytes," *Journal of Cellular and Molecular Medicine*, vol. 13, no. 9B, pp. 3632–3643, 2009.

[85] V. B. Pillai, N. R. Sundaresan, and M. P. Gupta, "Regulation of Akt signaling by sirtuins: its implication in cardiac hypertrophy and aging," *Circulation Research*, vol. 114, no. 2, pp. 368–378, 2014.

[86] E. Morselli, G. Mariño, M. V. Bennetzen et al., "Spermidine and resveratrol induce autophagy by distinct pathways converging on the acetylproteome," *The Journal of Cell Biology*, vol. 192, no. 4, pp. 615–629, 2011.

[87] D. Tsitsipatis, L. O. Klotz, and H. Steinbrenner, "Multifaceted functions of the forkhead box transcription factors FoxO1 and FoxO3 in skin," *Biochimica et Biophysica Acta (BBA)-General Subjects*, vol. 1861, no. 5, pp. 1057–1064, 2017.

[88] "Long live FOXO: unraveling the role of FOXO proteins in aging and longevity," *Aging Cell*, vol. 15, no. 2, pp. 196–207, 2016.

[89] H. Tanaka, Y. Murakami, I. Ishii, and S. Nakata, "Involvement of a forkhead transcription factor, FOXO1A, in UV-induced changes of collagen metabolism," *The Journal of Investigative Dermatology Symposium Proceedings*, vol. 14, no. 1, pp. 60–62, 2009.

[90] A. van der Horst and B. M. Burgering, "Stressing the role of FoxO proteins in lifespan and disease," *Nature Reviews Molecular Cell Biology*, vol. 8, no. 6, pp. 440–450, 2007.

[91] K. E. van der Vos, P. Eliasson, T. Proikas-Cezanne et al., "Modulation of glutamine metabolism by the PI(3)K-PKB-FOXO network regulates autophagy," *Nature Cell Biology*, vol. 14, no. 8, pp. 829–837, 2012.

[92] N. Hariharan, Y. Maejima, J. Nakae, J. Paik, R. A. Depinho, and J. Sadoshima, "Deacetylation of FoxO by Sirt1 plays an essential role in mediating starvation-induced autophagy in cardiac myocytes," *Circulation Research*, vol. 107, no. 12, pp. 1470–1482, 2010.

[93] S. A. Ham, E. S. Kang, H. Lee et al., "PPARδ Inhibits UVB-Induced Secretion of MMP-1 through MKP-7-Mediated Suppression of JNK Signaling," *The Journal of Investigative Dermatology*, vol. 133, no. 11, pp. 2593–2600, 2013.

[94] X. Palomer, E. Capdevila-Busquets, G. Botteri et al., "PPARβ/δ attenuates palmitate-induced endoplasmic reticulum stress and induces autophagic markers in human cardiac cells," *International Journal of Cardiology*, vol. 174, no. 1, pp. 110–118, 2014.

[95] C. G. Evans, L. Chang, and J. E. Gestwicki, "Heat shock protein 70 (hsp70) as an emerging drug target," *Journal of Medicinal Chemistry*, vol. 53, no. 12, pp. 4585–4602, 2010.

[96] N. V. Bobkova, M. Evgen'ev, D. G. Garbuz et al., "Exogenous Hsp70 delays senescence and improves cognitive function in aging mice," *Proceedings of the National Academy of Sciences of the United States of America*, vol. 112, no. 52, pp. 16006–16011, 2015.

[97] T. Haarmann-Stemmann, F. Boege, and J. Krutmann, "Adaptive and maladaptive responses in skin: mild heat exposure protects against UVB-induced photoaging in mice," *The Journal of Investigative Dermatology*, vol. 133, no. 4, pp. 868–871, 2013.

[98] K. Dokladny, O. B. Myers, and P. L. Moseley, "Heat shock response and autophagy–cooperation and control," *Autophagy*, vol. 11, no. 2, pp. 200–213, 2015.

[99] R. Hjerpe, J. S. Bett, M. J. Keuss et al., "UBQLN2 mediates autophagy-independent protein aggregate clearance by the proteasome," *Cell*, vol. 166, no. 4, pp. 935–949, 2016.

[100] A. Walker, A. Singh, E. Tully et al., "Nrf2 signaling and autophagy are complementary in protecting breast cancer cells during glucose deprivation," *Free Radical Biology & Medicine*, vol. 120, pp. 407–413, 2018.

[101] J. L. Zhong, G. P. Edwards, C. Raval, H. Li, and R. M. Tyrrell, "The role of Nrf2 in ultraviolet A mediated heme oxygenase 1 induction in human skin fibroblasts," *Photochemical & Photobiological Sciences*, vol. 9, no. 1, pp. 18–24, 2010.

[102] A. Hirota, Y. Kawachi, M. Yamamoto, T. Koga, K. Hamada, and F. Otsuka, "Acceleration of UVB-induced photoageing in Nrf2 gene-deficient mice," *Experimental Dermatology*, vol. 20, no. 8, pp. 664–668, 2011.

[103] N. Kubben, W. Zhang, L. Wang et al., "Repression of the antioxidant NRF2 pathway in premature aging," *Cell*, vol. 165, no. 6, pp. 1361–1374, 2016.

[104] M. Pajares, N. Jiménez-Moreno, Á. J. García-Yagüe et al., "Transcription factor NFE2L2/NRF2 is a regulator of macroautophagy genes," *Autophagy*, vol. 12, no. 10, pp. 1902–1916, 2016.

[105] M. Komatsu, H. Kurokawa, S. Waguri et al., "The selective autophagy substrate p62 activates the stress responsive transcription factor Nrf2 through inactivation of Keap1," *Nature Cell Biology*, vol. 12, no. 3, pp. 213–223, 2010.

[106] V. E. Reeve and R. M. Tyrrell, "Heme oxygenase induction mediates the photoimmunoprotective activity of UVA radiation in the mouse," *Proceedings of the National Academy of Sciences of the United States of America*, vol. 96, no. 16, pp. 9317–9321, 1999.

[107] S. W. Ryter, J. Alam, and A. M. Choi, "Heme oxygenase-1/carbon monoxide: from basic science to therapeutic applications," *Physiological Reviews*, vol. 86, no. 2, pp. 583–650, 2006.

[108] L. E. Otterbein, M. P. Soares, K. Yamashita, and F. H. Bach, "Heme oxygenase-1: unleashing the protective properties of heme," *Trends in Immunology*, vol. 24, no. 8, pp. 449–455, 2003.

[109] A. Loboda, M. Damulewicz, E. Pyza, A. Jozkowicz, and J. Dulak, "Role of Nrf2/HO-1 system in development, oxidative stress response and diseases: an evolutionarily conserved mechanism," *Cellular and Molecular Life Sciences*, vol. 73, no. 17, pp. 3221–3247, 2016.

[110] L. A. Applegate, A. Noel, G. Vile, E. Frenk, and R. M. Tyrrell, "Two genes contribute to different extents to the heme oxygenase enzyme activity measured in cultured human skin fibroblasts and keratinocytes: implications for protection against oxidant stress," *Photochemistry and Photobiology*, vol. 61, no. 3, pp. 285–291, 1995.

[111] G. F. Vile, S. Basu-Modak, C. Waltner, and R. M. Tyrrell, "Heme oxygenase 1 mediates an adaptive response to oxidative stress in human skin fibroblasts," *Proceedings of the National Academy of Sciences of the United States of America*, vol. 91, no. 7, pp. 2607–2610, 1994.

[112] A. Rossi and M. G. Santoro, "Induction by prostaglandin A1 of haem oxygenase in myoblastic cells: an effect independent of expression of the 70 kDa heat shock protein," *The Biochemical Journal*, vol. 308, no. 2, pp. 455–463, 1995.

[113] R. M. Tyrrell, "Activation of mammalian gene expression by the UV component of sunlight–from models to reality," *BioEssays*, vol. 18, no. 2, pp. 139–148, 1996.

[114] P. Waltz, E. H. Carchman, A. C. Young et al., "Lipopolysaccaride induces autophagic signaling in macrophages via a TLR4, heme oxygenase-1 dependent pathway," *Autophagy*, vol. 7, no. 3, pp. 315–320, 2011.

[115] E. H. Carchman, J. Rao, P. A. Loughran, M. R. Rosengart, and B. S. Zuckerbraun, "Heme oxygenase-1-mediated autophagy protects against hepatocyte cell death and hepatic injury from infection/sepsis in mice," *Hepatology*, vol. 53, no. 6, pp. 2053–2062, 2011.

[116] Y. Devary, C. Rosette, J. A. DiDonato, and M. Karin, "NF-kappa B activation by ultraviolet light not dependent on a nuclear signal," *Science*, vol. 261, no. 5127, pp. 1442–1445, 1993.

[117] F. G. Osorio, C. Barcena, C. Soria-Valles et al., "Nuclear lamina defects cause ATM-dependent NF-κB activation and link accelerated aging to a systemic inflammatory response," *Genes & Development*, vol. 26, no. 20, pp. 2311–2324, 2012.

[118] J. S. Tilstra, A. R. Robinson, J. Wang et al., "NF-κB inhibition delays DNA damage-induced senescence and aging in mice," *The Journal of Clinical Investigation*, vol. 122, no. 7, pp. 2601–2612, 2012.

[119] G. J. Fisher, S. C. Datta, H. S. Talwar et al., "Molecular basis of sun-induced premature skin ageing and retinoid antagonism," *Nature*, vol. 379, no. 6563, pp. 335–339, 1996.

[120] E. L. O'Dea, J. D. Kearns, and A. Hoffmann, "UV as an amplifier rather than inducer of NF-kappaB activity," *Molecular Cell*, vol. 30, no. 5, pp. 632–641, 2008.

[121] M. M. Simon, Y. Aragane, A. Schwarz, T. A. Luger, and T. Schwarz, "UVB light induces nuclear factor kappa B (NF kappa B) activity independently from chromosomal DNA damage in cell-free cytosolic extracts," *The Journal of Investigative Dermatology*, vol. 102, no. 4, pp. 422–427, 1994.

[122] K. Bender, M. Gottlicher, S. Whiteside, H. J. Rahmsdorf, and P. Herrlich, "Sequential DNA damage-independent and -dependent activation of NF-kappaB by UV," *The EMBO Journal*, vol. 17, no. 17, pp. 5170–5181, 1998.

[123] Z. H. Wu, Y. Shi, R. S. Tibbetts, and S. Miyamoto, "Molecular linkage between the kinase ATM and NF-kappaB signaling in response to genotoxic stimuli," *Science*, vol. 311, no. 5764, pp. 1141–1146, 2006.

[124] J. Dujic, S. Kippenberger, S. Hoffmann et al., "Low concentrations of curcumin induce growth arrest and apoptosis in skin keratinocytes only in combination with UVA or visible light," *The Journal of Investigative Dermatology*, vol. 127, no. 8, pp. 1992–2000, 2007.

[125] O. Reelfs, R. M. Tyrrell, and C. Pourzand, "Ultraviolet A Radiation-Induced Immediate Iron Release Is a Key Modulator of the Activation of NF-κB in Human Skin Fibroblasts," *The Journal of Investigative Dermatology*, vol. 122, no. 6, pp. 1440–1447, 2004.

[126] R. A. Swerlick and N. J. Korman, "UVA and NF-kappaB activity: ironing out the details," *The Journal of Investigative Dermatology*, vol. 122, no. 6, pp. xi–xii, 2004.

[127] Z. Zhong, A. Umemura, E. Sanchez-Lopez et al., "NF-κB restricts inflammasome activation via elimination of damaged mitochondria," *Cell*, vol. 164, no. 5, pp. 896–910, 2016.

[128] C. P. Chang, Y. C. Su, P. H. Lee, and H. Y. Lei, "Targeting NFKB by autophagy to polarize hepatoma-associated macrophage differentiation," *Autophagy*, vol. 9, no. 4, pp. 619–621, 2013.

[129] T. G. Sommermann, H. I. Mack, and E. Cahir-McFarland, "Autophagy prolongs survival after NFκB inhibition in B-cell lymphomas," *Autophagy*, vol. 8, no. 2, pp. 265–267, 2012.